1-1-2012

Throughput Analysis of Opportunistic Channel Access Techniques in Cognitive Radio Systems

Sivasothy Sen Senthuran
Ryerson University

Throughput Analysis of Opportunistic Channel Access Techniques in Cognitive Radio Systems

by

Sivasothy (Sen) Senthuran

B.Sc.Eng., University of Moratuwa, Sri Lanka, 2003

M.Eng., Asian Institute of Technology, Thailand, 2006

M.Sc., Telecom SudParis, France, 2006

A Dissertation

presented to Ryerson University

in partial fulfilment of the requirements for the degree of

Doctor of Philosophy in the

Program of Electrical and Computer Engineering

Toronto, Ontario, Canada, 2012

AUTHORS DECLARATION FOR ELECTRONIC SUBMISSION OF A DISSERTATION

I hereby declare that I am the sole author of this dissertation. This is a true copy of the dissertation, including any required final revisions, as accepted by my examiners.

I authorize Ryerson University to lend this dissertation to other institutions or individuals for the purpose of scholarly research.

I further authorize Ryerson University to reproduce this dissertation by photocopying or by other means, in total or in part, at the request of other institutions or individuals for the purpose of scholarly research.

I understand that my dissertation may be made electronically available to the public.

Abstract

Throughput Analysis of Opportunistic Channel Access Techniques in Cognitive Radio Systems

Doctor of Philosophy

Electrical and Computer Engineering

Ryerson University

In recent studies it was found out that previously allocated frequency spectrum is not fully utilized in all the wireless systems. Cognitive radio is the new concept to access this under-utilized spectrum and, also a promising technology to cope with the ever increasing bandwidth demand for next generation wireless networks. Cognitive radio network can be classified into three different categories: interweave, underlay and overlay. In an interweave cognitive radio system, the unoccupied spectrum holes can be shared by cognitive users with minimal collision with primary users (spectrum owners) whereas in an underlay system, concurrent transmission is allowed with an interference threshold to the primary users. In an underlay system, cognitive users generally transmit at very low power. In an overlay system, cognitive users, similar to underlay cognitive radio systems, concurrently transmit with primary users but cognitive users may know the codewords of the primary transmitter. Hence, using that knowledge, cognitive transmitter may adopt different coding techniques to cancel/mitigate the interference at the primary receiver and/or it may assist the primary system by relaying primary user's data. In this thesis, we improve the throughput/bit error rate performance of a cognitive radio system by effectively accessing the channels. Throughout the thesis we assume that cognitive user can sense only one channel at a time and we analyze the performance with perfect and imperfect sensing.

First, we propose a novel opportunistic access scheme for cognitive radios in an interweave cognitive system, that considers the channel gain as well as the predicted idle channel probability (primary user occupancy: busy/idle). In contrast to previous work where a cognitive user vacates a channel only when that channel becomes busy, the proposed scheme requires the cognitive user to switch to the channel with the next highest idle probability if the current channel's gain is below a certain threshold. We derive the threshold values that maximize the long term throughput for various primary user transition probabilities and cognitive user's relative movement (Doppler spread). Then, we propose a three state Markov model to analyze the performance of a hybrid interweave-underlay system where the primary user's occupancy states are hidden, but their activity statistics, ranges of transmission, and interference thresholds are known. The primary user is assumed to be in one of the three transmission modes as seen by the cognitive user: busy, concurrent and idle. We derive the transmission mode selection criteria (interweave/underlay) to improve the long term throughput of a cognitive user based on the primary user traffic characteristics and the achievable throughput ratio between the two modes of operation. Later, we incorporate the sensing error in our analysis where we study the optimal access strategy. Since the optimal policy requires the channel to be sensed in each time-slot, we propose and analyze a forward algorithm based cross-layer frame based sensing policy.

Finally, we focus on the overlay cognitive radio system where cognitive relay nodes assist the primary transmission. As an initial study, we select a two-hop decode-and-forward orthogonal frequency and code division multiplexing based relay network. For this system, we propose adaptive channel allocation and, power allocation strategies and the bit error rate performance is numerically evaluated. This preliminary analysis can be extended to overlay cognitive systems.

Acknowledgment

This dissertation would not be possible without the help and support of many people. A few words mentioned here cannot adequately express my appreciation.

First and foremost, I would like to express my deepest gratitude toward my supervisors, Professors Alagan Anpalagan and Olivia Das for giving me this opportunity. I am extraordinarily grateful to Dr. Anpalagan for his criticism, patience, invaluable support and guidance throughout my research program at the Ryerson University. His helpful, detailed criticism has sharpened my scientific and communication abilities, and his professional discipline and diligence inspire me to the same. I am also very grateful for his positive encouragement at numerous times during my graduate studies. Dr. Das has cheered me since Day 1 and I am grateful for her kindness, enthusiasm, and articulate advice. Her help with Markov analysis was outstanding and made my thesis stronger.

I would like to extend my gratitude to Professors S. Krishnan , L. Zhao and V. Misic from the Ryerson University, and Professor E. Hossain from University of Manitoba for serving in my doctoral dissertation exam committee. Their insightful advice and comments have improved the quality of this dissertation. I am grateful to these astute researchers and scientists, and it is a privilege to have had my work refined by their hands and minds. I am very grateful to Dr. Ashok Karmokar for the research collaboration in chapter 4, and sharing his knowledge and technical expertise in Markov analysis. Special thanks to my masters program advisor Professor N. Rajatheva for general discussion on wireless communication.

I gratefully acknowledge Ryerson University for the continuous support for my studies. Also, I acknowledge the Natural Sciences and Engineering Research Council (NSERC) for funding this research work. I would like to acknowledge the support of my lab mates, who have helped me during each stage of my graduate studies. Thanks for offering a sympathetic

ear and sage advice.

Finally, I am deeply grateful to my family, for their patient encouragement throughout my every adventure, including graduate school. Their unconditional love reminds me that my value as a person does not hinge upon my completion of this degree or upon professional accolades. Additionally, this would not have been possible without the love, laughter, and prayers of many friends.

Dedication

To my late father

Nagalingam Sivasothy

Contents

List of Tables

List of Figures

List of Abbreviations

4G	Fourth Generation
ACK/NAK	Positive/Negative Acknowledgment
BER	Bit Error Rate
BPSK	Binary Phase Shift Keying
CDMA	Code Division Multiple Access
CSI	Channel State Information
C-CSI	Cooperative CSI
MAC	Medium Access Control
PHY	Physical Layer
POMDP	Partially Observable Markov Decision Process
OFCDM	Orthogonal Frequency and Code Division Multiplexing
OFDM	Orthogonal Frequency Division Multiplexing
SINR	Signal to Interference and Noise Ratio
SNR	Signal to Noise Ratio

Chapter 1

Introduction

Wireless communication has become an integral part of human life. Recent exponential growth in the use of wireless phones has been attributed to the advances in device technology and applications development in addition to various communication technologies. One of them is the advent of cognitive radio technology.

1.1 Cognitive Radio System

The under-utilization of the scarce spectrum triggered the need for opportunistic spectrum sharing among mobile radio users recently [1]. Cognitive radio is one of the most promising technologies to cope with the ever increasing bandwidth demand for future generation wireless networks. Due to current non-dynamic allocation of wireless spectrum, it is severely under-utilized in TV transmission band and amateur radio band, and extremely crowded in consumer radio communications band [2]. Motivated by the FCC study in the USA, the cognitive radio networks have been incepted for the dynamic and opportunistic utilization of the under-utilized spectrum, where an opportunistic cognitive user (also known as secondary user) can reuse an unoccupied piece of spectrum (also called a spectrum hole) licensed to

a primary user temporarily. The users who own the spectrum (primary users) usually get higher access privilege while the cognitive users usually look for opportunistic access [3].

There are three types of cognitive radio systems : interweave, underlay and overlay. In an interweave cognitive radio system, the unoccupied spectrum holes should be shared by cognitive users with minimal collision with primary users whereas in an underlay system, concurrent transmission and the interference threshold to the primary users are the main concerns [4–8]. Similar to underlay cognitive radio system, cognitive user transmits simultaneously in the same band as the primary transmitter in an overlay cognitive radio system but cognitive user may know the code words of the primary transmitter. Hence, using that knowledge, cognitive transmitter may adopt different coding techniques to cancel/mitigate the interference at the primary receiver and/or it may assist the primary system by relaying its data. We will briefly discuss this classification in the following.

1.1.1 Interweave Cognitive Radio System

Interweave communication is the first concept evolved with cognitive radio communication. It was found during the initial study by FCC that most of the assigned spectrum is not fully utilized [9]. That is, there exist temporary time-frequency-space voids and can be opportunistically used by cognitive users. Opportunistically using those spectrum holes by the cognitive users without affecting the primary users is called interweave communication. In an interweave communication, cognitive users are prohibited to transmit while primary user is occupying that spectrum. In order to use the spectrum holes with minimal collision with primary users, cognitive users must sense the spectrum before using it. Cognitive users may use the primary users' spectrum occupancy statistics in addition to spectrum sensing in order to effectively utilize the spectrum holes. Cognitive user should be intelligent enough to

sense the wide spectrum and opportunistically use the spectrum holes for its communication with minimal interference to the primary users. We use interweave communication system model in chapter 2 and, in chapters 3 and 4, it is used as a part of the interweave-underlay hybrid system.

1.1.2 Underlay Cognitive Radio System

In underlay cognitive radio systems, cognitive users transmit in the presence of primary users with the knowledge of interference caused by the cognitive transmitter to primary receivers [3]. Even though the concurrent transmission is allowed in underlay cognitive radio system, interference threshold to the primary receiver is highly respected. Interference to the primary receiver can be minimized using directional antennae at the cognitive transmitter. In most cases, the cognitive transmitter spreads its power across wider bands so that the transmission causes acceptable level of interference to the primary receiver [2]. This technique is used in ultra-wide-band communication. Cognitive transmitter can estimate the interference to the primary receiver via channel reciprocity if it can overhear cognitive receiver's signal. It can also adopt a conservative transmission policy that may result in shorter range of communication. If there is a mechanism to broadcast periodically the primary receiver's interference level, it would be easier to adopt the transmission policy at the cognitive transmitter. A discussion on underlay communication and fundamental limitations in resource allocations can be found in [10, 11]. Underlay cognitive system model is used in chapter 3 with perfect sensing and in chapter 4 with sensing error along with interweave cognitive system model in this thesis.

1.1.3 Overlay Cognitive Radio System

In overlay communication, cognitive transmitter is assumed to know the code words of the primary transmitter so that cognitive user can transmit at the same time in the same band without affecting the primary receiver. Primary users' codebooks may be publicly available or communicated to the cognitive user by broadcasting. Cognitive user may detect the signal and adopt a transmission scheme, such as dirty paper coding, so that it can mitigate/cancel the interference at the primary receiver [3]. In some cases, cognitive transmitter assists the primary user transmission by relaying the primary user's data. Cognitive user may split the transmission power between its own transmission and in assisting primary user. In unlicensed bands, sharing the codebooks allows cognitive users to mitigate the interference. In licensed bands, they can use that knowledge to cancel the interference or in assisting the primary receiver. The overlay system model is used in the chapter 4.

1.1.4 Channel Sensing and Access

In order to reuse spectrum holes, a cognitive user must perform out-of-band sensing. If a spectrum hole is found, the cognitive user can use it for its data transmission. However, it needs to also conduct in-band sensing periodically so that it can vacate the acquired channel when the incumbent user re-appears. In IEEE 802.22 Wireless Regional Area Networks, primary users should be detected within two seconds of their reappearance with the sensing error probabilities no greater than 0.1 [12]. In order to avoid interference among multiple sensors and achieve reliable sensing, all the cognitive users should sense the channel during the quiet period. In the quiet period, all cognitive users should postpone their transmission so that any sensor monitoring the channel may observe the presence/absence of primary user signals without interference. Different physical (PHY) and medium access control (MAC)

layer techniques for efficient sensing and accessing exist in the literature. In [13], a decentralized MAC protocol for ad hoc cognitive radio networks has been proposed that senses channel in each time-slot and takes opportunistic channel access decision. The authors in [14] extended the partially observable Markov decision process (POMDP) based optimal and myopic greedy suboptimal techniques of [13] for cooperative sensing cognitive radio networks. In [15], the authors studied the problem of designing the sensing slot duration to maximize the achievable throughput. A comparative study of energy detection and feature detection in-band spectrum sensing techniques in wireless regional area networks can be found in [12]. While above works consider that the primary user's state may be in one of the two states, namely, busy and idle, we consider a third state that a primary user may occupy, and have studied opportunistic access strategies for hybrid cognitive radio networks. An information theoretic perspective of three paradigms, namely, underlay, overlay and interweave, has been given in [3].

Motivated by the above studies, in this thesis, we study the channel access schemes in a cognitive radio system in all three forms of cognitive radio systems.

1.2 Thesis Contribution

The key contributions of this thesis can be summarized as follows:

We considered a cognitive radio system where a cognitive user can sense only one primary channel at a time. For that system, we propose and analyze different channel access schemes. In an interweave cognitive radio system, cognitive user looks for an spectrum hole to access that primary channel. Based on the primary user occupancy statistics, cognitive user selects the best channel to sense, and if that is vacant then cognitive user can occupy the channel. We first propose an channel access/switching strategy based on the primary user occupancy

statistics as well as the cognitive user's received signal to noise ratio in a Rayleigh fading channel. Hence, we developed and analyzed an effective channel access strategy for a system with two primary channel as well as multiple channels. Based on the analysis, effective throughput of a cognitive user can be increased by implementing the proposed strategy.

Further, in a cognitive radio system, there are opportunities to access the spectrum in underlay or interweave modes. Hence, there is need for an effective access strategy for selecting the best mode of transmission. We propose a three state Markov framework to analyze the interweave-underlay mode of transmission. Based on the primary user traffic characteristics and effective throughput ratio between the two mode of transmissions, optimal channel access strategy is proposed, analyzed and verified through simulations.

In practice, there is uncertainty in sensing. Therefore, we incorporated the sensing error in the above interweave-underlay cognitive radio system to find an optimal access strategy. The problem is formulated as finite-horizon POMDP and the optimal solution technique is given using incremental-pruning algorithm that optimizes the throughput and avoids the interference to primary users. We studied the throughput and collision performance analysis via simulation for different primary user occupancy characteristics.

Finally, we considered the overlay cognitive radio system where cognitive relay nodes assist the primary user transmission. In our study, we considered an orthogonal frequency and code division multiplexing (OFCDM) based decode-and-forward relay and we propose an adaptive channel (OFCDM subcarrier) allocation scheme to improve the system throughput based on the primary and cognitive user links (channel gains). The analysis mainly focuses on the performance of the cognitive relay assisted primary user throughput. At system level, the optimal power allocation between the primary user and cognitive relay is also analyzed.

Most of the works reported in this dissertation can be found in peer reviewed research publications [16–23]. chapter 2 appeared in [16, 17]. The work of chapter 3 can be found

in [18, 19]. The work in chapter 4 can be found in [20] and chapter 5 in [21–23].

1.3 Thesis Organization

The snap shot of the thesis work is shown in the Fig. 1.1. In this dissertation, we propose novel Markov model for the analysis of different cognitive radio systems and different access strategies to improve the system performance.

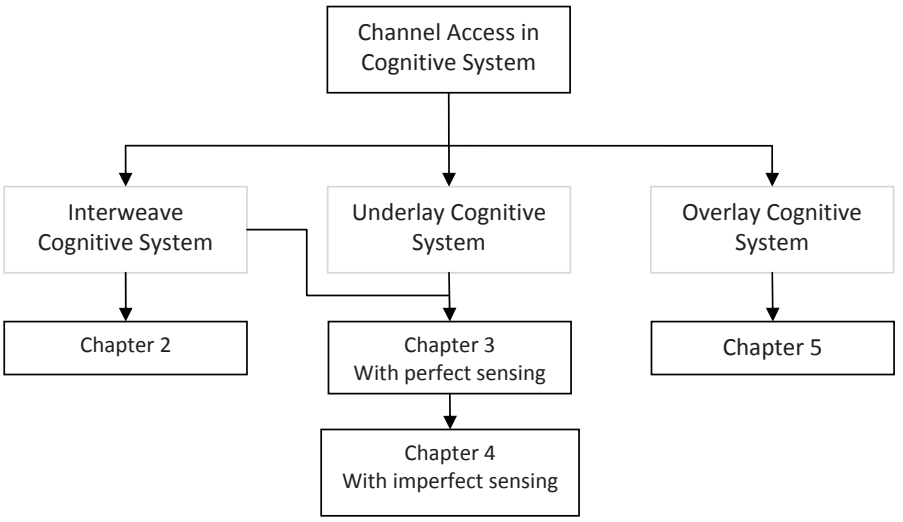

Figure 1.1: Chapter organization.

The thesis is organized as follows:

In chapter 2, we propose and analyze a channel access scheme for a cognitive user that operates in an interweave system, based on the traffic characteristics of the primary system and Doppler spread of the cognitive user. Throughput performance is analytically evaluated and verified via simulations.

In chapter 3, the above work is extended to hybrid interweave-underlay cognitive radio system. In this chapter, we propose a three state model for the analysis and study the transmission mode selection with channel access in a hybrid underlay-interweave cognitive

radio systems based on cognitive user throughput ratio between underlay and interweave transmission modes and the primary user traffic statistics while cognitive user can sense only one channel. Again the analytical work is verified with simulation.

The chapter 3 work is extended to a system with sensing error in chapter 4. In this chapter, we study the channel access and power adaptation techniques for a hybrid interweave-underlay cognitive radio system. We first study the optimal channel access and power adaptation strategy by formulating the problem as a finite-horizon POMDP. The optimal solution technique is given using incremental-pruning algorithm that optimizes the throughput and avoids the interference to primary users. Since the optimal algorithm requires channel to be sensed in every time-slot, we propose a novel cross-layer forward algorithm based technique that updates the state belief using spectrum sensing result in the first time-slot and then using positive/negative acknowledgment (ACK/NAK) information of the previous time-slot (obtained from data link layer) in the rest of the frame. We study the throughput and collision performance results via simulation for different cases of primary user channel mixing rates and error occurrence both in sensing and in feedback.

Chapter 5 presents the channel and power allocation of an overlay cognitive radio system. In this chapter, we first propose an adaptive channel allocation algorithm for a two-hop decode-and-forward OFCDM based cognitive relay system and then its performance is formulated and numerically evaluated via Monte-Carlo simulation. The effect of considering the CSI of source-base station and source-cognitive relay links are evaluated in an overlay cognitive radio system. In addition to that, different power allocation schemes between the source and the cognitive relay nodes are analyzed and numerically evaluated for a two-hop decode-and-forward OFCDM based cognitive relay network.

The contributions of this dissertation is summarized in chapter 6. In addition, the future research directions relevant to the works in this thesis are discussed.

Chapter 2

Channel Access in Interweave Cognitive Radio System

Opportunistic communication over fading channels is a well studied subject where the adaptive radio resource allocation and multiuser selection in transmission often exploit the channel fading characteristics [24]. The limited frequency spectrum and under-utilization of the assigned spectrum triggered the need for opportunistic spectrum sharing [1] among users. The users who own the spectrum get higher access privilege, and the opportunistic users (also known as cognitive users) usually look for opportunistic channel access. In an interweave cognitive radio system, the unoccupied spectrum holes should be shared by cognitive users with minimal collision [2]. That is, an effective sensing scheme should be used to find the vacant channels in order to avoid collision. There are many spectrum sensing algorithms proposed in the literature with different techniques [25].

The objective of a channel access scheme is to maximize the long-term throughput of a cognitive user with minimal interference to the primary users. In [26], multi-channel opportunistic sensing was proposed where a cognitive user senses the channel before the

access and the cognitive user is limited to sense only one channel at a time. This problem is treated as partially observable Markov decision process for generally correlated channels and their proposed optimal access scheme is intractable and computationally complex. A simple myopic access scheme was proposed in [27, 28] and it was designed to maximize the throughput of each slot neglecting the impact on the future potential throughput. Hence, this myopic scheme was modeled as a static optimization problem rather than a sequential decision making process. It was not only simple and robust, but also proved to be optimal under the i.i.d. Gilbert-Elliot channel model [29]. It was proposed in [28] that a cognitive user senses the most probable idle channel in each slot, and if primary user's traffic is positively correlated, the cognitive user occupies that channel until it becomes busy, i.e., until the primary user starts to use that channel. In that work, the channel fading characteristic was not considered; hence, even if the cognitive user occupies a weak channel, it will stay with that channel until it becomes busy. There could be other channels with good channel gains that are potentially idle for use by cognitive users. This motivates us to investigate a new channel switching strategy in cognitive radio systems.

In this chapter, a channel switching scheme based on the primary user channel occupancy statistics as well as the cognitive user's received signal to noise ratio (SNR) is proposed, analyzed and verified for a cognitive radio system. Rather than staying in a channel when the cognitive user's received SNR goes below a threshold, a cognitive radio switches to the channel with the next highest idle probability to improve the throughput. Following the formulation of this channel switching problem, optimal switching thresholds that maximize the long term throughput of the cognitive radios are analytically found for different primary users' traffic characteristics using a Markov chain model. Our contributions in this chapter can be summarized as follows:

- Analytically evaluating the throughput performance of a cognitive user with channel switching for different traffic characteristics of primary users and the relative motion (Doppler spread) of cognitive users.

- Proposing an opportunistic channel switching algorithm and analytically obtaining the optimal channel switching threshold for an interweave cognitive radio system.

The rest of the chapter is organized as follows. Section 2.1 describes the system model under consideration. Section 2.2 analyzes the performance of the proposed interweave access scheme with two primary channels and a system with multiple primary channels is analyzed in Section 2.3. Finally, the chapter is summarized in Section 2.4.

2.1 Interweave System Model

We assume that there are many primary user channels, and one cognitive user pair tries to access an idle channel. Also, we assume that a cognitive user can sense/access only one channel during a time slot and occupies that channel if it is idle; otherwise, it waits for the next time slot. After each sensing, the cognitive user updates the belief vector (Π^O) of the primary user occupancy as given in (2.1). If the first slot is idle, then it will transmit in that slot and updates the belief vector (Π^H) of the cognitive user's received SNR. During the next time slot, if that current channel's primary user occupancy and cognitive user's SNR prediction are favorable, then the cognitive user will sense the same channel. Otherwise, based on the primary users occupancy prediction (Π^O), the cognitive user will switch the sensing to the most probable idle channel other than the current channel. The primary user's occupancy state prediction and received SNR state prediction models are explained in subsection 2.1.1 and subsection 2.1.2 respectively.

In this work, the initial analysis is done for a system that has two identical but independent primary channels and one cognitive user that tries to opportunistically occupy a primary user channel as shown in Fig. 2.1.

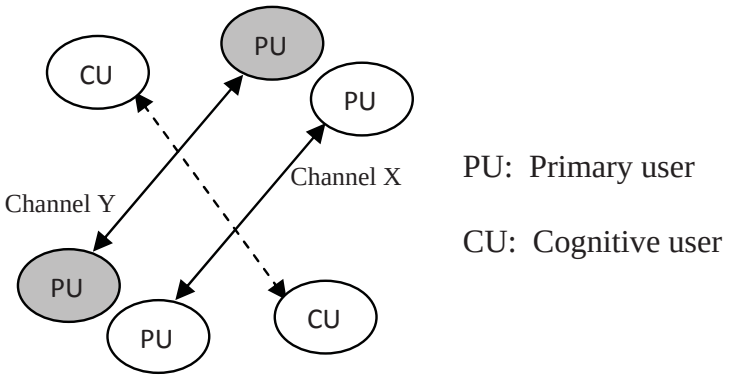

Figure 2.1: System model (2 primary user channels and 1 cognitive user pair).

2.1.1 Channel Occupancy State

We use a multi-channel cognitive radio system to develop our access scheme. There are N independent, stochastically identical slotted channels, each of which is modeled using a two state Markov chain [29] as in Fig. 2.2. The busy and idle state of the channel are denoted with *State B* and *State I* respectively. The transition probability of this Markov chain is denoted by $\{P_{qr}\}_{q,r=B,I}$. P_{II} denotes the probability that a channel becomes idle in the next time slot given that it is idle during the current slot. P_{BI} denotes the probability that a channel becomes idle given that the channel is currently busy; that is, the probability that a primary user leaves the channel during the next time slot after occupying the current slot. The idle probability of channel i (Π_i^O) is updated after each slot based on the sensing outcome [26]. That is,

$$\Pi_i^O(t+1) = \begin{cases} P_{II}, & \text{Case } \theta_1; \\ P_{BI}, & \text{Case } \theta_2; \\ \Pi_i^O(t)P_{II} + (1-\Pi_i^O(t))P_{BI}, & \text{Case } \theta_3, \end{cases} \tag{2.1}$$

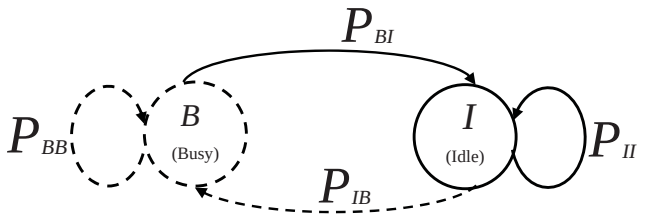

Figure 2.2: Markov channel model for occupancy of a primary user.

where Case θ_1 and Case θ_2 denote that at time t, the channel i is selected for sensing and it is idle (*State I*) and busy (*State B*) respectively. Case θ_3 denotes that at time t, the channel i is not selected for sensing. The cognitive user communicates opportunistically by using the idle channels of the primary users. The primary user channel state (busy or idle) predication is incorporated with our channel switching strategy. When $P_{II}>P_{BI}$, the probability of an idle channel (*State I*) during the current slot becoming idle in the following slot (P_{II}) is higher than that of a busy channel (*State B*) becoming idle (P_{BI}). Therefore, when a cognitive user senses a channel as idle and when $P_{II}>P_{BI}$, it is better to transmit during that slot and stay in that channel, since there is a higher probability that the channel will become idle during the next time slot. On the other hand, when $P_{BI}>P_{II}$, the probability of an idle channel during the current slot becoming idle in the following slot (P_{II}) is lower than that of a busy channel becoming idle (P_{BI}). Therefore, when a cognitive user senses a channel as idle and when $P_{BI}>P_{II}$, it is better to transmit during that slot and move out of that channel in the next slot, since there is a higher probability that the channel will become busy during the next time slot. The steady state probability if *State I* and *State B* can be written as $P_I = P_{BI}/(P_{BI} + P_{IB})$ and $P_B = 1 - P_I$ respectively.

2.1.2 Channel Gain State

In a rich multipath propagation environment, the instantaneous received signal amplitude is commonly modeled with the Rayleigh distribution. A slowly varying Rayleigh channel can be modeled as a finite state Markov channel [30] by partitioning the received SNR, which is proportional to the squared of the received signal amplitude, into a finite number of K non-overlapping states. As mentioned in [31], this first order Markov model accurately models the practical fading channel for packet/block level communication when the block length is sufficiently large. Let h be the normalized SNR at the receiver when the transmitter power is P_{power}. The pdf of h is exponentially distributed and can be written as (cf. [32]), where h_0 is the average received SNR.

$$p(h) = \frac{1}{h_0} e^{\left(-\frac{h}{h_0}\right)}, \quad \text{for } h \geq 0; \tag{2.2}$$

Let $H = \{H_l, H_h\}$ denote the state space of the finite state Markov channel. The Rayleigh

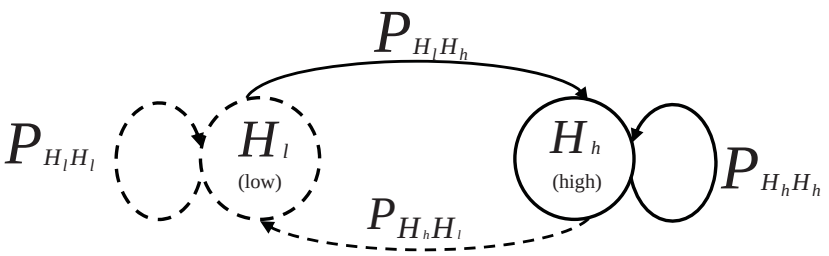

Figure 2.3: Two sate Markov channel model for gain state (SNR) of a cognitive user.

fading channel is said to be in state H_l and H_h when the received SNR is in the interval $[0, \Gamma)$ and $[\Gamma, \infty)$ respectively. Let P_{H_l} and P_{H_h}denote the steady state probabilities associated with states H_l and H_h respectively. Hence, $P_{H_l} = \int_0^{\Gamma} p(h)dh = 1 - \exp(-\frac{\Gamma}{h_0})$ and $P_{H_h} = \exp(-\frac{\Gamma}{h_0})$. We assume that the Rayleigh fading channel is slow enough so that the received SNR remains within the certain state for the duration of a block.

The transition probability, $P_{H_l H_h}$ from state H_l to state H_k is approximated by the ratio of the expected number of level crossings at the received SNR (Γ), and the average transmission rate in state H_l. Similarly, the transition probability, $P_{H_h H_l}$ from state H_h to state H_l is approximated by the ratio of the expected number of level crossings at the received SNR Γ and the average transmission rate in state H_h. Let the number of blocks per second of the block-fading channel be R_B, so the average number of blocks/second during which the channel is in state H_l is $R_B^l = P_{H_l} R_B$ [33]. Therefore, the crossover transition probabilities can be written as,

$$P_{H_l H_h} \approx \frac{N(\Gamma)}{R_B^l},$$

and similarly,

$$P_{H_h H_l} \approx \frac{N(\Gamma)}{R_B^h},$$

where $N(\Gamma)$ is the expected number of times per second the received SNR passes downward across the corresponding threshold Γ and is given by,

$$N(\Gamma) = \sqrt{\frac{2\pi\Gamma}{h_0}} f_m e^{\left(\frac{\Gamma}{h_0}\right)}.$$

In this expression, $f_m = v/\lambda$ is the maximum Doppler frequency, where v is the speed of the mobile terminal and λ is the wavelength of the radio wave. The transition probability of staying in the same state can be found as, $P_{H_l H_l} = 1 - P_{H_l H_h}$ and $P_{H_h H_h} = 1 - P_{H_h H_l}$. Average channel capacity (R_{H_h}) in state H_h (assuming unit bandwidth) can be calculated as follows:

$$R_{H_h} = \int_{\Gamma}^{\infty} \log_2(1+h) \frac{1}{h_0} e^{\frac{-h}{h_0}} dh,$$
$$R_{H_h} = \frac{1}{h_0 \ln(2)} \int_{\Gamma}^{\infty} \ln(1+h) e^{\frac{-h}{h_0}} dh,$$

by substituting $1 + h = \psi$,

$$
\begin{aligned}
R_{H_h} &= \frac{1}{h_0 \ln(2)} \int_{1+\Gamma}^{\infty} \ln(\psi) e^{\frac{-(\psi-1)}{h_0}} d\psi, \\
&= \frac{e^{h_0{}^{-1}}}{h_0 \ln(2)} \int_{1+\Gamma}^{\infty} \ln(\psi) e^{\frac{-\psi}{h_0}} d\psi, \\
&= \frac{e^{h_0{}^{-1}}}{h_0 \ln(2)} (-ho) \left(\left[e^{\frac{\psi}{-h_0}} \ln|\psi| \right]_{1+\Gamma}^{\infty} - \int_{1+\Gamma}^{\infty} \frac{e^{\frac{\psi}{-h_0}}}{\psi} d\psi \right), \\
&= \frac{e^{\frac{1}{h_0}}}{\ln(2)} \left[\frac{\ln(1+\Gamma)}{e^{\frac{1+\Gamma}{h_0}}} + E_1\left(\frac{1+\Gamma}{ho}\right) \right], \qquad (2.3)
\end{aligned}
$$

where $\mathrm{E}_1(x) = \int_1^{\infty} t^{-1} e^{-xt} dt$, $x \geq 0$. Similarly, R_{H_l} can be found.

The probability of a channel i being in state H_h (Π_i^H)is updated after each slot based on the sensing outcome. That is,

$$
\Pi_i^H(t+1) = \begin{cases} P_{H_h H_h}, & \text{Case } \chi_1; \\ P_{H_l H_h}, & \text{Case } \chi_2; \\ \Pi_i^H(t) P_{H_h H_h} + (1 - \Pi_i^H(t)) P_{H_l H_h}, & \text{Case } \chi_3, \end{cases} \qquad (2.4)
$$

where Case χ_1 and Case χ_2 denote that at time t, the channel i is selected for sensing and it is sensed as idle. During the transmission it is found that the channel is state H_h and H_l respectively. Case χ_3 denotes that at time t, the channel i is not selected for sensing or sensed as busy.

2.1.3 Channel Access Scheme

As mentioned earlier, our proposed access scheme incorporates prediction of the primary user occupancy state and SNR of the cognitive user. Therefore, even when the current channel has higher probability to become idle during the next time slot, if the cognitive user's predicted SNR is below a threshold (Γ), then the cognitive user switches the sensing

to the other channel to potentially improve the throughput in the proposed scheme. The cognitive user switches the channel for sensing due to the following two cases:

i) Case 1: The cognitive user's predicted SNR of the current channel for the next slot is lower than the threshold (Γ) or,

ii) Case 2: The cognitive user senses that the channel is busy (when $P_{II}>P_{BI}$) or idle (when $P_{BI}>P_{II}$) during the current slot.

The proposed channel access scheme is described as follows: (See Fig. 2.4 for corresponding flow chart):

---

1. Initially the idle probability for all the channels is set to their steady state probability ($P_{BI}/(P_{BI}+P_{IB})$), if not known.

2. Select the most (or second most, from step 4) probable idle channel ($\arg\max \Pi_i^O(t)$) and sense. Update the occupancy belief (2.1)

3. If it is available, occupy that channel (transmit and update the channel gain belief (2.4)) during that slot else go to step 2 and wait for the next slot.

4. During the transmission if the corresponding received SNR is above a specified threshold, go to step 2 and sense the most probable idle channel or else sense the second most probable idle channel.

We consider in the following sections that primary user's occupancy and cognitive user's received SNR are positively correlated. That is, $P_{II} > P_{BI}$ and $P_{H_hH_h} > P_{H_lH_h}$. In that case, the algorithm will be simplified as follows:

1. Sense the channel, if it is idle (*State I*) transmit during that slot and go to step 2 else switch[1] the channel and wait for the next slot to sense again (step 1)

2. During the transmission if the received SNR is in *State* H_h, stay in that channel and go to step 1 else switch the channel and go to step 1

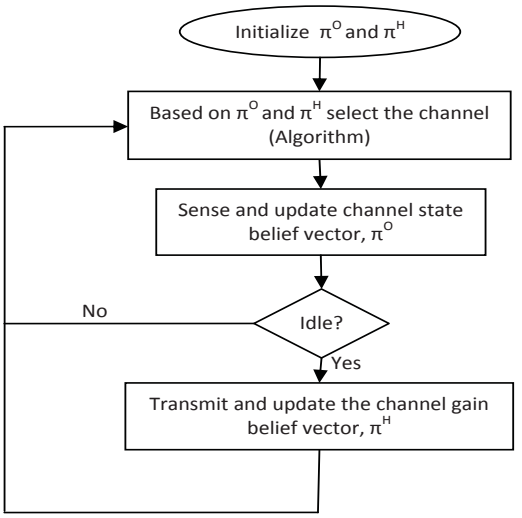

Figure 2.4: Flow chart: Channel access scheme in an interweave cognitive system

We assume that the cognitive user stays in a channel continuously for L (≥ 1) slots. The cognitive user's stay in a channel is modeled as in Fig. 2.5.

2.2 Two-Channel System

In this section, we analyze a cognitive radio system with two primary channels. As we mentioned in subsection 2.1.3, if the predicted SNR is low or the predicted occupancy state is busy, then cognitive user will switch the channel. We combine occupancy state transition (shown in Fig. 2.2) channel gain transition (shown in Fig. 2.3) into a four state model in

[1]round-robin scheme based on a circular ordering is proved to be optimal [28]

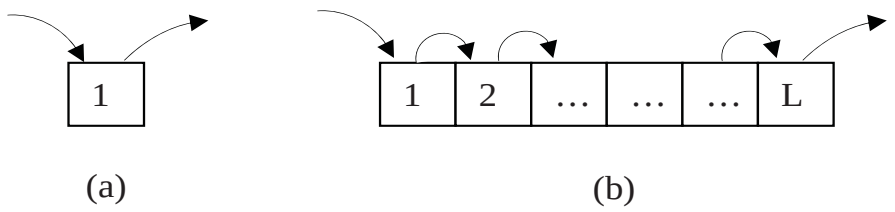

Figure 2.5: Sensing cycle: One cognitive user accesses the primary user channels when $P_{II} > P_{BI}$. Cognitive user switches the channel either due to, the current sensed channel is in busy state or the predicted SNR of the current channel for the next slot is lower than the specific threshold.

this chapter and assume these notations $P_{IB} = \alpha$, $P_{BI} = \beta$, $P_{H_h H_l} = \gamma$ and $P_{H_l H_h} = \delta$. The combined transition matrix can be defined using four states IH_h, IH_l, BH_h and BH_l and denoted by ξ_1, ξ_2, ξ_3 and ξ_4 respectively. The combined transition matrix T_C can be defined as,

$$T_C = \begin{array}{c} \\ \xi_1 \rightarrow \\ \xi_2 \rightarrow \\ \xi_3 \rightarrow \\ \xi_4 \rightarrow \end{array} \begin{array}{c} \begin{array}{cccc} \xi_1(IH_h) & \xi_2(IH_l) & \xi_3(BH_h) & \xi_4(BH_l) \end{array} \\ \begin{pmatrix} (1-\alpha)(1-\gamma) & (1-\alpha)\gamma & \alpha(1-\gamma) & \alpha\gamma \\ (1-\alpha)\delta & (1-\alpha)(1-\delta) & \alpha\delta & \alpha(1-\delta) \\ \beta(1-\gamma) & \beta\gamma & (1-\beta)(1-\gamma) & (1-\beta)\gamma \\ \beta\delta & \beta(1-\delta) & (1-\beta)\delta & (1-\beta)(1-\delta) \end{pmatrix} \end{array}. \quad (2.5)$$

A cognitive user may leave a channel if, either the occupancy state of the channel is busy (ξ_3) or the predicted SNR during the next slot is low (ξ_2) or both (ξ_4). If the channel is in state ξ_1, cognitive user may stay in that channel. For the analysis purpose, we model the problem into nine different states based on the last state of the current channel and previous channel as in Table 2.1. Based on the state classification, the state transitions possibilities can be derived as in (2.6).

State	State of the last slot of the previous channel	State of the last slot of the current channel
S_1	ξ_2	ξ_2
S_2	ξ_2	ξ_4
S_3	ξ_2	ξ_3
S_4	ξ_4	ξ_2
S_5	ξ_4	ξ_4
S_6	ξ_4	ξ_3
S_7	ξ_3	ξ_2
S_8	ξ_3	ξ_4
S_9	ξ_3	ξ_3

Table 2.1: State classification for analysis purpose

$$T = \begin{array}{c} \\ S_1 \\ S_2 \\ S_3 \\ S_4 \\ S_5 \\ S_6 \\ S_7 \\ S_8 \\ S_9 \end{array} \begin{array}{c} \begin{array}{ccccccccc} S_1 & S_2 & S_3 & S_4 & S_5 & S_6 & S_7 & S_8 & S_9 \end{array} \\ \begin{pmatrix} * & * & * & - & - & - & - & - & - \\ - & - & - & * & * & * & - & - & - \\ - & - & - & - & - & - & * & * & * \\ * & * & * & - & - & - & - & - & - \\ - & - & - & * & * & * & - & - & - \\ - & - & - & - & - & - & * & * & * \\ * & * & * & - & - & - & - & - & - \\ - & - & - & * & * & * & - & - & - \\ - & - & - & - & - & - & * & * & * \end{pmatrix} \end{array}. \tag{2.6}$$

We do the analysis based on the above nine states. Each of these nine states can be divided

into more than one state depending on the number of slots that the cognitive user stays in a channel continuously. S_K^L denotes that cognitive users stay for L slots (L=1,2,3...) continuously in a channel in state S_K (K=1,2,3,..,9.). Fig. 2.6 shows the channel switching between two channels and its state transitions. For example, consider the following scenario. At time t=3, a cognitive user switches the channel from Channel B to Channel A, as Channel B was in State ξ_3. It again switches back to Channel B as it finds the state of the Channel A as ξ_4. We consider this one slot stay (at t=4) of the cognitive user in Channel A. The state of the last slot of the current channel (Channel A, t=4) is ξ_4 and previous channel (Channel B, t=3) is ξ_3, from Table 2.1. Then, we can decide the state of that stay as S_8. Further, as the cognitive user stayed for only one slot, that stay is denoted by S_8^1. Similarly, if we consider the three slots stay in Channel B (t=10 to t=12), cognitive user is leaving the channel B during the current visit at t=12 as it is in State ξ_2 and cognitive user left previous channel (Channel A, t=9) as it was in State ξ_3, then that stay is denoted by S_7^3.

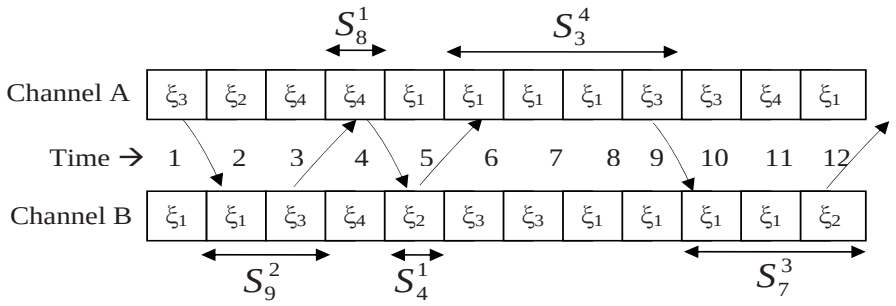

Figure 2.6: One cognitive user accesses two primary user channels.

$T_{S_{K_1}^n S_{K_2}^m}$ denotes the transition probability of a cognitive user that stays in State S_{K_1} for n slots continuously and then moves to State S_{K_2} and stays for m slots before leaving that channel. In Fig. 2.6, cognitive user moves from Channel A to Channel B at t=4 with transition probability $T_{S_8^1 S_4^1}$. As the previous channel's (Channel A, t=4) state is S_8^1, we can say that the state of the last slot during the last visit of the Channel B should be ξ_3 (t=3)

from Table 2.1. Similarly, as the current state is S_4^1, we can say that cognitive user leaves the channel after staying for one slot and the state of that channel is ξ_3 (Channel B, t=5) from Table 2.1. As the cognitive user stayed only one slot in the Channel A (S_8^1) during the last channel switch, the transition probability can be written as $T^{(2)}_{\xi_3\xi_2}$. That is, $T^{(2)}_{\xi_3\xi_2}$ denotes the transition probability from State ξ_3 to State ξ_2 after two slots and it can be found from (2.5). Similarly, at t=5, the cognitive user switches from State S_4^1 to S_9^4. That implies, the cognitive user left the Channel A in the previous visit when the last slot was ξ_4 and stayed one slot in Channel B, then switched back to Channel A and stays for four slots and leave the channel as it is in State ξ_3. We split the transition probability calculation into three parts as $T_{t=4\to t=6} = T^{(2)}_{\xi_4\xi_1}$, $T_{t=6\to t=8} = (T_{\xi_1\xi_1})^2$ and $T_{t=8\to t=9} = T_{\xi_1\xi_2}$. Hence, the transition probability can be written as $T_{S_3^4 S_7^3} = T^{(2)}_{\xi_4\xi_1}(T_{\xi_1\xi_1})^2 T_{\xi_1\xi_2}$

Similarly, we can find the other transition probabilities that are listed below.

$$
\begin{aligned}
T_{S_1^n S_1^1} = T_{S_2^n S_4^1} = T_{S_3^n S_7^1} &= T^{(n+1)}_{\xi_2\xi_2}, \\
T_{S_1^n S_2^1} = T_{S_2^n S_5^1} = T_{S_3^n S_8^1} &= T^{(n+1)}_{\xi_2\xi_4}, \\
T_{S_1^n S_3^1} = T_{S_2^n S_6^1} = T_{S_3^n S_9^1} &= T^{(n+1)}_{\xi_2\xi_3}, \\
T_{S_1^n S_1^m} = T_{S_2^n S_4^m} = T_{S_3^n S_7^m} &= T^{(n+1)}_{\xi_2\xi_1}(T_{\xi_1\xi_1})^{m-2} T_{\xi_1\xi_2}, \\
T_{S_1^n S_2^m} = T_{S_2^n S_5^m} = T_{S_3^n S_8^m} &= T^{(n+1)}_{\xi_2\xi_1}(T_{\xi_1\xi_1})^{m-2} T_{\xi_1\xi_4}, \\
T_{S_1^n S_3^m} = T_{S_2^n S_6^m} = T_{S_3^n S_9^m} &= T^{(n+1)}_{\xi_2\xi_1}(T_{\xi_1\xi_1})^{m-2} T_{\xi_1\xi_3}, \\
T_{S_4^n S_1^1} = T_{S_5^n S_4^1} = T_{S_6^n S_7^1} &= T^{(n+1)}_{\xi_3\xi_2}, \\
T_{S_4^n S_2^1} = T_{S_5^n S_5^1} = T_{S_6^n S_8^1} &= T^{(n+1)}_{\xi_3\xi_4}, \\
T_{S_4^n S_3^1} = T_{S_5^n S_6^1} = T_{S_6^n S_9^1} &= T^{(n+1)}_{\xi_3\xi_3}, \\
T_{S_4^n S_1^m} = T_{S_5^n S_4^m} = T_{S_6^n S_7^m} &= T^{(n+1)}_{\xi_3\xi_1}(T_{\xi_1\xi_1})^{m-2} T_{\xi_1\xi_2}, \\
T_{S_4^n S_2^m} = T_{S_5^n S_5^m} = T_{S_6^n S_8^m} &= T^{(n+1)}_{\xi_3\xi_1}(T_{\xi_1\xi_1})^{m-2} T_{\xi_1\xi_4},
\end{aligned}
$$

$$
\begin{aligned}
T_{S_4^n S_3^m} = T_{S_5^n S_6^m} = T_{S_6^n S_9^m} &= T^{(n+1)}_{\xi_3\xi_1}(T_{\xi_1\xi_1})^{m-2}T_{\xi_1\xi_3}, \\
T_{S_7^n S_1^1} = T_{S_8^n S_4^1} = T_{S_9^n S_7^1} &= T^{(n+1)}_{\xi_4\xi_2}, \\
T_{S_7^n S_2^1} = T_{S_8^n S_5^1} = T_{S_9^n S_8^1} &= T^{(n+1)}_{\xi_4\xi_4}, \\
T_{S_7^n S_3^1} = T_{S_8^n S_6^1} = T_{S_9^n S_9^1} &= T^{(n+1)}_{\xi_4\xi_3}, \\
T_{S_7^n S_1^m} = T_{S_8^n S_4^m} = T_{S_9^n S_7^m} &= T^{(n+1)}_{\xi_4\xi_1}(T_{\xi_1\xi_1})^{m-2}T_{\xi_1\xi_2}, \\
T_{S_7^n S_2^m} = T_{S_8^n S_5^m} = T_{S_9^n S_8^m} &= T^{(n+1)}_{\xi_4\xi_1}(T_{\xi_1\xi_1})^{m-2}T_{\xi_1\xi_4}, \\
T_{S_7^n S_3^m} = T_{S_8^n S_6^m} = T_{S_9^n S_9^m} &= T^{(n+1)}_{\xi_4\xi_1}(T_{\xi_1\xi_1})^{m-2}T_{\xi_1\xi_3}.
\end{aligned}
$$

2.2.1 Steady State Analysis

In this section, we show the steady state analysis and throughput evaluation of the considered system. If we consider the State $P_{S_1^2}$, we can write the steady state equation as,

$$
\begin{aligned}
P_{S_1^2} &= P_{S_1^1}T_{S_1^1S_1^2} + P_{S_4^1}T_{S_4^1S_1^2} + P_{S_7^1}T_{S_7^1S_1^2} \\
&+ P_{S_1^2}T_{S_1^2S_1^2} + P_{S_1^3}T_{S_1^3S_1^2} + P_{S_1^4}T_{S_1^4S_1^2}..... \\
&+ P_{S_4^2}T_{S_4^2S_1^2} + P_{S_4^3}T_{S_4^3S_1^2} + P_{S_4^4}T_{S_4^4S_1^2}..... \\
&+ P_{S_7^2}T_{S_7^2S_1^2} + P_{S_7^3}T_{S_7^3S_1^2} + P_{S_7^4}T_{S_7^4S_1^2}.....
\end{aligned}
$$

From the transition probabilities found in Section 2.2, we can re-write it as follows:

$$
\begin{aligned}
P_{S_1^2} &= P_{S_1^1}T^{(2)}_{\xi_2\xi_1}T_{\xi_1\xi_2} + P_{S_4^1}T^{(2)}_{\xi_3\xi_1}T_{\xi_1\xi_2} + P_{S_7^1}T^{(2)}_{\xi_4\xi_1}T_{\xi_1\xi_2} \\
&+ P_{S_1^2}T^{(3)}_{\xi_2\xi_1}T_{\xi_1\xi_2} + P_{S_1^3}T^{(4)}_{\xi_2\xi_1}T_{\xi_1\xi_2} + P_{S_1^4}T^{(5)}_{\xi_2\xi_1}T_{\xi_1\xi_2}..... \\
&+ P_{S_4^2}T^{(3)}_{\xi_3\xi_1}T_{\xi_1\xi_2} + P_{S_4^3}T^{(4)}_{\xi_3\xi_1}T_{\xi_1\xi_2}..... \\
&+ P_{S_7^2}T^{(3)}_{\xi_4\xi_1}T_{\xi_1\xi_2} + P_{S_7^3}T^{(4)}_{\xi_4\xi_1}T_{\xi_1\xi_2}.....
\end{aligned} \tag{2.7}
$$

Similarly, if we write the steady state equations for states $P_{S_K^i}$ ($i = 2, 3, ..$and $K = 1, 2, ..., 9.$), we can find the relationship as:

$$P_{S_K^i} = (T_{\xi_1\xi_1})^{i-2} P_{S_K^2}. \tag{2.8}$$

From (2.7) and (2.8) we get,

$$\begin{aligned}
P_{S_1^2} &= P_{S_1^1} T^{(2)}_{\xi_2\xi_1} T_{\xi_1\xi_2} + P_{S_4^1} T^{(2)}_{\xi_3\xi_1} T_{\xi_1\xi_2} + P_{S_7^1} T^{(2)}_{\xi_4\xi_1} T_{\xi_1\xi_2} \\
&+ P_{S_1^2}(T^{(3)}_{\xi_2\xi_1} + (T_{\xi_1\xi_1}) T^{(4)}_{\xi_2\xi_1} + (T_{\xi_1\xi_1})^2 T^{(5)}_{\xi_2\xi_1} .....) T_{\xi_1\xi_2} \\
&+ P_{S_4^2}(T^{(3)}_{\xi_3\xi_1} + (T_{\xi_1\xi_1}) T^{(4)}_{\xi_3\xi_1} .....) T_{\xi_1\xi_2} \\
&+ P_{S_7^2}(T^{(3)}_{\xi_4\xi_1} + (T_{\xi_1\xi_1}) T^{(4)}_{\xi_4\xi_1} .....) T_{\xi_1\xi_2}
\end{aligned}$$

$$\begin{aligned}
P_{S_1^2} &= P_{S_1^1} T^{(2)}_{\xi_2\xi_1} T_{\xi_1\xi_2} + P_{S_4^1} T^{(2)}_{\xi_3\xi_1} T_{\xi_1\xi_2} + P_{S_7^1} T^{(2)}_{\xi_4\xi_1} T_{\xi_1\xi_2} \\
&+ \left(P_{S_1^2} \sum_{i=2}^{\infty} (T_{\xi_1\xi_1})^{i-2} T^{(i+1)}_{\xi_2\xi_1} + P_{S_4^2} \sum_{i=2}^{\infty} (T_{\xi_1\xi_1})^{i-2} T^{(i+1)}_{\xi_3\xi_1} + P_{S_7^2} \sum_{i=2}^{\infty} (T_{\xi_1\xi_1})^{i-2} T^{(i+1)}_{\xi_4\xi_1} \right) T_{\xi_1\xi_2}.
\end{aligned} \tag{2.9}$$

Similarly, for other states with two slot stay, we can write the steady state equations as follows:

$$\begin{aligned}
P_{S_2^2} &= P_{S_1^1} T^{(2)}_{\xi_2\xi_1} T_{\xi_1\xi_4} + P_{S_4^1} T^{(2)}_{\xi_3\xi_1} T_{\xi_1\xi_4} + P_{S_7^1} T^{(2)}_{\xi_4\xi_1} T_{\xi_1\xi_4} \\
&+ \left(P_{S_1^2} \sum_{i=2}^{\infty} (T_{\xi_1\xi_1})^{i-2} T^{(i+1)}_{\xi_2\xi_1} + P_{S_4^2} \sum_{i=2}^{\infty} (T_{\xi_1\xi_1})^{i-2} T^{(i+1)}_{\xi_3\xi_1} + P_{S_7^2} \sum_{i=2}^{\infty} (T_{\xi_1\xi_1})^{i-2} T^{(i+1)}_{\xi_4\xi_1} \right) T_{\xi_1\xi_4},
\end{aligned} \tag{2.10}$$

$$\begin{aligned}
P_{S_3^2} &= P_{S_1^1} T^{(2)}_{\xi_2\xi_1} T_{\xi_1\xi_3} + P_{S_4^1} T^{(2)}_{\xi_3\xi_1} T_{\xi_1\xi_3} + P_{S_7^1} T^{(2)}_{\xi_4\xi_3} T_{\xi_1\xi_3} \\
&+ \left(P_{S_1^2} \sum_{i=2}^{\infty} (T_{\xi_1\xi_1})^{i-2} T^{(i+1)}_{\xi_2\xi_1} + P_{S_4^2} \sum_{i=2}^{\infty} (T_{\xi_1\xi_1})^{i-2} T^{(i+1)}_{\xi_3\xi_1} + P_{S_7^2} \sum_{i=2}^{\infty} (T_{\xi_1\xi_1})^{i-2} T^{(i+1)}_{\xi_4\xi_1} \right) T_{\xi_1\xi_3},
\end{aligned} \tag{2.11}$$

$$\begin{aligned}
P_{S_4^2} &= P_{S_3^1} T^{(2)}_{\xi_2\xi_1} T_{\xi_1\xi_2} + P_{S_6^1} T^{(2)}_{\xi_3\xi_1} T_{\xi_1\xi_2} + P_{S_9^1} T^{(2)}_{\xi_4\xi_1} T_{\xi_1\xi_2} \\
&+ \left(P_{S_3^2} \sum_{i=2}^{\infty} (T_{\xi_1\xi_1})^{i-2} T^{(i+1)}_{\xi_2\xi_1} + P_{S_6^2} \sum_{i=2}^{\infty} (T_{\xi_1\xi_1})^{i-2} T^{(i+1)}_{\xi_3\xi_1} + P_{S_9^2} \sum_{i=2}^{\infty} (T_{\xi_1\xi_1})^{i-2} T^{(i+1)}_{\xi_4\xi_1} \right) T_{\xi_1\xi_2},
\end{aligned} \tag{2.12}$$

$$\begin{aligned}
P_{S_5^2} &= P_{S_3^1} T^{(2)}_{\xi_2\xi_1} T_{\xi_1\xi_4} + P_{S_6^1} T^{(2)}_{\xi_3\xi_1} T_{\xi_1\xi_4} + P_{S_9^1} T^{(2)}_{\xi_4\xi_1} T_{\xi_1\xi_4} \\
&+ \left(P_{S_3^2} \sum_{i=2}^{\infty} (T_{\xi_1\xi_1})^{i-2} T^{(i+1)}_{\xi_2\xi_1} + P_{S_6^2} \sum_{i=2}^{\infty} (T_{\xi_1\xi_1})^{i-2} T^{(i+1)}_{\xi_3\xi_1} + P_{S_9^2} \sum_{i=2}^{\infty} (T_{\xi_1\xi_1})^{i-2} T^{(i+1)}_{\xi_4\xi_1} \right) T_{\xi_1\xi_4},
\end{aligned} \tag{2.13}$$

$$
\begin{aligned}
P_{S_6^2} &= P_{S_3^1} T^{(2)}_{\xi_2\xi_1} T_{\xi_1\xi_3} + P_{S_6^1} T^{(2)}_{\xi_3\xi_1} T_{\xi_1\xi_3} + P_{S_9^1} T^{(2)}_{\xi_4\xi_3} T_{\xi_1\xi_3} \qquad (2.14)\\
&+ \left(P_{S_3^2} \sum_{i=2}^{\infty} (T_{\xi_1\xi_1})^{i-2} T^{(i+1)}_{\xi_2\xi_1} + P_{S_6^2} \sum_{i=2}^{\infty} (T_{\xi_1\xi_1})^{i-2} T^{(i+1)}_{\xi_3\xi_1} + P_{S_9^2} \sum_{i=2}^{\infty} (T_{\xi_1\xi_1})^{i-2} T^{(i+1)}_{\xi_4\xi_1} \right) T_{\xi_1\xi_3},\\
P_{S_7^2} &= P_{S_2^1} T^{(2)}_{\xi_2\xi_1} T_{\xi_1\xi_2} + P_{S_5^1} T^{(2)}_{\xi_3\xi_1} T_{\xi_1\xi_2} + P_{S_8^1} T^{(2)}_{\xi_4\xi_1} T_{\xi_1\xi_2} \qquad (2.15)\\
&+ \left(P_{S_2^2} \sum_{i=2}^{\infty} (T_{\xi_1\xi_1})^{i-2} T^{(i+1)}_{\xi_2\xi_1} + P_{S_5^2} \sum_{i=2}^{\infty} (T_{\xi_1\xi_1})^{i-2} T^{(i+1)}_{\xi_3\xi_1} + P_{S_8^2} \sum_{i=2}^{\infty} (T_{\xi_1\xi_1})^{i-2} T^{(i+1)}_{\xi_4\xi_1} \right) T_{\xi_1\xi_2},\\
P_{S_8^2} &= P_{S_2^1} T^{(2)}_{\xi_2\xi_1} T_{\xi_1\xi_4} + P_{S_5^1} T^{(2)}_{\xi_3\xi_1} T_{\xi_1\xi_4} + P_{S_8^1} T^{(2)}_{\xi_4\xi_1} T_{\xi_1\xi_4} \qquad (2.16)\\
&+ \left(P_{S_2^2} \sum_{i=2}^{\infty} (T_{\xi_1\xi_1})^{i-2} T^{(i+1)}_{\xi_2\xi_1} + P_{S_5^2} \sum_{i=2}^{\infty} (T_{\xi_1\xi_1})^{i-2} T^{(i+1)}_{\xi_3\xi_1} + P_{S_8^2} \sum_{i=2}^{\infty} (T_{\xi_1\xi_1})^{i-2} T^{(i+1)}_{\xi_4\xi_1} \right) T_{\xi_1\xi_4},\\
P_{S_9^2} &= P_{S_2^1} T^{(2)}_{\xi_2\xi_1} T_{\xi_1\xi_3} + P_{S_5^1} T^{(2)}_{\xi_3\xi_1} T_{\xi_1\xi_3} + P_{S_8^1} T^{(2)}_{\xi_4\xi_3} T_{\xi_1\xi_3} \qquad (2.17)\\
&+ \left(P_{S_2^2} \sum_{i=2}^{\infty} (T_{\xi_1\xi_1})^{i-2} T^{(i+1)}_{\xi_2\xi_1} + P_{S_5^2} \sum_{i=2}^{\infty} (T_{\xi_1\xi_1})^{i-2} T^{(i+1)}_{\xi_3\xi_1} + P_{S_8^2} \sum_{i=2}^{\infty} (T_{\xi_1\xi_1})^{i-2} T^{(i+1)}_{\xi_4\xi_1} \right) T_{\xi_1\xi_3}.
\end{aligned}
$$

If we consider the one slot stay, we can write the steady state equations as follows:

$$
\begin{aligned}
P_{S_1^1} &= P_{S_1^1} T^{(2)}_{\xi_2\xi_2} + P_{S_4^1} T^{(2)}_{\xi_3\xi_2} + P_{S_7^1} T^{(2)}_{\xi_4\xi_2} \qquad (2.18)\\
&+ \left(P_{S_1^2} \sum_{i=2}^{\infty} (T_{\xi_1\xi_1})^{i-2} T^{(i+1)}_{\xi_2\xi_2} + P_{S_4^2} \sum_{i=2}^{\infty} (T_{\xi_1\xi_1})^{i-2} T^{(i+1)}_{\xi_3\xi_2} + P_{S_7^2} \sum_{i=2}^{\infty} (T_{\xi_1\xi_1})^{i-2} T^{(i+1)}_{\xi_4\xi_2} \right),\\
P_{S_2^1} &= P_{S_1^1} T^{(2)}_{\xi_2\xi_4} + P_{S_4^1} T^{(2)}_{\xi_3\xi_4} + P_{S_7^1} T^{(2)}_{\xi_4\xi_4} \qquad (2.19)\\
&+ \left(P_{S_1^2} \sum_{i=2}^{\infty} (T_{\xi_1\xi_1})^{i-2} T^{(i+1)}_{\xi_2\xi_4} + P_{S_4^2} \sum_{i=2}^{\infty} (T_{\xi_1\xi_1})^{i-2} T^{(i+1)}_{\xi_3\xi_4} + P_{S_7^2} \sum_{i=2}^{\infty} (T_{\xi_1\xi_1})^{i-2} T^{(i+1)}_{\xi_4\xi_4} \right),\\
P_{S_3^1} &= P_{S_1^1} T^{(2)}_{\xi_2\xi_3} + P_{S_4^1} T^{(2)}_{\xi_3\xi_3} + P_{S_7^1} T^{(2)}_{\xi_4\xi_3} \qquad (2.20)\\
&+ \left(P_{S_1^2} \sum_{i=2}^{\infty} (T_{\xi_1\xi_1})^{i-2} T^{(i+1)}_{\xi_2\xi_3} + P_{S_4^2} \sum_{i=2}^{\infty} (T_{\xi_1\xi_1})^{i-2} T^{(i+1)}_{\xi_3\xi_3} + P_{S_7^2} \sum_{i=2}^{\infty} (T_{\xi_1\xi_1})^{i-2} T^{(i+1)}_{\xi_4\xi_3} \right),\\
P_{S_4^1} &= P_{S_3^1} T^{(2)}_{\xi_2\xi_2} + P_{S_6^1} T^{(2)}_{\xi_3\xi_2} + P_{S_9^1} T^{(2)}_{\xi_4\xi_2} \qquad (2.21)\\
&+ \left(P_{S_3^2} \sum_{i=2}^{\infty} (T_{\xi_1\xi_1})^{i-2} T^{(i+1)}_{\xi_2\xi_2} + P_{S_6^2} \sum_{i=2}^{\infty} (T_{\xi_1\xi_1})^{i-2} T^{(i+1)}_{\xi_3\xi_2} + P_{S_9^2} \sum_{i=2}^{\infty} (T_{\xi_1\xi_1})^{i-2} T^{(i+1)}_{\xi_4\xi_2} \right),\\
P_{S_5^1} &= P_{S_3^1} T^{(2)}_{\xi_2\xi_4} + P_{S_6^1} T^{(2)}_{\xi_3\xi_4} + P_{S_9^1} T^{(2)}_{\xi_4\xi_4} \qquad (2.22)\\
&+ \left(P_{S_3^2} \sum_{i=2}^{\infty} (T_{\xi_1\xi_1})^{i-2} T^{(i+1)}_{\xi_2\xi_4} + P_{S_6^2} \sum_{i=2}^{\infty} (T_{\xi_1\xi_1})^{i-2} T^{(i+1)}_{\xi_3\xi_4} + P_{S_9^2} \sum_{i=2}^{\infty} (T_{\xi_1\xi_1})^{i-2} T^{(i+1)}_{\xi_4\xi_4} \right),\\
P_{S_6^1} &= P_{S_3^1} T^{(2)}_{\xi_2\xi_3} + P_{S_6^1} T^{(2)}_{\xi_3\xi_3} + P_{S_9^1} T^{(2)}_{\xi_4\xi_3} \qquad (2.23)\\
&+ \left(P_{S_3^2} \sum_{i=2}^{\infty} (T_{\xi_1\xi_1})^{i-2} T^{(i+1)}_{\xi_2\xi_3} + P_{S_6^2} \sum_{i=2}^{\infty} (T_{\xi_1\xi_1})^{i-2} T^{(i+1)}_{\xi_3\xi_3} + P_{S_9^2} \sum_{i=2}^{\infty} (T_{\xi_1\xi_1})^{i-2} T^{(i+1)}_{\xi_4\xi_3} \right),
\end{aligned}
$$

$$
\begin{aligned}
P_{S_7^1} &= P_{S_2^1} T^{(2)}_{\xi_2\xi_2} + P_{S_5^1} T^{(2)}_{\xi_3\xi_2} + P_{S_8^1} T^{(2)}_{\xi_4\xi_2} \qquad (2.24)\\
&+ \left(P_{S_2^2} \sum_{i=2}^{\infty} (T_{\xi_1\xi_1})^{i-2} T^{(i+1)}_{\xi_2\xi_2} + P_{S_5^2} \sum_{i=2}^{\infty} (T_{\xi_1\xi_1})^{i-2} T^{(i+1)}_{\xi_3\xi_2} + P_{S_8^2} \sum_{i=2}^{\infty} (T_{\xi_1\xi_1})^{i-2} T^{(i+1)}_{\xi_4\xi_2} \right),\\
P_{S_8^1} &= P_{S_2^1} T^{(2)}_{\xi_2\xi_4} + P_{S_5^1} T^{(2)}_{\xi_3\xi_4} + P_{S_8^1} T^{(2)}_{\xi_4\xi_4} \qquad (2.25)\\
&+ \left(P_{S_2^2} \sum_{i=2}^{\infty} (T_{\xi_1\xi_1})^{i-2} T^{(i+1)}_{\xi_2\xi_4} + P_{S_5^2} \sum_{i=2}^{\infty} (T_{\xi_1\xi_1})^{i-2} T^{(i+1)}_{\xi_3\xi_4} + P_{S_8^2} \sum_{i=2}^{\infty} (T_{\xi_1\xi_1})^{i-2} T^{(i+1)}_{\xi_4\xi_4} \right),\\
P_{S_9^1} &= P_{S_2^1} T^{(2)}_{\xi_2\xi_3} + P_{S_5^1} T^{(2)}_{\xi_3\xi_3} + P_{S_8^1} T^{(2)}_{\xi_4\xi_3} \qquad (2.26)\\
&+ \left(P_{S_2^2} \sum_{i=2}^{\infty} (T_{\xi_1\xi_1})^{i-2} T^{(i+1)}_{\xi_2\xi_3} + P_{S_5^2} \sum_{i=2}^{\infty} (T_{\xi_1\xi_1})^{i-2} T^{(i+1)}_{\xi_3\xi_3} + P_{S_8^2} \sum_{i=2}^{\infty} (T_{\xi_1\xi_1})^{i-2} T^{(i+1)}_{\xi_4\xi_3} \right).
\end{aligned}
$$

Further, we can write

$$
\begin{aligned}
\sum_{K=1}^{9} \sum_{i=1}^{\infty} P_{S_K^i} &= 1,\\
\sum_{K=1}^{9} \left(P_{S_K^i} + \sum_{i=2}^{\infty} P_{S_K^i} \right) &= 1. \qquad (2.27)
\end{aligned}
$$

From (2.8) and (2.27),

$$
\begin{aligned}
\sum_{K=1}^{9} \left(P_{S_K^1} + P_{S_K^2} \sum_{i=2}^{\infty} (T_{\xi_1\xi_1})^{i-2} \right) &= 1,\\
\sum_{K=1}^{9} \left(P_{S_K^1} + \frac{P_{S_K^2}}{(T_{\xi_1\xi_1})^{i-2}} \right) &= 1. \qquad (2.28)
\end{aligned}
$$

The series sum in (2.9)-(2.26) can be calculated using eigenvalue decomposition. The square matrix T_C defined in (2.5) can be written as,

$$T_C = VDV^{-1},$$

where D and V denote a diagonal matrix of eigenvalues and a full matrix whose columns are the corresponding eigenvectors of matrix T_C respectively. The diagonal elements of the matrix D can be denoted by λ_1, λ_2, λ_3 and λ_4. Using the above properties, $T^{(i+1)}_{\xi_1\xi_3}$, for any positive integer i, can be calculated as $T^{(i+1)}_{\xi_1\xi_3} = (VD^{i+1}V^{-1})_{(1,3)}$. The infinite series sum can be found as shown below,

$$\sum_{i=2}^{\infty} (T_{\xi_1\xi_3})^{i-2} T^{(i+1)}_{\xi_1\xi_1} = (V\bar{D}V^{-1})_{(1,3)},$$

where

$$\bar{D} = \begin{pmatrix} \frac{(\lambda_1)^3}{1-T_{\xi_1\xi_1}\lambda_1} & 0 & 0 & 0 \\ 0 & \frac{(\lambda_2)^3}{1-T_{\xi_1\xi_1}\lambda_2} & 0 & 0 \\ 0 & 0 & \frac{(\lambda_3)^3}{1-T_{\xi_1\xi_1}\lambda_3} & 0 \\ 0 & 0 & 0 & \frac{(\lambda_4)^3}{1-T_{\xi_1\xi_1}\lambda_4} \end{pmatrix}.$$

Similarly, we can find the other infinite series sum. Solving the linear equations (2.9)-(2.26) and (2.28), we can find the steady state probabilities of all the states. The average continuous stay in a channel can be found as follows:

$$\begin{aligned} \bar{L} &= \sum_{K=1}^{9} \left(P_{S_K^1} + \sum_{i=2}^{\infty} i \times P_{S_K^i} \right), \qquad (2.29) \\ &= \sum_{K=1}^{9} \left(P_{S_K^1} + P_{S_K^2} \sum_{i=2}^{\infty} i \times (T_{\xi_1\xi_1})^{i-2} \right), \\ &= \sum_{K=1}^{9} \left(P_{S_K^1} + P_{S_K^2} \frac{2 - T_{\xi_1\xi_1}}{(1 - T_{\xi_1\xi_1})^2} \right). \end{aligned}$$

The cognitive user switches a channel in the states S_1, S_4 and S_7 only because of the predicted SNR is low even though the channel is idle (ξ_2). Therefore, a cognitive user may transmit during that last slot and leave that channel. On the other hand, cognitive user leaves the other states as the primary channel is busy. Hence, cognitive user will not transmit during the last of those six states. The last slot throughput can be written as,

$$\begin{aligned} C_1 &= R_{H_l} \sum_{i=1}^{\infty} (S_1^i + S_4^i + S_7^i), \\ &= R_{H_l} \left(S_1^1 + S_4^1 + S_7^1 + \frac{S_1^2 + S_4^2 + S_7^2}{1 - T_{\xi_1\xi_1}} \right), \end{aligned}$$

and during the other slots, gain state of the channel would be higher. Hence, throughput (for $L > 2$) can be written as,

$$
\begin{aligned}
C_2 &= R_{H_h} \sum_{K=1}^{9} \sum_{i=2}^{\infty} ((i-1) S_K^i), \\
&= R_{H_h} \sum_{K=1}^{9} \left(\frac{S_K^2}{(1 - T_{\xi_1 \xi_1})^2} \right).
\end{aligned}
$$

The average throughput can be written as,

$$
\bar{C} = \frac{C_1 + C_2}{\bar{L}}.
$$

2.2.2 Analytical Results and Discussion

In this section we discuss the results of the cognitive radio system with two primary channels. In Fig. 2.7, we verify the accuracy of the analytical results using Monte Carlo simulations for a positively correlated channel with $P_{BI} = 0.4$,$P_{IB} = 0.1$ and Doppler spread $f_m = 150$Hz.

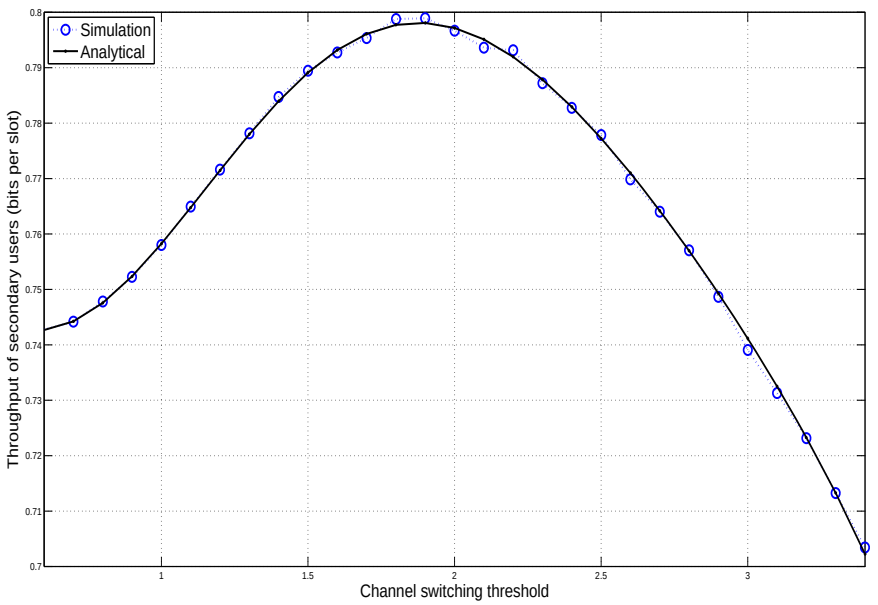

Figure 2.7: Throughput performance for different channel switching threshold ($P_{BI} = 0.4, P_{IB} = 0.1, f_m = 150$Hz).

Fig. 2.8 shows the optimal channel switching thresholds for different P_{BI} for a system with Doppler spread f_m=20Hz and P_{IB}=0.1. When P_{BI}=0.3, if the predicted SNR is below 1.8, it is better to switch the channel and if it is above then better to stay in that channel until it becomes busy. Similarly for different scenarios, we can find the optimal channel switching strategy.

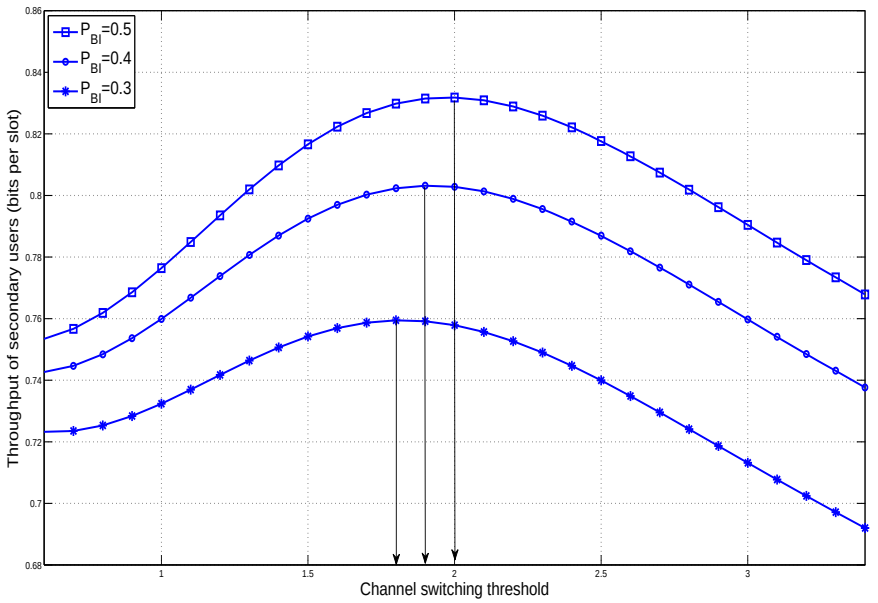

Figure 2.8: Throughput performance for different channel switching threshold (P_{IB} = 0.1, f_m = 20Hz).

2.3 Multi-Channel system

In this section, we analyze the performance of a cognitive radio system with multiple primary user channels. We assume that there are more than $N(> 2)$ primary channels and a cognitive user can access any channel if it is not occupied by the primary user. As we consider the round robin access, if there are enough channels, the state of the first slot of a channel that

the cognitive user accessed long time back will have steady state probabilities after few time slots. That assumption made the analysis simpler compare to the two channel case

2.3.1 Steady State Analysis

As we consider channel occupancy state (B or I) and SNR state (H_l or H_h), the first slot can be in any combination. If the sensed channel is busy (B), or idle (I) with lower SNR (H_l), the cognitive user will leave that channel. In that case, it is considered as cognitive user stayed only one slot ($L = 1$) in that channel (Fig. 2.5(a)). If that channel is in busy state, without transmission, cognitive user will switch the channel. If that channel is idle but with lower SNR, with probability $P_I P_{H_l}/(P_B + P_I P_{H_l})$, it will transmit during that slot and leave that channel right after. Probability of success in accessing the first slot (fs) of a primary channel can be written, using the steady state probabilities, as $P_{fs} = P_I P_{H_h}$. Therefore, if cognitive user stays only one slot, the reward can be written as

$$R_{L=1} = (1 - P_{fs}) \frac{P_I P_{H_l}}{P_B + P_I P_{H_l}} R_{H_l},$$

where R_{H_l} denotes the reward (throughput) during the low SNR (State H_l) transmission.

When sensing, if the channel is idle (I) and having higher gain (H_h), then cognitive user will transmit and will stay in that channel to sense during the next time slot. Probability of staying in the same channel during the next slot (ns) can be written as $P_{ns} = P_{II} P_{H_h H_h}$ and probability of leaving a currently occupied channel can be written as $(1 - P_{ns})$.

When the cognitive user stays L (> 1) number of slots, it may leave the channel when the channel occupancy state becomes busy or the SNR state becomes H_l (Fig. 2.5(b)). If a cognitive user leaves the channel due to busy state, it will not transmit in the last slot. Hence, the reward during the last slot can be written, considering one slot before the last

slot was in state I with H_h, as:

$$R_{LastSlot} = \frac{P_{II}P_{H_hH_l}}{P_{IB} + P_{II}P_{H_hH_l}} R_{H_l}.$$

Therefore, if a cognitive user stays in a channel for $L(> 1)$ slots, the reward can be written as,

$$R = (1 - P_{fs})\frac{P_I P_{H_l}}{P_B + P_I P_{H_l}} R_{H_l} + P_{fs}\left(\frac{1}{1 - P_{ns}} R_{H_h} + \frac{P_{II}P_{H_hH_l}}{P_{IB} + P_{II}P_{H_hH_l}} R_{H_l}\right). \tag{2.30}$$

2.3.2 Analytical Results and Discussion

In this section, we present and discuss the throughput performance of the proposed access scheme for a cognitive radio system with multiple primary channels. The proposed channel switching scheme provides the optimal channel switching threshold for a given traffic characteristics of primary users and the relative motion (Doppler spread) of cognitive user given that cognitive user can sense only one channel.

The cognitive user's throughput performance for different channel switching thresholds is shown for different primary user occupancy statistics. For Doppler spread $f_m = 20$Hz, $P_{BI} = 0.1$ and $P_{IB} = 0.1$, the optimal channel switching threshold, $\Gamma = 2.6$, can be found in Fig. 2.9. That is, when the received SNR is below 2.6, it is better to switch the channel for long term throughput benefit even the current channel is in idle state. Also we can find that $\Gamma = 2.8$ when $P_{BI} = 0.5$. In a positively correlated primary user traffic, the cognitive user leaves a channel when it finds that channel is in State B. When a cognitive user switches the channel, it expects that the channels were in busy state during its previous visit may be in idle state after few slots. If the channel's P_{BB} is higher, there is lower probability that the switched channel will be in idle state compared to the channel with lower P_{BB}. Therefore, it is better to stay in the same channel if it is idle even the predicted SNR is not good. We can observe in Fig. 2.9 that when P_{BI} decreases (or P_{BB} increases) the channel switching

threshold also decreases. That is, the access scheme encourages the users to stay in the same channel if it is idle even the predicted SNR is not good for the long term throughput advantage when P_{BB} increases ($P_{BB} = 1 - P_{BI}$).

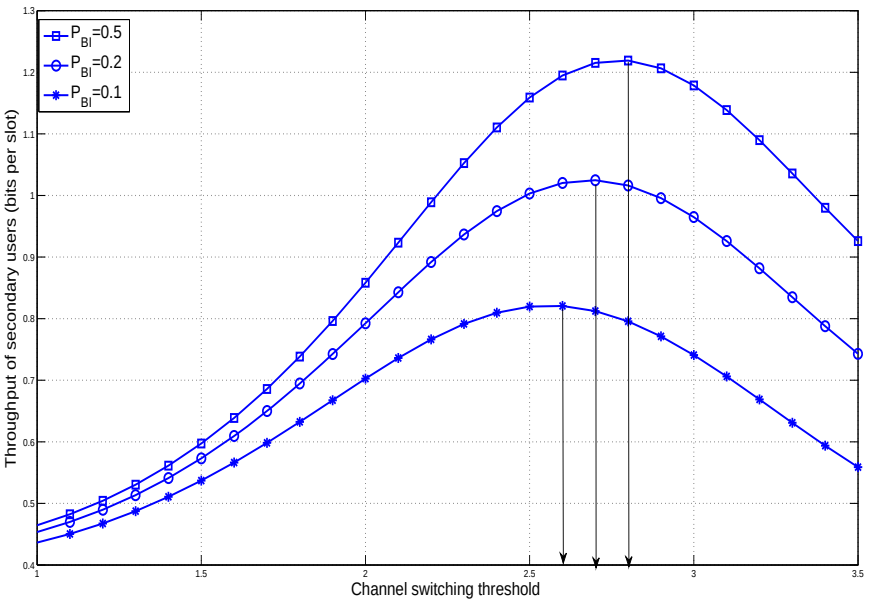

Figure 2.9: Throughput performance for different channel switching threshold ($P_{IB} = 0.1, f_m = 20$Hz).

Further, when P_{II} increases (P_{IB} decreases), the channel switching threshold also increases. We can observe in Fig. 2.10 that Γ increases from 2.5 to 2.8 when P_{IB} decreases from 0.3 to 0.1 for $P_{BI} = 0.4$ and $f_m = 20$Hz.

Fig. 2.11 shows the throughput performance for different Doppler spreads. When the Doppler spread increases, the SNR prediction is not reliable and hence, the channel switching threshold decreases. That is, in a dynamic environment the channel switching based on the channel gain is discouraged for the long term throughput benefit of the cognitive user. We can observe that in Fig. 2.11 for $P_{BI} = P_{IB} = 0.1$, when Doppler spread f_m increases from

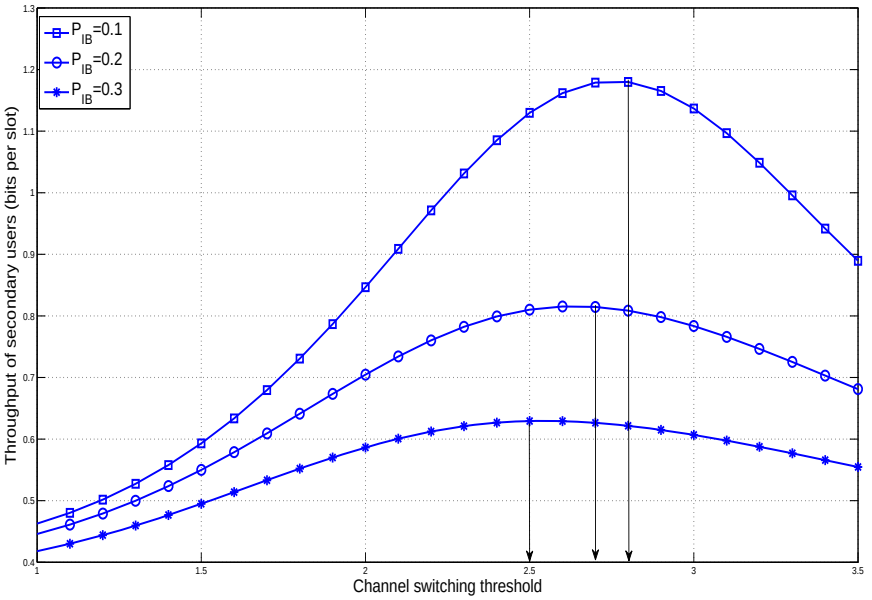

Figure 2.10: Throughput performance for different channel switching threshold ($P_{BI} = 0.4$, $f_m = 20$Hz).

20Hz to 200Hz, the optimal channel switching threshold increases from 2.2 to 2.6.

2.4 Chapter Summary

In this chapter, we analyzed a channel access scheme for a cognitive user that operates in an interweave system, based on the traffic characteristics of the primary system and Doppler spread of the cognitive user. In a positively correlated primary user traffic, the cognitive user switches the channel either when the sensed primary channel is busy or predicted SNR is below a specific threshold. It is found that, when the primary user traffic is highly correlated (higher P_{BB} and P_{II}) or cognitive user is more dynamic (higher f_m), it is not beneficial to switch the channel frequently in order to gain long term throughput advantage. For given statistics about primary user traffic, an optimal channel switching threshold can be found

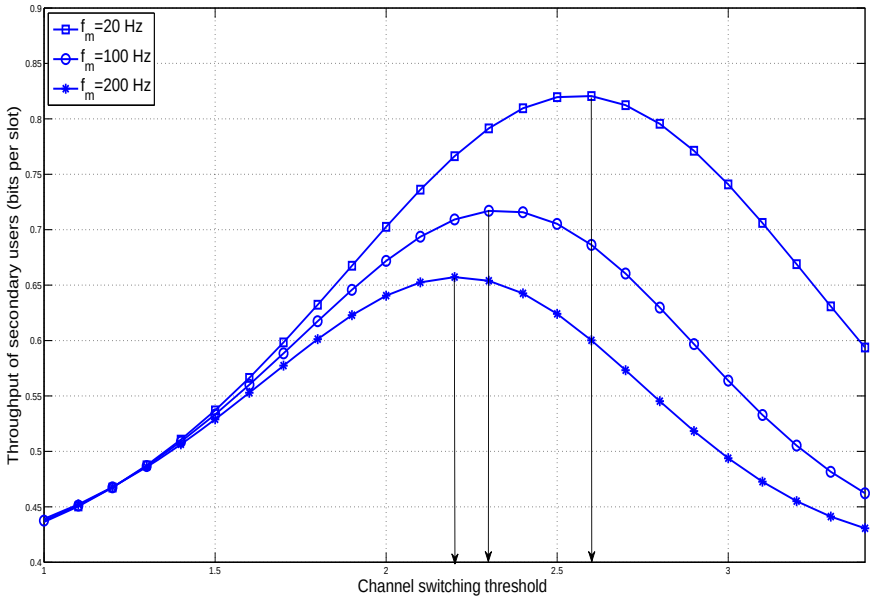

Figure 2.11: Throughput performance for different channel switching threshold ($P_{IB} = 0.1, P_{BI} = 0.1$).

from the analysis that maximizes the long term throughput of a cognitive user. In the next chapter, we analyze the channel switching strategy of a cognitive user in a hybrid interweave-underlay cognitive radio system

Chapter 3

Channel Access in Interweave-Underlay Cognitive Radio System with Perfect Sensing

In the last chapter, we studied the performance of an interweave cognitive radio system where we showed that a cognitive radio can switch the channel sensing for possible transmission and hence improve throughput based on primary user traffic characteristics. In reality, the cognitive user may get opportunity to transmit both in interweave and underlay modes of transmission in future wireless systems [3]. Therefore, in this chapter, we evaluate the throughput performance of a cognitive user in both transmission modes and develop a framework for the transmission mode selection. Our contributions in this chapter can be summarized as follows:

- Proposing a new analytical study on transmission mode selection with channel switching in hybrid underlay-interweave systems based on cognitive user throughput ratio between underlay and interweave transmission modes (R_U/R_I) and the primary user

traffic statistics (T) while cognitive user can sense only one channel,

- Developing a three-state Markov framework to analyze such a hybrid mode of transmission for a positively correlated primary user traffic,
- Analytically deriving the optimal thresholds for transmission mode selection considering throughput performance of a cognitive user and,
- Showing both analytically and via simulation that proper transmission mode selection can provide up to 8% throughput advantage in hybrid cognitive radio networks.

The rest of the chapter is organized as follows. Section 3.1 describes the system model under consideration. Section 3.2 analyzes the performance of the proposed hybrid system and results are given in Section 3.3 Finally, the chapter is summarized in Section 3.4.

3.1 Interweave-Underlay System Model with Perfect Sensing

In this work, the initial analysis is done for a system that has two identical but independent primary channels and one cognitive user that tries to opportunistically occupy a primary user channel as shown in Fig. 3.1. The detailed system description of primary and cognitive users are given in the following subsections.

3.1.1 Primary User

In a cognitive radio network, the cognitive users use the primary channels opportunistically. We classify the state of a primary user channel into three states in the view of a cognitive user. They are:

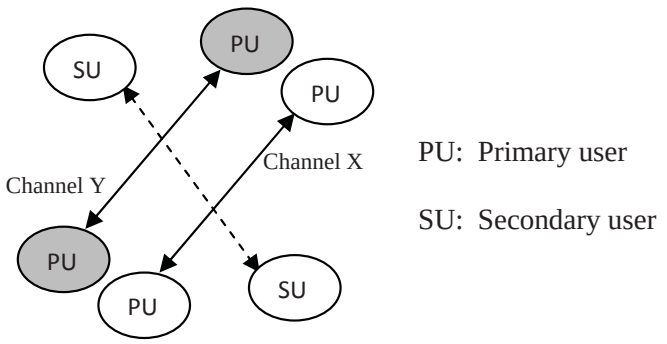

Figure 3.1: System model (2 primary user channels and 1 cognitive user pair).

1. The channel is not being used by the primary user and hence the channel is said to be idle. The cognitive user can opportunistically use that channel and its state is denoted by *State I* (idle).

2. The primary user occupies the channel and the cognitive user occupancy will cause interference to the primary user. Since the primary users get higher priority, the cognitive users are not allowed to use that channel. This state of the channel is denoted by *State B* (busy).

3. In few instances (where the interference caused by the cognitive users to the primary user is below a certain threshold), cognitive users are allowed to share the channel with primary users. In that case, both primary and cognitive users share the channel but cognitive user transmits with low power. Hence, the data rate would be lower. This channel state is denoted by *State U* (similar to underlay).

Therefore, we use a three state Markov chain to model each primary user channel as shown in Fig. 3.2. The states are defined for a single primary user channel as summarized below:

- *State I*: The channel is idle and it can be occupied by the cognitive user.

- *State B*: The channel is occupied by the primary user and no cognitive user can share this channel.

- *State U*: The channel is occupied by the primary user but it can be used by the cognitive user with low transmit power.

The transition probability from *State B* to *State I* is denoted by P_{BI}. Similarly, other transition probabilities are denoted. The corresponding transition matrix is given by,

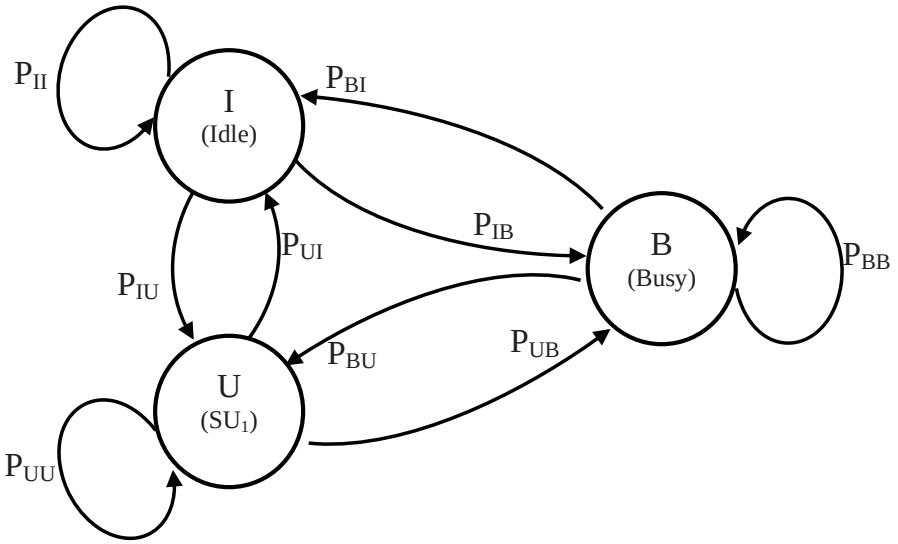

Figure 3.2: Markov channel model for a primary user channel.

$$T = \begin{pmatrix} P_{BB} & P_{BI} & P_{BU} \\ P_{IB} & P_{II} & P_{IU} \\ P_{UB} & P_{UI} & P_{UU} \end{pmatrix}. \tag{3.1}$$

3.1.2 Cognitive User

The cognitive user is not having any pre-assigned channels to transmit and it uses the primary channels opportunistically. During the interweave (when the state is idle) transmission, the

cognitive user gains throughput advantage compared to the underlay transmission as it can transmit at maximum power. The cognitive user makes the transmission strategy based on the state and traffic characteristics of the primary users as well as the throughput ratio between the interweave and underlay transmissions. In this section, we consider the following two transmission strategies.

1. *Strategy A*: cognitive user occupies the primary user channel when the channel is in either *State I* (idle) or in *State U* (share with the primary user with lower data rate).

2. *Strategy B*: cognitive user occupies the channel only when it is idle (*State I*) (no co-existence with the primary user).

We assume that the cognitive user can sense only one channel at a time. Therefore, cognitive user does not know the states of the other channels when cognitive user senses one channel, but it can predict the states of the other channels based on the previously sensed data and the state transition probabilities of the primary user using the Bayes rule [28].

The state of a channel k at time slot t is denoted by $S_k(t)$ and the channel sensed during the time slot t is denoted by $a(t)$. The predicted state probability of a channel k (k=1,2 for two channel system), during the time slot t, being in *State B*, *State I* and *State U* are denoted by $\omega_{k_B}(t)$, $\omega_{k_I}(t)$ and $\omega_{k_U}(t)$ respectively. They can be calculated as follows,

$$\omega_{k_X}(t+1) = \begin{cases} P_{BX}, & a(t)=k,\ S_{a(t)}(t)=B; \\ P_{IX}, & a(t)=k,\ S_{a(t)}(t)=I; \\ P_{UX}, & a(t)=k,\ S_{a(t)}(t)=U; \\ \omega_{k_B}(t)P_{BX} + \omega_{k_I}(t)P_{IX} + \omega_{k_U}(t)P_{UX}, & a(t)\neq k. \end{cases}$$

where $X \in \{B, I, U\}$, $P_{BU} = 1 - P_{BB} - P_{BI}$, $P_{IU} = 1 - P_{IB} - P_{II}$, $P_{UU} = 1 - P_{UB} - P_{UI}$ and $\omega_{k_B}(t) + \omega_{k_I}(t) + \omega_{k_U}(t) = 1$.

We also assume that, based on the sensing result and predefined interference threshold, cognitive user decides whether to share the channel with primary user or not. Let Γ_S be the sensed power level, and Γ_O and Γ_U ($> \Gamma_O$) be the sensed power thresholds for interweave and underlay (sharable) modes respectively. All these parameters are defined at the cognitive transmitter. Primary receiver interference threshold is denoted by γ_S. The detail operational descriptions are stated in the subsection 3.2.3.

- If $\Gamma_S > \Gamma_U$, then no transmission is allowed.
- If $\Gamma_S < \Gamma_O$, then interweave mode of transmission. The interweave threshold is tighter to protect primary user transmission during time slots (with the acceptable tolerance of mis-detection and false alarm). During that slot, cognitive user will operate with its full power to gain maximum throughput.
- If $\Gamma_O < \Gamma_S < \Gamma_U$, then underlay mode of transmission. Underlay threshold is little compromised to allow for limited cognitive user transmission. When the cognitive user finds that the sensed power level is above the interweave threshold but safely below the underlay threshold, then it will transmit with lower power to gain some throughput.

Hence, based on the sensing result of the primary user's signal and the predefined thresholds, the cognitive user decides whether the primary user channel is in state U or B [34] [35].

The cognitive user's behaviour is analyzed using a Markov chain where each state represents the length of the continuous stay of a cognitive user in terms of time slots ($L = 1, 2, 3, \ldots$) before switching to another channel. It is shown in Fig. 3.3, where P_{nm} denotes the transition probability of cognitive user for staying in a channel for $L = n$ slots and switching to the other channel for $L = m$ slots. The probability of staying in a channel for a consecutive L slots is written as P_L. Note that each primary user channel is modeled as in Fig. 3.2 and each cognitive user's stay in a channel is modeled as in Fig. 3.3.

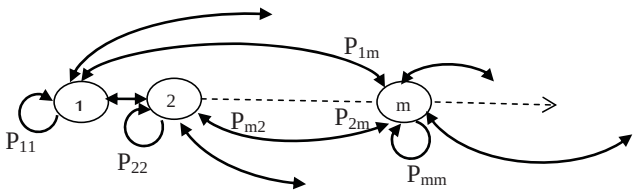

Figure 3.3: Markov chain model for the cognitive user: states represent the length (L) of the stay of a cognitive user in a channel continuously.

In the literature, for a two state case (B or I), the analysis was done for positively and negatively correlated primary user traffic . The positively correlated primary user traffic implies that $P_{BB} > P_{IB}$. A myopic strategy was proposed in [28] as, in positively correlated traffic, the cognitive user switches the channel when it senses the primary channel as busy; and in negatively correlated traffic, the cognitive user stays in that channel when it senses the channel as busy. Cognitive user does the opposite when it senses as idle.

In our case with three states, we consider a scenario in which the primary user traffic is positively correlated with time. That is, when a primary user occupies a channel, it stays in that channel for few slots ($P_{BB} > \{P_{IB}$ or $P_{UB}\}$). Hence, if the currently sensed channel is busy, then the predicted state of that channel during the next slot will be busy with higher probability. In that case, the cognitive user prefers to switch the channel expecting to transmit in the other channel. In a negatively correlated traffic, it would be other way. That is, the cognitive user may find it beneficial to stay in that channel without any transmission when the sensed slot is busy and it will wait for the next slot hoping that the primary user may vacate that channel. We believe that positively correlated primary user traffic represents a more common case of a stable system with enough data at primary user for transmission. Therefore, we assume that cognitive user switches the channel when it senses the primary channel as busy in the analysis. The detailed operational details are given in Section 3.2.3.

3.2 Throughput Analysis

As mentioned earlier, the analysis is done for a two-primary user channel system with one cognitive user. The objective is to maximize the throughput of a cognitive user without affecting the primary users. We assume that the cognitive user has enough data to transmit continuously and it looks for a better selection of a primary user channel to transmit its data.

The critical decision for a cognitive user is whether to stay in a channel and transmit at a lower rate or, leave that channel and sense the other channels when the currently sensed channel is in *State U*. The other channel can be in one of the three states. If it is in *State I*, then the switching would be beneficial. If it is in the *State B*, then it would reduce the throughput.

3.2.1 Strategy A: Cognitive access with simultaneous channel sharing

In this strategy, the cognitive user occupies a channel when it is in *State I* (idle) or *State U* (coexistence with primary user). When the channel state becomes *State B*, cognitive user leaves that channel without transmitting as we assume that primary user traffic is positively correlated. In order to compute the cognitive user's throughput in this strategy, we need to find both the transition and the steady state probabilities of the Markov chain described in Fig. 3.3.

The calculation of a transition probability in a two-primary user channel system can be illustrated using an example as follows: A cognitive user had stayed in the first channel (say channel X) for $L = m$ slots, then moved to the second channel (say channel Y) when the channel X became busy (*State B*). Then it stayed in the channel Y for $L = n$ slots before

moving back to the channel X in our two-primary user channel system as shown in Fig. 3.4. Here, m and n can be any positive integers but we first consider the case for $n \geq 2$. Always a cognitive user switches the channel if that channel becomes busy to allow for primary user's privileged access. If the first slot of the channel Y is in *State I* (slot $m+1$), then the transition probability should be $P_{BI}^{(m+1)}$ where $P_{BI}^{(m+1)}$ denotes the transition probability of a channel becoming *State I* from *State B* after $m+1$ slots. Similarly, if the slot $m+1$ is in *State U*, then the transition probability should be $P_{BU}^{(m+1)}$. For staying the rest of $n-1$ slots in the channel Y, the channel should be in either *State I* or *U* for the next $n-2$ slots $((m+2)-(m+n-1))$ and of course, the last slot ($(m+n)^{th}$ slot) should be in *State B*. We consider an extracted transition matrix $\bar{T}$ as defined in (3.2) from the original transition matrix T to characterize the channel transition. The transition probability for staying in a channel for $L = n, (n \geq 2)$ slots provided that cognitive user had stayed in the other channel for $L = m$ slots before switching to this channel can be written as shown below for four different scenarios.

$$P_{mn} = \begin{cases} P_{BI}^{(m+1)} \bar{P}_{II}^{(n-2)} P_{IB}, & \text{Slot } (m+1) \text{ and } (m+n-1) \text{ are in } \textit{State I}; \\ P_{BI}^{(m+1)} \bar{P}_{IU}^{(n-2)} P_{UB}, & \text{Slot } (m+1) \text{ and } (m+n-1) \text{ are in } \textit{State I} \text{ and } \textit{State U} \text{ respectively}; \\ P_{BU}^{(m+1)} \bar{P}_{UI}^{(n-2)} P_{IB}, & \text{Slot } (m+1) \text{ and } (m+n-1) \text{ are in } \textit{State U} \text{ and } \textit{State I} \text{ respectively}; \\ P_{BU}^{(m+1)} \bar{P}_{UU}^{(n-2)} P_{UB}, & \text{Slot } (m+1) \text{ and } (m+n-1) \text{ are in } \textit{State U}. \end{cases}$$

Hence,

$$P_{mn} = P_{BI}^{(m+1)} (\bar{P}_{II}^{(n-2)} P_{IB} + \bar{P}_{IU}^{(n-2)} P_{UB}) + P_{BU}^{(m+1)} (\bar{P}_{UI}^{(n-2)} P_{IB} + \bar{P}_{UU}^{(n-2)} P_{UB}),$$

where $\bar{P}_{II}^{(n-2)}$ is defined as transition probability of a channel from *State I* to become *State I* after $n-2$ slots (there should not be any *State B* within $n-2$ slots) and other notations can also be interpreted similarly. The transition probabilities are calculated from the transition

matrix $\bar{T}$ which is defined as,

$$\bar{T} = \begin{pmatrix} P_{II} & P_{IU} \\ P_{UI} & P_{UU} \end{pmatrix}. \tag{3.2}$$

Finally, for the case when $n = 1$, the cognitive user stays only one time slot because the

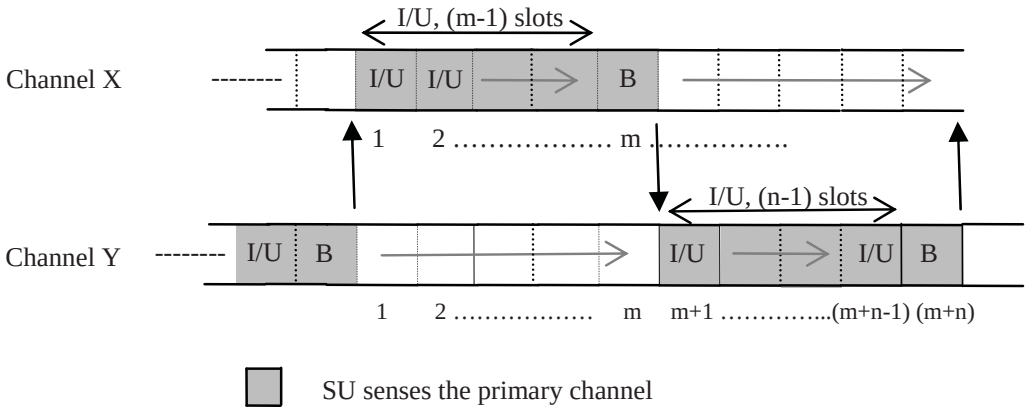

Figure 3.4: Sensing: One cognitive user accesses two primary channels.

primary channel is in *State B*. Hence, the transition probability for that case can be written as $P_{m,1} = P_{BB}^{(m+1)}$.

In the steady sate, we can write the steady state equation for the first two states ($L = 1, 2$) as,

$$P_1 = \sum_{i=1}^{\infty} P_i P_{BB}^{(i+1)}, \tag{3.3}$$

$$P_2 = \sum_{i=1}^{\infty} P_i (P_{BI}^{(i+1)} P_{IB} + P_{BU}^{(i+1)} P_{UB}), \tag{3.4}$$

with

$$\sum_{i=1}^{\infty} P_i = 1. \tag{3.5}$$

Further, we can write the steady state equation for the states $L > 2$ as,

$$P_L = \sum_{i=1}^{\infty} P_i \left(P_{BI}^{(i+1)} (\bar{P}_{II}^{(L-2)} P_{IB} + \bar{P}_{IU}^{(L-2)} P_{UB}) + P_{BU}^{(i+1)} (\bar{P}_{UI}^{(L-2)} P_{IB} + \bar{P}_{UU}^{(L-2)} P_{UB}) \right). \quad (3.6)$$

In order to solve (3.3)-(3.5), we need to simplify the infinite series. For that we need to find the relationship between the states. The states are sub-divided as shown below to find the relationships among them. From (3.4), we can write:

$$P_2 = P_{2_1} + P_{2_2}, \quad (3.7)$$

where $P_{2_1} = \sum_{i=1}^{\infty} P_i P_{BI}^{(i+1)} P_{IB}$ and $P_{2_2} = \sum_{i=1}^{\infty} P_i P_{BU}^{(i+1)} P_{UB}$. Also, from (3.6) for a specific state $L, L > 2$, we can write

$$P_L = P_{L_1} + P_{L_2} + P_{L_3} + P_{L_4},$$

where

$$\begin{aligned}
P_{L_1} &= \sum_{i=1}^{\infty} P_i P_{BI}^{(i+1)} \bar{P}_{II}^{(L-2)} P_{IB}, \\
P_{L_2} &= \sum_{i=1}^{\infty} P_i P_{BI}^{(i+1)} \bar{P}_{IU}^{(L-2)} P_{UB}, \\
P_{L_3} &= \sum_{i=1}^{\infty} P_i P_{BU}^{(i+1)} \bar{P}_{UI}^{(L-2)} P_{IB}, \\
P_{L_4} &= \sum_{i=1}^{\infty} P_i P_{BU}^{(i+1)} \bar{P}_{UU}^{(L-2)} P_{UB}.
\end{aligned}$$

From the above we can find the relationship as,

$$P_{L_1} = P_{2_1} \bar{P}_{II}^{(L-2)}, \quad (3.8a)$$

$$P_{L_2} = P_{2_1} \frac{P_{UB}}{P_{IB}} \bar{P}_{IU}^{(L-2)}, \quad (3.8b)$$

$$P_{L_3} = P_{2_2} \frac{P_{IB}}{P_{UB}} \bar{P}_{UI}^{(L-2)}, \quad (3.8c)$$

$$P_{L_4} = P_{2_2} \bar{P}_{UU}^{(L-2)}, \quad (3.8d)$$

and from (3.3), (3.7) and (3.8),

$$P_1 = P_1 P_{BB}^{(2)} + P_2 P_{BB}^{(3)} + \sum_{i=3}^{\infty} \left(P_{L_1} + P_{L_2} + P_{L_3} + P_{L_4}\right) P_{BB}^{(i+1)},$$

$$\begin{aligned} P_1 = P_1 P_{BB}^{(2)} + P_2 P_{BB}^{(3)} \quad &+ \quad P_{2_1} \sum_{i=3}^{\infty} \left(\bar{P}_{II}^{(i-2)} + \frac{P_{UB}}{P_{IB}} \bar{P}_{IU}^{(i-2)} \right) P_{BB}^{(i+1)} \\ &+ \quad P_{2_2} \sum_{i=3}^{\infty} \left(\frac{P_{IB}}{P_{UB}} \bar{P}_{UI}^{(i-2)} + \bar{P}_{UU}^{(i-2)} \right) P_{BB}^{(i+1)}. \end{aligned} \tag{3.9}$$

The series sum can be calculated using eigenvalue decomposition. The square matrix T defined in (3.1) can be written as,

$$T = VDV^{-1},$$

where D and V denote a diagonal matrix of eigenvalues and a full matrix whose columns are the corresponding eigenvectors of matrix T respectively. The diagonal elements of the matrix D can be denoted by λ_1, λ_2 and λ_3. Similarly the matrix $\bar{T}$, defined in (3.2) can be written as $\bar{T} = \bar{V}\bar{D}\bar{V}^{-1}$ where the diagonal elements are denoted by $\bar{D}_{(1,1)} = \mu_1$ and $\bar{D}_{(2,2)} = \mu_2$ where $D_{(m,n)}$ denotes the mth row and n^{th} column element of the matrix $\bar{D}$ for any positive integer m, n. Using the above properties, $P_{BU}^{(i)}$, for any positive integer i, can be calculated as $P_{BU}^{(i)} = (VD^iV^{-1})_{(1,3)}$. The infinite series sum can be found as shown below,

$$\sum_{i=3}^{\infty} \bar{P}_{II}^{(i-2)} P_{BI}^{(i+1)} \quad = \quad (\bar{V}_{(1,1)} \bar{V}_{(1,1)}^{-1} W_{\mu_1})_{(1,2)} + (\bar{V}_{(1,2)} \bar{V}_{(2,1)}^{-1} W_{\mu_2})_{(1,2)},$$

where

$$W_{\mu_1} = V \begin{pmatrix} \frac{\mu_1(\lambda_1)^4}{1-\lambda_1\mu_1} & 0 & 0 \\ 0 & \frac{\mu_1(\lambda_2)^4}{1-\lambda_1\mu_1} & 0 \\ 0 & 0 & \frac{\mu_1(\lambda_3)^4}{1-\lambda_1\mu_1} \end{pmatrix} V^{-1},$$

$$W_{\mu_2} = V \begin{pmatrix} \frac{\mu_2(\lambda_1)^4}{1-\lambda_1\mu_2} & 0 & 0 \\ 0 & \frac{\mu_2(\lambda_2)^4}{1-\lambda_1\mu_2} & 0 \\ 0 & 0 & \frac{\mu_2(\lambda_3)^4}{1-\lambda_1\mu_2} \end{pmatrix} V^{-1}.$$

Similarly, we can find the other infinite series sum. Solving the linear equations (3.3)-(3.5) after simplifying them as shown above, we can find the steady state probabilities of each state analytically.

The steady state probability P_L gives the probability that a cognitive user continuously stays in a channel for L number of slots. The last slot should be in *State B* and previous $L-1$ slots can be in either *State I* or *State U*. As mentioned earlier, if it is in *State U*, the cognitive user shares the channel with primary user and the throughput would be reduced. Therefore, we need to identify the probability distribution of *State I* and *State U* for each state P_L in the throughput calculation. That is, for each state $L \geq 2$, the probability of staying in *State I* (P_{L_I}) and *State U* (P_{L_U}) needs to be calculated. This can be done using a tree diagram [36] concept. For that calculation, we need to know the probability of the first slot being in *State I* (P_{I_f}) and *State U* (P_{U_f}) for the states $L \geq 2$ and P_{I_f} can be found as,

$$P_{I_f} = \sum_{i=1}^{\infty} P_i P_{BI}^{(i+1)},$$

and similar equation can be written for the probability of the first slot being in *State U* (P_{U_f}). We assume that the cognitive user's data rate is R_I when it is in *State I* and R_U when the channel is in *State U*. Then the transmitted data can be defined as,

$$C_I = \sum_{i=2}^{\infty} (i-1) P_i (P_{i_I} R_I + P_{i_U} R_U). \tag{3.10}$$

The average length of a continuous stay of a cognitive user in a channel (in number of slots) can be found as,

$$\bar{L}_I = \sum_{i=1}^{\infty} i P_i. \tag{3.11}$$

Using (3.10) and (3.11), we can write the throughput of the cognitive user as,

$$\bar{C}_I = \frac{C_I}{\bar{L}_I}.$$

3.2.2 Strategy B: Cognitive access without simultaneous channel sharing

In this section, the Strategy B is discussed with throughput analysis. Note that Strategy B is cognitive user occupies the channel only when it is idle (*State I*) (no co-existence with the primary user). In the analysis, as defined earlier in Fig. 3.3, an infinite state Markov chain having states $L = 1, 2, 3 \ldots$ is used. As cognitive user senses only one channel at a time, the state of the other channel ($B/U/I$) is predicted from the last visit. If a channel was visited n slots before and it was in *State B*, then the probability of being in *State I* in the next slot would be $P_{BI}^{(n+1)}$. Similarly, we can predict the other transition probabilities. In this prediction, we are using the state of the channel when it was sensed during the last visit.

In Strategy B, a cognitive user occupies a channel only when it is in *State I* (idle) and leaves a channel if the sensed channel was in either *State B* or *State U*. That is, if a cognitive user senses the channel as in either *State B* or *State U*, then it switches the sensing to the next channel in the next slot. During the sensing slot, if that channel is in *State B*, the cognitive user will not transmit during that slot; on the other hand, if the sensed channel is in *State U*, then cognitive user will transmit with lower power during that slot and switch the sensing to the other channel. Hence, it is noted that cognitive user stays in only one slot ($L = 1$) even though it does not transmit when the channel is in *State B*, and it transmits only in one slot at lower rate when the sensed channel is in *State U* before switching the sensing to the other channel. It is considered in the throughput calculation of state $L = 1$. For $L \geq 2$ states, the first $L - 1$ slots are in *State I* and the last slot is *State B* or *State U*. In the analysis, we denote it with W, that is channel state of the last slot can be either *State B* or *State U*. The probability of last slot being in *State U* before the cognitive user

leaves a channel can be written as $\delta = P_{IU}/(P_{IU} + P_{IB})$ for $L \geq 2$. Similarly, we can write that probability of last slot being in *State B* as $1 - \delta$.

As mentioned earlier, the $L = 1$ state is either due to *State B* or *State U*. For the analytical purpose, the *State* $L = 1$ is divided into 6 states ($1_{B_B}, 1_{B_U}, 1_{U_U}, 1_{U_B}, 1_{B_W}$ and 1_{U_W}) and for $L \geq 2$, each state is divided into 3 states (L_B, L_U and L_W) based on the state of the previous visit. That is, *State* 1_{B_U} denotes that cognitive user stays in only one slot ($L = 1$) (during the sensing slot) and then, leaves it as that channel is in *State B*; and the cognitive user had left that channel on its previous visit as it was in *State U* (denoted by the subscript letter U). For simplicity in notation, we use B_B instead of 1_{B_B} (state notation without "1"). The corresponding steady state probabilities are denoted by $P_{B_B}, P_{B_U}, P_{U_U}, P_{U_B}, P_{B_W}$ and P_{U_W} for the state $L = 1$, and P_{L_B}, P_{L_U} and P_{L_W} for the states $L \geq 2$, where $P_1 = P_{B_B} + P_{B_U} + P_{U_U} + P_{U_B} + P_{B_W} + P_{U_W}$, and $P_L = P_{L_B} + P_{L_W} + P_{L_U}$ for $L \geq 2$.

The modified representation of Fig. 3.3 is shown in Fig. 3.5. This modification is done to facilitate the analysis for Strategy B. The subscript of the state notation denotes the state of channel during the previous visit. That is, L_B denotes that the cognitive user stays L slots continuously in a channel and the state of the channel during cognitive user's previous visit was *State B*. L_U and L_B states are only one step transition states. That is, whenever a cognitive user moves from a $L = 1$ state to L (≥ 2) states, it will go to one of the L_U states ($L \geq 2$) if its previous state was $L = 1$ and *State U* or it will go to one of the L_B states ($L \geq 2$) if its previous state was $L = 1$ and *State B*. Since L_B and L_U are transition states, there will not be any transitions within L_B or L_U states or between L_B and L_U states. After staying L (≥ 2) slots in either L_B or L_U state, cognitive user can move to either *State* B_W ($L = 1$ and *State B*) or *State* U_W ($L = 1$ and *State U*) or *State* L_W ($L \geq 2$, the first $L - 1$ slots are in *State I* and last slot is in either *State B* or *State U*). That is, the transition

depends on the state of the newly switched channel. The state transitions are possible within *State* L_W. That is, we can find the transition probability, if the cognitive user moves from any *State* L_W ($L \geq 2$) to any *State* L_W ($L \geq 2$).

The state descriptions are summarized below. The state of the channel during the last visit is used in the transition probability calculations.

- B_B - The cognitive user left the channel on its previous visit as the channel was in *State B*, it stays in only one slot ($L = 1$) during the current sensing slot, and then leaves that channel as the channel is in *State B*.

- B_U - The cognitive user left the channel on its previous visit as the channel was in *State U*, it stays in only one slot ($L = 1$) during the current sensing slot, and then leaves that channel as the channel is in *State B*.

- U_B - The cognitive user left the channel on its previous visit as the channel was in *State B*, it stays in only one slot ($L = 1$) during the current sensing slot, and then leaves that channel as the channel is in *State U*.

- U_U - The cognitive user left the channel on its previous visit as the channel was in *State U*, it stays in only one slot ($L = 1$) during the current sensing slot, and then leaves that channel as the channel is in *State U*.

- B_W - The cognitive user left the channel on its previous visit as the channel was in either *State B* or *State U*, it stays in only one slot ($L = 1$) during the current sensing slot, and then leaves that channel as the channel is in *State B* .

- U_W - The cognitive user left the channel on its previous visit as the channel was in *State B* or *State U*, it stays in only one slot ($L = 1$) during the sensing slot, and then leaves that channel as the channel is in *State U*.

- L_B - The cognitive user left the channel on its previous visit as the channel was in *State B*, it stays in L slots during the current visit.

- L_U - The cognitive user left the channel on its previous visit as the channel was in *State U*. it stays in L slots during the current visit.

- L_W - The cognitive user left the channel on its previous visit as the channel was in either *State B* or *State U*. it stays in L slots during the current visit.

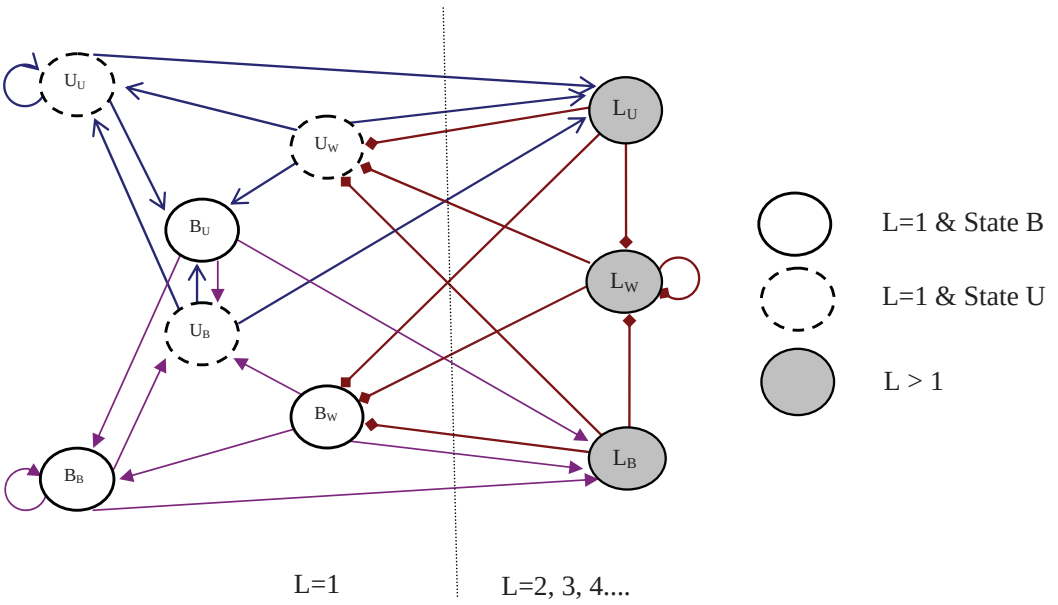

Figure 3.5: Modified Markov chain model for the cognitive user: states represent length of the stay of a cognitive user (L) in a channel continuously.

At steady state, we can write the steady state equation for *State* 2_B ($L = 2$) as follows:

$$P_{2_B} = P_{B_B} P_{BI}^{(2)} (P_{IB} + P_{IU}) + P_{B_U} P_{UI}^{(2)} (P_{IB} + P_{IU}) + P_{B_W} (\delta P_{UI}^{(2)} + (1-\delta) P_{BI}^{(2)})(P_{IB} + P_{IU}),$$

where $\delta = P_{IU}/(P_{IU} + P_{IB})$. For $L > 2$,

$$\begin{aligned} P_{L_B} &= P_{B_B} P_{BI}^{(2)} P_{II}^{L-2}(P_{IB} + P_{IU}) + P_{B_U} P_{UI}^{(2)} P_{II}^{L-2}(P_{IB} + P_{IU}), \\ &= P_{B_W}(\delta P_{UI}^{(2)} + (1-\delta) P_{BI}^{(2)}) P_{II}^{L-2}(P_{IB} + P_{IU}), \end{aligned}$$

and hence we can write,

$$P_{L_B} = P_{2_B} P_{II}^{L-2}. \tag{3.12a}$$

Similarly, the following relationships can be found.

$$P_{L_W} = P_{2_W} P_{II}^{L-2}, \tag{3.12b}$$

$$P_{L_U} = P_{2_U} P_{II}^{L-2}. \tag{3.12c}$$

Using (3.12),

$$\begin{aligned} 1 = \sum_{i=1}^{\infty} P_i &= (P_{B_B} + P_{B_U} + P_{B_W} + P_{U_B} + P_{U_U} + P_{U_W}) + \frac{P_{2_B} + P_{2_W} + P_{2_U}}{1 - P_{II}}, \quad (3.13) \\ 1 &= P_1 + \frac{P_2}{1 - P_{II}}. \end{aligned}$$

In Strategy B, the cognitive user stays in the same channel only when the state of the channel is *State I*. As mentioned earlier, we consider a two primary channel system (say, channel X and Y). The *State* U_B denotes that state of the current channel (say channel X) is *State U* and stays in only one slot ($L = 1$). The state of the previous channel (channel Y) was *State B* denoted by the subscript. Since the cognitive user stays in only one slot in channel X (as it is in *State* U_B) and switches back to the previous channel (channel Y), we can find the transition probability of a channel (in this example, channel Y) from *State B* to *State B* after 2 slots as $P_{BB}^{(2)}$. Note that, $P_{BB}^{(2)}$ denotes the transition probability of a channel becoming *State B* from *State B* after 2 slots. Hence, we can write the transition probability from *State* U_B to *State* B_U as $P_{BB}^{(2)}$. Similarly, we can write the transition probability from *State* U_U to *State* B_U as $P_{UB}^{(2)}$. Next we will find the transition probability from *State* U_W to

State B_U. The *State* U_W denotes that the current state of the channel is *State* U and $L = 1$, and the state of the previous channel's last slot was either *State* B or *State* U (denoted by subscript W). That is, the cognitive user stayed in the previous channel for L (≥ 2) slots and left that channel since the last slot of that channel was either *State* B or *State* U. Since the cognitive user was in that channel for more than one slot, the one before the last slot should be *State* I. Hence, the probability of last slot being in *State* U can be written as $\delta = P_{IU}/(P_{IU} + P_{IB})$ and last slot being in *State* B can be written as $1 - \delta$. Hence we can write the transition probability from *State* U_W to *State* B_U as $\delta P_{UB}^{(2)} + (1 - \delta)P_{BB}^{(2)}$. As we already know the transition probabilities from *State* U_U to *State* B_U, *State* U_B to *State* B_U and *State* U_W to *State* B_U, we can write the steady state equation for the State B_U as,

$$P_{B_U} = P_{UB}^{(2)} P_{U_U} + P_{BB}^{(2)} P_{U_B} + (\delta P_{UB}^{(2)} + (1 - \delta)P_{BB}^{(2)})P_{U_W}.$$

Similarly, we can write the steady state equations for the other states as,

$$\begin{aligned}
P_{U_U} &= P_{UU}^{(2)} P_{U_U} + P_{BU}^{(2)} P_{U_B} + (\delta P_{UU}^{(2)} + (1 - \delta)P_{BU}^{(2)})P_{U_W}, && (3.14a)\\
P_{U_B} &= P_{BU}^{(2)} P_{B_B} + (\delta P_{UU}^{(2)} + (1 - \delta)P_{BU}^{(2)})P_{B_W} + P_{UU}^{(2)} P_{B_U}, && (3.14b)\\
P_{2_B} &= P_{BI}^{(2)}(P_{IB} + P_{IU})P_{B_B} + P_{UI}^{(2)}(P_{IB} + P_{IU})P_{B_U} \\
&+ (\delta P_{UI}^{(2)}(1 - \delta)P_{BI}^{(2)})(P_{IB} + P_{IU})P_{B_W}, && (3.14c)\\
P_{B_B} &= P_{BB}^{(2)} P_{B_B} + (\delta P_{UB}^{(2)} + (1 - \delta)P_{BB}^{(2)})P_{B_W} + P_{UB}^{(2)} P_{B_U}, && (3.14d)\\
P_{2_U} &= P_{UI}^{(2)}(P_{IB} + P_{IU})P_{U_U} + P_{BI}^{(2)}(P_{IB} + P_{IU})P_{U_B} \\
&+ (\delta P_{UI}^{(2)} + (1 - \delta)P_{BI}^{(2)})(P_{IB} + P_{IU})P_{U_W}, && (3.14e)\\
P_{B_W} &= \left(P_{BB}^{(3)} P_{2_B} + (\delta P_{UB}^{(3)} + (1 - \delta)P_{BB}^{(3)})P_2 + P_{UB}^{(3)} P_{2_U}\right), \\
&+ \left(P_{BB}^{(4)} P_{3_B} + (\delta P_{UB}^{(4)} + (1 - \delta)P_{BB}^{(4)})P_3 + P_{UB}^{(4)} P_{3_U}\right) \ldots\ldots \\
&= \sum_{i=2}^{\infty} P_{BB}^{(i+1)} P_{i_B} + (\delta P_{UB}^{(i+1)} + (1 - \delta)P_{BB}^{(i+1)})P_i + P_{UB}^{(i+1)} P_{i_U}.
\end{aligned}$$

Using (3.12),

$$\begin{aligned} P_{B_W} &= P_{2_B}\sum_{i=2}^{\infty} P_{BB}^{(i+1)} P_{II}^{i-2} + P_2 \sum_{i=2}^{\infty} (\delta P_{UB}^{(i+1)} + (1-\delta) P_{BB}^{(i+1)}) P_{II}^{i-2} + P_{2_U} \sum_{i=2}^{\infty} P_{UB}^{(i+1)} P_{II}^{i-2}, \\ &= W_{(1,1)} P_{2_B} + W_{(3,1)} P_{2_U} + (\delta W_{(3,1)} + (1-\delta) W_{(1,1)}) P_2, \end{aligned} \tag{3.14f}$$

where

$$W = V \begin{pmatrix} \frac{(\lambda_1)^3}{1-P_{II}\lambda_1} & 0 & 0 \\ 0 & \frac{(\lambda_2)^3}{1-P_{II}\lambda_1} & 0 \\ 0 & 0 & \frac{(\lambda_3)^3}{1-P_{II}\lambda_1} \end{pmatrix} V^{-1}.$$

Similarly, we can write

$$P_2 = \left(W_{(1,2)} P_{2_B} + W_{(3,2)} P_{2_U}\right)(P_{IB} + P_{IU}) + (\delta W_{(3,2)} + (1-\delta) W_{(1,2)})(P_{IB} + P_{IU}) P_2.$$

Solving these linear equations (3.14) with (3.13), we can find the steady state probabilities of each state. The average length of a continuous stay of a cognitive user in a channel can be found (in number of slots) as,

$$\begin{aligned} \bar{L}_{II} &= \sum_{i=1}^{\infty} i P_i, \\ &= P_1 + \frac{P_2(2-P_{II})}{(1-P_{II})^2}. \end{aligned} \tag{3.15}$$

When $L = 1$, the cognitive user switches the channel after staying in only one slot and that slot, should be either *State U* or *State B*. If it is in *State U*, then cognitive user transmits at lower rate (R_U) before the switch. On the other hand, if the channel is in *State B*, cognitive user leaves that channel without transmitting as we assume that primary user traffic is positively correlated. Then the transmitted data can be calculated based on the probability of *State U* when $L = 1$ as,

$$C_a = (P_{U_U} + P_{U_B} + P_{U_W}) R_U. \tag{3.16}$$

For $L \geq 2$, in the last slot, the cognitive user leaves the channel due to the channel becoming either *State U* or *State B*. If the reason for leaving the channel was due to *State U*, then the cognitive user would have transmitted in the last slot with a lower rate before leaving. Hence, the transmitted data in the last slot can be calculated as,

$$C_b = \sum_{i=2}^{\infty} P_i \delta R_U = \frac{P_2}{1 - P_{II}} \delta R_U, \tag{3.17}$$

where as defined earlier, $\delta = \frac{P_{IU}}{P_{IU}+P_{IB}}$. When $L \geq 2$, the data transmitted in other than the last slot is definitely due to the *State I* of the channel; hence, it can be calculated as,

$$C_c = \sum_{i=2}^{\infty} (i-1) P_i R_I = \frac{P_2}{(1 - P_{II})^2} R_I. \tag{3.18}$$

The throughput can be calculated as,

$$\bar{C}_{II} = \frac{C_a + C_b + C_c}{\bar{L}_{II}},$$

where the average length of a continuous stay of a cognitive user in a channel in terms of slots $\bar{L}_{II}$ is given in (3.15).

3.2.3 Operational Details

As we discussed earlier, the cognitive user should accurately detect the presence of the primary user in the interweave transmission. When the primary user is not active or not within the range of the cognitive user transmission, the cognitive user can transmit. There are many sensing algorithms in the literature [25, 27] that can be used to detect the primary user transmission. On the other hand, in an underlay transmission mode, a cognitive user can transmit while a primary user is active as long as the interference to the primary system is within the threshold.

We propose to use two different power levels P_O and P_U ($< P_O$) during the interweave (when the state is idle) and underlay modes of transmission of cognitive users; however, more

than two levels can also be considered. As these power levels are known to the cognitive transmitter, the throughput ratio (R_U/R_I) of the cognitive user between the interweave and underlay transmission modes can be roughly calculated before the transmission. In our implementation, noting that achievable data rate is proportional to transmit power, we initially set $R_U/R_I = P_U/P_I$ where P_U and P_I are underlay and interweave mode transmission power respectively. During the transmission, throughput can be reported back to the cognitive transmitter by the cognitive receiver and hence fine-tuned.

We use the interference region model commonly used in [37–39] as shown in Fig. 3.6. In this model, it is assumed that a cognitive user knows the pilot power of the primary transmitter (P_p), interference threshold at the primary receiver (γ_s) and communication range of the primary transmitter (R). With the pilot power, the distance between the primary and cognitive transmitters can be calculated ($R + D$) where D is the interference range of the cognitive transmitter.

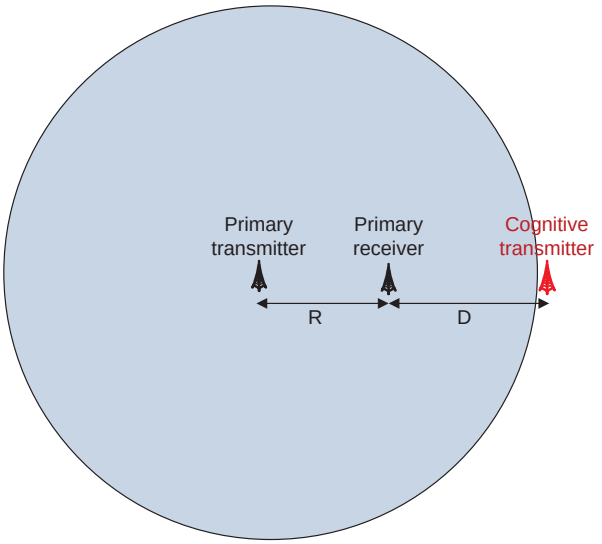

Figure 3.6: System model: Cognitive user in the presence of primary transceiver.

If the cognitive user's underlay mode transmission with power P_U is not causing interfer-

ence to the primary receiver, then the underlay transmission is possible. This interference threshold constraint can be written as $\frac{P_P L(R)}{P_U L(D)+P_n} > \gamma_s$, where $L(d)$ and P_n are denoted by total path loss at distance d from the transmitter, and the noise power level at the primary receiver respectively [37]. After estimating the distance of the primary user with the detected primary signal level during the sensing at the cognitive transmitter, the above interference constraint can be checked to see if it is met or not; and if it is, underlay transmission with power P_U is decided.

We re-define the following notations with additional details:

γ_s The interference threshold at the primary receiver. If the SINR is below this threshold, primary receiver cannot decode the signal properly.

Γ_S The sensed power level at the cognitive transmitter.

Γ_O Power threshold at cognitive transmitter that determines the presence of the primary user transmission. If the sensed power level at the cognitive transmitter is below this threshold (i.e., $\Gamma_S < \Gamma_O$), then it can be assumed safely that primary user is not active on that sensed channel. This threshold can be calculated based on the probability of false alarm and detection requirements [40] and [15].

Γ_U Power threshold at cognitive transmitter for underlay transmission. If the sensed power level (Γ_S) is such that $\Gamma_O < \Gamma_S < \Gamma_U$, then it can be assumed that cognitive user can safely transmit in underlay mode without exceeding the interference threshold of the primary receiver. If the sensed power level at the cognitive transmitter is above this threshold (i.e., $\Gamma_S > \Gamma_U$), then it can be assumed that the primary user is active and underlay transmission of the cognitive user may affect the primary system. This threshold can be calculated using the sensed signal level $P_p L(R + D)$. Following, the

location of the primary transmitter can be estimated $(R+D)$ and then the interference range D can be calculated. Hence, with the received signal level Γ_S, the distance and the corresponding interference level can be calculated for a specific transmission power level P_U. Note that Γ_U is a specific sensed power level, at which the underlay transmission with power P_U causes interference to exceed the interference threshold (γ_s) to the primary system.

The above discussed scenarios are summarized as follows:

- State B : $\Gamma_S > \Gamma_U$, No transmission
- State I : $\Gamma_S < \Gamma_O$, Interweave transmission
- State U : $\Gamma_U > \Gamma_S > \Gamma_O$, Underlay transmission

As mentioned in Section 3.1.2, in a cognitive radio system with positively correlated primary user traffic, cognitive user will stay or leave a primary channel when the sensed state of that channel is idle or busy respectively. When the channel is in State U, the cognitive user can stay in that channel with underlay transmission until that channel becomes State B or, cognitive user can switch that channel and look for interweave transmission (State I). When switching, cognitive user may end up with a channel with State B and it may reduce the throughput. Following our framework and analysis, a cognitive user can decide, based on the primary user network statistics, which mode of transmission (underlay/interweave) gives better long term throughput as evident from the figures from Section 3.3.

Further, we assume that the primary user's transition matrix (T) as a long term statistic and not instantaneous quantity. The cognitive user can monitor the network over a period of time and, based on the sensed power level of the primary user Γ_S with the thresholds Γ_O and Γ_U, it can build and model the primary user statistics (state transition matrix,

T) [30]. Also, the cognitive users can use any learning algorithms to model the primary user statistics [41] [42]. Another approach is to use databases where these statistics can be stored and provided to cognitive users upon request.

3.3 Analytical Results and Discussion

In this section, we present and discuss the performance difference between the two schemes. The transition probabilities are randomly picked to do the analysis. The Monte-Carlo simulation results are compared with analytical results in Fig. 3.8 for different transition probabilities of P_{BI} (busy to idle) when the data ratio $\frac{R_U}{R_I}$ is 0.6. As noted in the figure, analytical and simulation results are in close agreement. We verified the analysis with simulation results for other transition probabilities as well.

As we mentioned earlier, we assume that the primary user traffic is positively correlated with time. That is, when a primary user occupies the channel, it stays in that channel for few slots ($P_{BB} > \{P_{IB}$ or $P_{UB}\}$). Based on this assumption, we evaluated the underlay-interweave mode selection strategy for the cognitive user. Our analysis and simulation show the best strategy selection under this scenario (that is, cognitive user switches the channel when it senses the primary channel as busy). The strategy selection may change for other scenarios such as with ($P_{IB} > \{P_{BB}$ or $P_{UB}\}$) or ($P_{UB} > \{P_{IB}$ or $P_{BB}\}$) and, those cases are not shown in the plots. We believe the analysis for other scenarios can be done similarly by following the same steps and principles for the considered case.

3.3.1 Different primary user characteristics in channel sharing mode

When the primary user occupies the channel, it can stay in that channel for longer/shorter duration or it can share the channel with the cognitive user. Longer the primary user occupies the channel alone, lower the throughput of the cognitive user will be. In Fig. 3.9, the throughput performance for different transition probabilities P_{BU} are considered for the above scenario. As $P_{BB} + P_{BI} + P_{BU}$=1, for a specific P_{BI}, if P_{BU} is higher, then P_{BB} would be lower. That is, if a primary user uses the channel (busy) for a short duration then the cognitive user's throughput would be higher. We can see from Fig. 3.9 that depending on the length of stay of a primary user, different strategies can be chosen by the cognitive user. When the primary users stays longer in a channel (i.e., P_{BB} is higher), the Strategy A is useful. That is, cognitive user should look for an idle/sharing channel. The exact strategy switching thresholds can be found from the analysis for different primary user characteristics. In Fig. 3.9, it is found that the Strategy B performs better when $P_{BI} > 0.1$ for $P_{BU} = 0.4$ and when $P_{BI} > 0.22$ for $P_{BU} = 0.1$ respectively. Similarly, we can select the best strategy provided the statistical data of primary users are given.

3.3.2 Different data rates in channel sharing

The strategy selection not only depends on the primary user characteristics but also on the data rate of the cognitive user when sharing the channel. As discussed earlier, there exists a strategy switching threshold that directs the best strategy to follow. This threshold changes with different data rates. We consider the ratio between the data rate of the cognitive user when sharing the channel with primary user (R_U) and the data rate when using the channel alone (R_I). We do not assume any specific data rates, rather consider the ratio to make

the analysis more generic. The throughput performance comparison is shown in Fig. 3.10 and Fig. 3.11 for different data rates while sharing the channel with primary user for the ratio of 0.3 and 0.6 respectively. As expected, Strategy A performs better when the $\frac{R_U}{R_I}$ ratio increases. Hence, we can also see that for $P_{IU} = 0.1$, the strategy switching point shifts from $P_{IB} = 0.3$ to $P_{IB} = 0.2$ when $\frac{R_U}{R_I}$ changes from 0.3 to 0.6 while other transition probabilities are kept fixed. That is, when the shared channel data rate (R_U) of a cognitive user increases, the Strategy A performs better. These analytical figures give better understanding of the throughput performance of the cognitive users in these different strategies. In Fig. 3.10, we can see that proper use of strategy gives up to 8% throughput advantage when $P_{IB} = 0.1$. Similarly, we can find different thruput advantage for different conditions.

In Fig. 3.12, the strategy selection criteria for different throughput ratio (R_U/R_I) are shown for different set of primary user statistics. For example, when $R_U/R_I = 0.6$ and $P_{BI} > 0.23$, it is better to select Strategy B. Also, we can see from Fig. 10 that for higher R_U/R_I, the strategy selection is towards Strategy B (underlay) when the probability P_{UU} is higher. These data can be calculated analytically form our framework for different primary user statistics and can be stored in a lookup table, if needed, to speed up the decision process by the cognitive users to select the optimal transmission mode.

3.4 Chapter Summary

In this chapter, we analyzed two different opportunistic access strategies with different primary user channel conditions where the cognitive user can use an idle channel alone or can share with primary user under certain circumstances. When the primary user channel characteristics are given, we can find the best access strategy for the cognitive user from our analysis. When the data rate ratio (R_U/R_I) increases, the Strategy A (underlay access,

sharing the channel) performs better for a positively correlated primary user traffic. That is, it is beneficial for a cognitive user to look for an idle/shared channel. If the ratio decreases, it is better to look for an idle channel only (Strategy B (interweave), access without sharing the channel). If a primary user occupies the channel (busy) for a long period, then it is better to look for Strategy A. The exact strategy switching thresholds (mode selection) can be found from our analysis and it depends on the transition probabilities of the primary user and the throughput ratio between the two modes of operation. The proper strategy selection can provide throughput gain over the other based on the scenario. The performance loss due to imperfect sensing and the gain due to sensing of multiple channels can be evaluated when using the proposed transmission mode selection.

In this chapter we assumed perfect sensing of channel in the interweave-underlay cognitive system. However, in practice, there would be errors in both sensing and acknowledgement. Hence, in the following chapter, we analyze the optimal access strategy of a cognitive user in a single primary channel of a hybrid interweave-underlay system with sensing and/or acknowledgement errors.

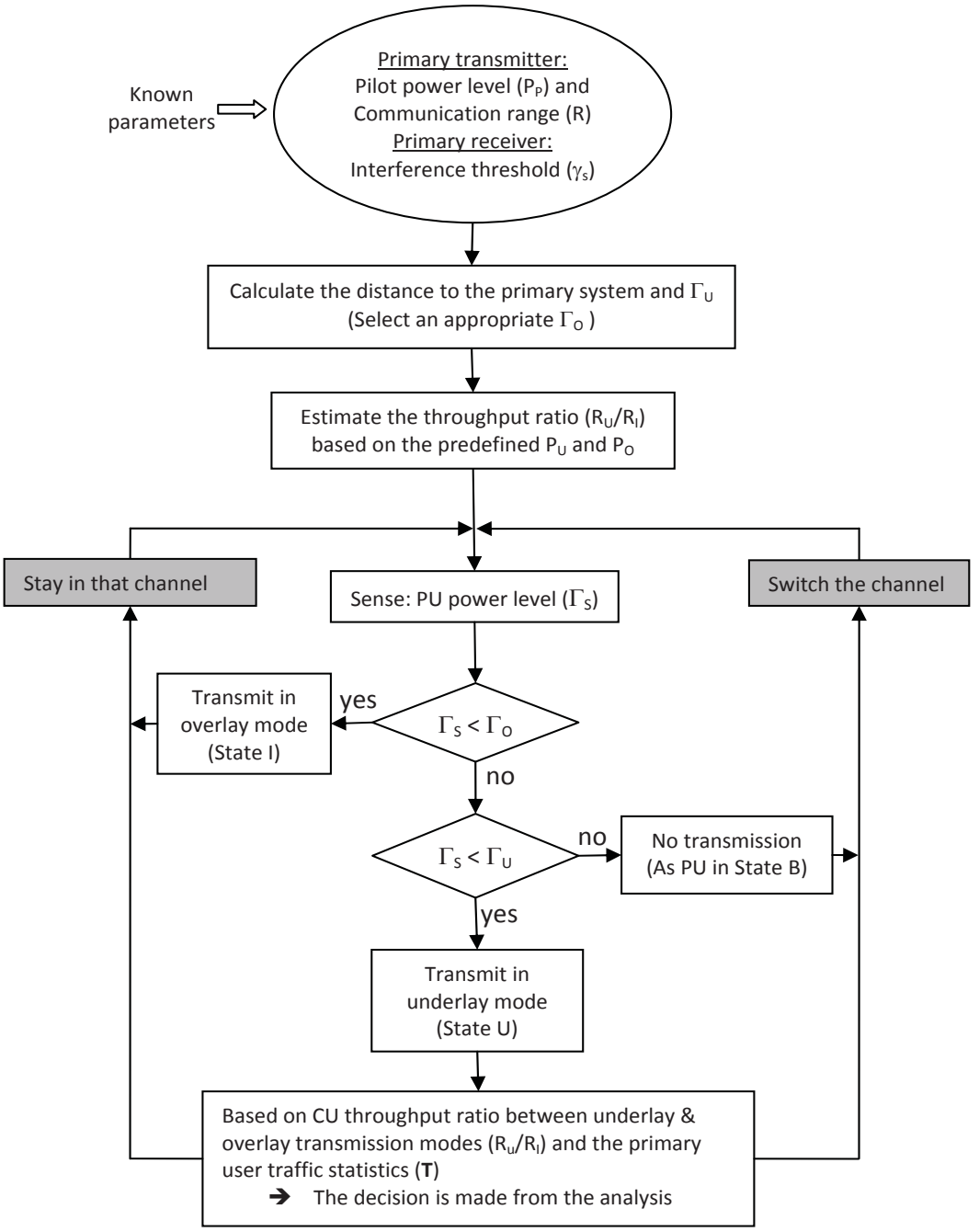

Figure 3.7: Flowchart: The decisions made in the shaded boxes are by assuming that the primary user occupancy is positively correlated with time.

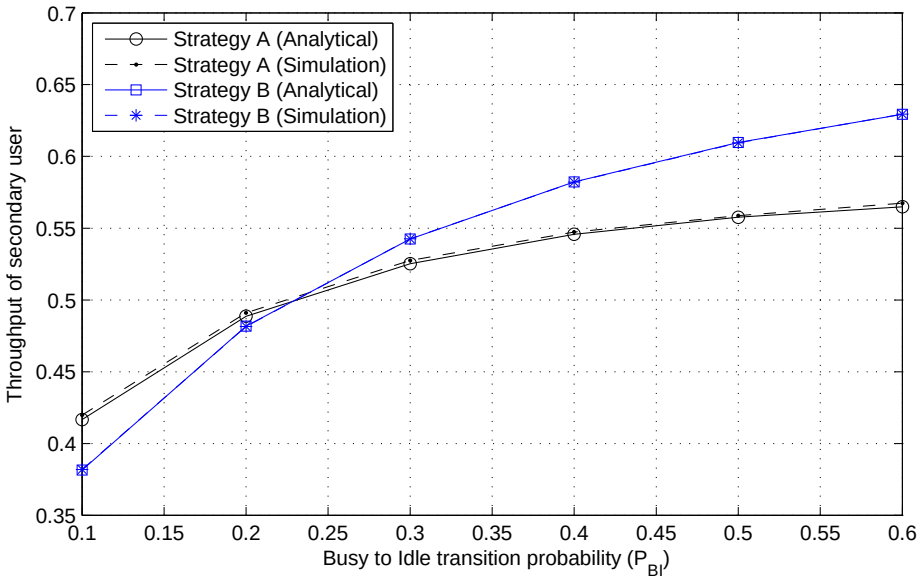

Figure 3.8: Analytical and simulation throughput performance comparison for different P_{BI}. $\frac{R_U}{R_I} = 0.6, P_{BU} = 0.1, P_{UB} = 0.3, P_{UI} = 0.1, P_{IU} = 0.3, P_{IB} = 0.2$.

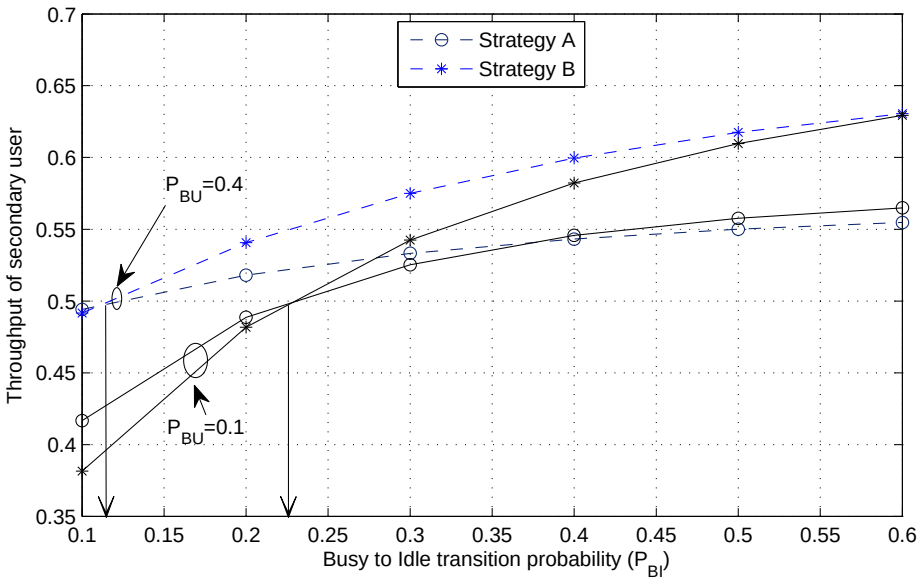

Figure 3.9: Throughput performance for different P_{BI} and P_{BU} for $\frac{R_U}{R_I} = 0.6$. $P_{UB} = 0.3, P_{UI} = 0.1, P_{IU} = 0.3, P_{IB} = 0.2$.

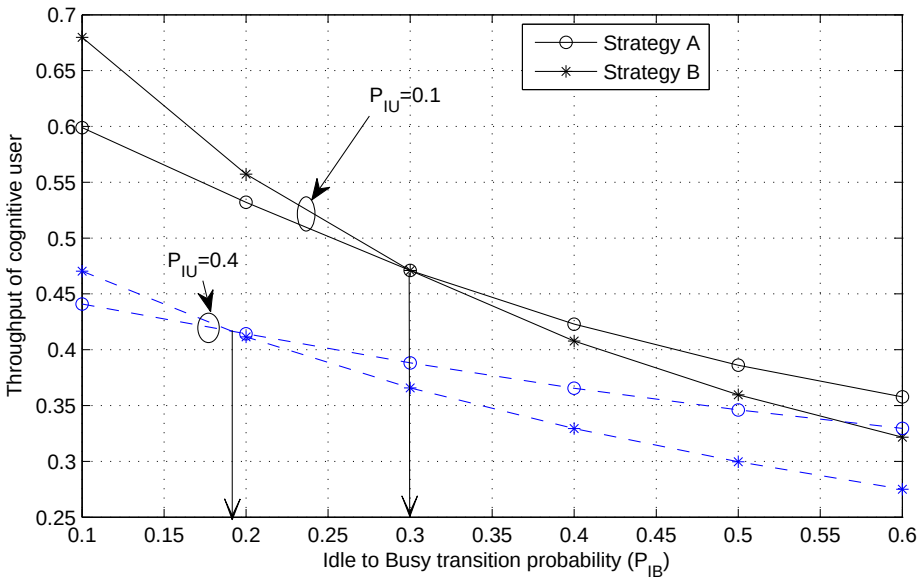

Figure 3.10: Throughput performance for different P_{IB} and P_{IU} for $\frac{R_U}{R_I} = 0.3$. $P_{UB} = 0.1, P_{UI} = 0.2, P_{BU} = 0.3, P_{BI} = 0.1$.

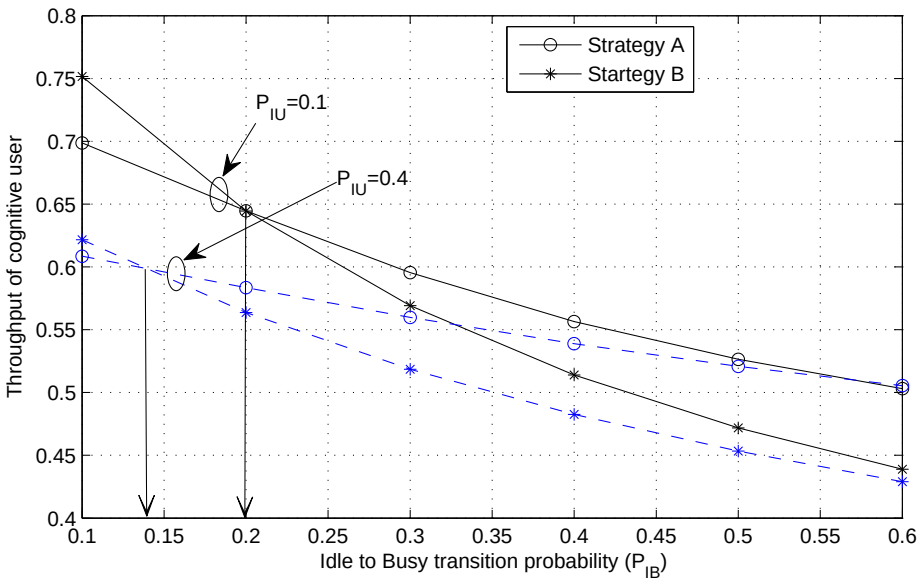

Figure 3.11: Throughput performance for different P_{IB} and P_{IU} for $\frac{R_U}{R_I} = 0.6$. $P_{UB} = 0.1, P_{UI} = 0.2, P_{BU} = 0.3, P_{BI} = 0.1$.

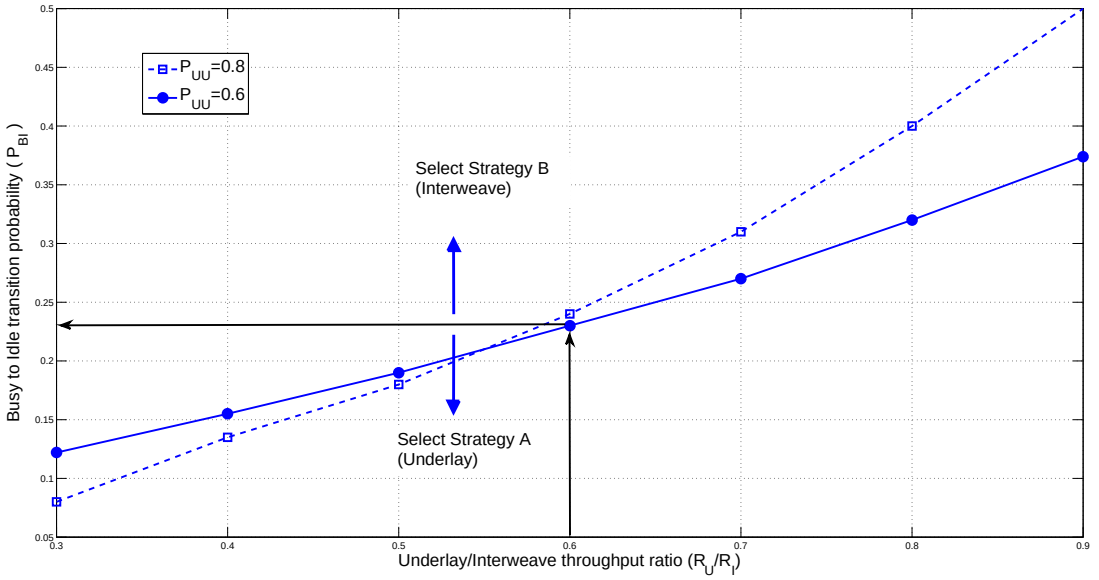

Figure 3.12: Strategy selection for different throughput ratio $(\frac{R_U}{R_I})$ $(P_{BU} = 0.1, P_{UB} = 0.3, P_{UI} = 0.1, P_{IU} = 0.3, P_{IB} = 0.2)$

Chapter 4

Channel Access in Interweave-Underlay Cognitive Radio System with Imperfect Sensing

In the previous chapter, we analyzed the channel switching strategy in a hybrid underlay-interweave system. There, we assumed that there are no channel sensing or receiver acknowledgement errors. In this chapter, we find an optimal access strategy of a primary channel given that the sensing is erroneous. While optimal and suboptimal myopic access strategies are investigated in the literature for two-state interweave primary user systems, in this chapter we consider and analyze the performance of a cognitive radio system when there are three possible hidden states. We propose *forward algorithm* to update the belief of the activity states of the primary user using information from two sources: the sensor output at the transmitter and the feedback signal from the receiver. Using these beliefs, the controller at the transmitter takes decision on the spectrum access and the power allocation based on the optimal alpha vectors calculated using finite-horizon POMDP formulation

and incremental redundancy solution technique. We compare the throughput that can be obtained using the forward algorithm based scheduler for partially observable state system with the optimal scheduler for completely observable state system. Our contributions in this chapter can be summarized as follows:

- Investigating the spectrum access and power adaptation techniques for an opportunistic cognitive user in a cognitive radio network to optimize its throughput with specified sensing error limit to avoid the unnecessary collision with the primary user where the primary users' states are hidden,

- Formulating the problem as a finite-horizon partially observable Markov decision process with the objective of maximizing the throughput, where the actions are no-transmission and transmission with any of the two pre-set power levels based on interweave/underlay modes.

- Proposing and analyzing a forward algorithm based technique that updates belief using the sensor output in the first slot and using the positive/negative acknowledgment (ACK/NAK) feedback of the previous time-slots in the rest of the slots of a frame to reduce the sensing burden to the cognitive user.

The chapter is organized as follows. In Section 4.1, we describe the system model for the considered problem. The formulation of the problem as a POMDP and its optimal solution techniques are given in Section 4.2. Above problem is analyzed with a practical limited sensing scenario in Section 4.3. We provide simulation results in Section 4.4 and conclude in Section 4.5.

4.1 Interweave-Underlay System Model with Sensing Error

We consider a cognitive radio system where the primary users own the channels and a cognitive user uses those channels when they are unused by the primary users. We assume that the time is discretized into time-slots of duration T_{slot} sec and several discrete time-slots constitute a radio frame of duration $T_f = H \times T_{slot}$, where H is called the horizon of the problem. Each time-slot possibly consists of sensing time T_s sec and data transmission time $T_d = T_{slot} - T_s$ sec as shown in Fig. 4.1(a). Data transmission time also includes the control and feedback signal times. At the beginning of a radio frame, a cognitive user decides how many channels and which channels to sense and then it carries out the out-of-band spectrum sensing. Our model is general enough to accommodate any physical layer (PHY) in-band channel sensing schemes. We assume that the performance of the channel sensing scheme only affects the accuracy of the mis-detection and false alarm probabilities, P_{MD} and P_{FA}. We assume that depending on the out-of-band sensing results, the cognitive user picks up one or more best channels and starts transmitting on that channels for the remaining of the time-slots. In the next time-slot of the frame, the cognitive user carries out in-band spectrum sensing and transmits packets if it is still free. In the next horizon, the cognitive user again starts the out-of-band or in-band channel sensing and selection depending on its strategy and the availability status of the previously occupied channel, and then repeats the transmission process. Upon receiving the data packet, the receiver sends an ACK/NAK feedback for the transmission. Let P_{fe} denote the probability of feedback error.

Problem Formulation: POMDP Based Interweave-Underlay Mode Selection

We are concerned with the problem of optimal utilization of the channel and adaptation of power based on interweave-underlay mode selection in order to maximize the throughput and avoid the collision occurrence in a cognitive radio system. Since the exact instantaneous state of the primary user is unknown to the cognitive user, but the cognitive user wants to adapt the transmission with respect to primary user activity, the problem falls in the scope of partially observable Markov decision process (POMDP), which has the following ingredients: a set of states $\mathcal{S}$, a set of actions $\mathcal{A}$, transition probability matrices $\mathcal{P}_s$, a set of observations $\mathcal{O}$, observation probability matrices $\mathcal{Q}$, and reward matrix $\mathcal{R}$.

System States

Let us assume that $\mathcal{S} = \{B, U, I\} = \{s_1, s_2, s_3\}$ denotes the set of activity modes of the primary users as determined by the cognitive user, where B, U and I correspond to busy (s_1), concurrent (s_2) and idle (s_3) states respectively.

The brief description of the states are given below:

1. Busy State $B(s_1)$: The primary user occupies the channel and does not expect any kind of channel access by the cognitive user. When a cognitive user tries to access the channel while primary user is in state B, it will cause undesirable interference to primary user.

2. Concurrent State $U(s_2)$: The cognitive user can transmit simultaneously with the primary user, possibly using lower transmission power than that in state I. In this state, the receivers of the primary user network do not need higher quality of service (QoS) requirement and it can tolerate a higher level of interference than normal (i.e., than in state B). In this state, the cognitive user transmitter may also use dirty paper

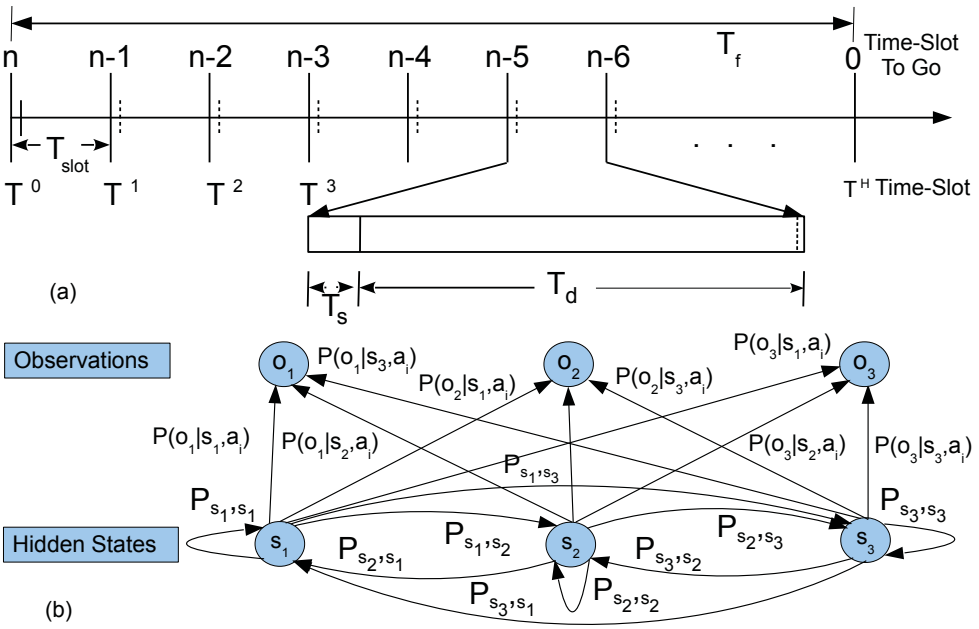

Figure 4.1: (a) An illustration of the radio frame and the slot structure. (b) The state diagram and observations for the POMDP problem.

coding techniques to zero-force interference for its own receiver's signal and uses a part of its power to amplify and relay primary user signal to compensate the interference it causes.

3. Idle State $I(s_3)$: The channel is completely free to use by the cognitive user. The cognitive user can use it with any actions. Although all actions are allowable in state I, higher power action is most preferable since it can transmit at higher rate with this action.

Power Adaptation Actions based on interweave-underlay mode selection

During a radio frame, at each time-slot, the controller of the cognitive transmitter takes decision whether or not to access the channel. The controller also decides what power it

will use to transmit data to the cognitive receiver if the channel is not in state B. Let $\mathcal{A} = \{a_1, a_2, a_3\} = \{\text{zero power, low power, high power}\}$ be the set of power actions, where each action corresponds to a specific transmission rate for the corresponding power. Note that action a_1 corresponds to no transmission when the primary user in state B. When the primary user is in state U (concurrent), low power transmission is available (underlay mode of transmission) and when the primary user is in state I (idle), cognitive user may transmit with high power (interweave mode of transmission).

State Transition Matrix

The transition probability matrix for a particular action expresses the probability of switching from one state to another, and for action $a_i \in \mathcal{A}$, it can be written as,

$$\mathcal{P}_s(a_i) = \begin{bmatrix} P_{BB}(a_i) & P_{BU}(a_i) & P_{BI}(a_i) \\ P_{UB}(a_i) & P_{UU}(a_i) & P_{UI}(a_i) \\ P_{IB}(a_i) & P_{IU}(a_i) & P_{II}(a_i) \end{bmatrix}. \tag{4.1}$$

Note that state transitions of the primary user activity are independent of the cognitive user's choice of action for the problem at hand. Therefore, we can write, $P_{s_i s_j}(a_i) = P_{s_i s_j}, \ \forall a_i \in \mathcal{A}$.

State Observation and its Probability

The sensing outcomes on the hidden system state form the observation vector $\mathcal{O}_s = \{o_1, \ o_2, \ o_3\} = \{\hat{B}, \ \hat{U}, \ \hat{I}\}$, where $o_1 = \hat{B}$, $o_2 = \hat{U}$ and $o_3 = \hat{I}$ are the spectrum sensor's outputs for corresponding hidden states B, U and I respectively. The relationship between the spectrum sensor outputs and the hidden states are shown in Fig. 4.1(b), where the probability of a state being in a particular state for a particular action is expressed in terms of observation probabilities $P(o_j|s_i, a_k), \ s_i \in \mathcal{S}, o_j \in \mathcal{O}, a_k \in \mathcal{A}$.

Reward Matrix

At the beginning of a time-slot, the system moves to the next state according to the state transition probability matrix of the hidden core process (primary user activity process) and an observation of the state is received through spectrum sensor. The controller at the cognitive user transmitter takes an action based on the updated belief of the state. The system also receives a reward or incurs a cost depending on the action choice. The controller chooses action that is expected to give best reward. Let $R_{s_i}(a)$ denote the reward value received in state s_i if action a is chosen. Therefore, the reward values for each state should be assigned in such way so that the controller chooses best action. In this chapter, unless specified otherwise, we use superscript t, $t = 0, 1, \cdots, H$ to denote a variable at time-slot T^t. For example, the state of the primary user at time-slot T^t is represented as s^t. Contrary, we use subscript n to denote n time-slots to go to reach the end of the horizon as shown in Fig. 4.1.

4.2 Optimal Solution Techniques

For the considered POMDP problem, the cognitive user transmitter only know the observations probabilities. Therefore unlike MDP problem (where the states of the system are completely observable, i.e., observation probability is either 1 or 0), the optimal solution for POMDP problem cannot be found using dynamic programming algorithm. However, information state vector, which can be tracked and updated with the observations, provides sufficient statistics for POMDP problem.

Information State

An information or belief vector, Z is a probability distribution over the set of states $\mathcal{S}$, where $Z(s)$ is the probability associated with hidden state s, called information state of state s. Note that the value of $Z(s)$ is a continuous positive real number and bounded by 0 and 1. The information state at time-slot T^t can be calculated when the sequence of observations and actions so far are known using relation: $Z(s^t) = P(s^t|a^{t-1}, o^{t-1}, \cdots, a^0, o^0, s^0)$, where o^0 and a^0 are the observation and corresponding action at the starting time-slot T^0. It can be noted that this conditional probability is essentially a filtering task, and the new information state can be calculated recursively from the previous information state and the new observation-action pair. At any time, information vector is a sufficient statistic of the past sequence of observations.

If $Z(s^t)$ is the previous information state, and the agent perceives observation o^t and takes action a^t, then the new information state at time-slot T^{t+1} is given by,

$$Z(s^{t+1}) = \alpha P(o^t|s^{t+1}, a^t) \sum_{s^t} P_{s^t,s^{t+1}}(a^t) Z(s^t), \tag{4.2}$$

where α is a normalizing constant that makes the information state sum to be 1. We can write transformation function $Z(s^{t+1}) = T(Z|a, o)$ as,

$$Z(s^{t+1}) = \frac{P(o^t|s^{t+1}, a^t) \sum_{s^t} P_{s^t,s^{t+1}}(a^t) Z(s^t)}{\sum_{s^{t+1}} P(o^t|s^{t+1}, a^t) \sum_{s^t} P_{s^t,s^{t+1}}(a^t) Z(s^t)}. \tag{4.3}$$

Transformation function $T(Z|a, o)$ updates the information state $Z(s^t)$, $\forall s^t \in \mathcal{S}$ at time-slot T^t to the information state $Z(s^{t+1})$, $\forall s^{t+1} \in \mathcal{S}$ at time-slot T^{t+1}. Once the observation probabilities are known, we can find the term $P(o^t|s^{t+1}, a^t)$, $\forall s^{t+1} \in \mathcal{S}$ by $P(o^t|s^{t+1}, a^t) = \sum_{s^t \in \mathcal{S}} P(o^t|s^t, a^t) P_{s^t,s^{t+1}}(a^t)$. It can be noted that the observation probability of a state is dependent only on the underlying hidden state and is independent of the action. Therefore, we can write $P(o^t|s_i, a^t) = P(o^t|s_i)$, $\forall o^t \in \mathcal{O}$, $s_i \in \mathcal{S}$.

Value Function

The value functions are mappings from the information states to expected discounted total reward. Let $V_n(Z)$ be the maximum expected reward that the system can accrue during the lifetime of the process if the current information vector is Z and there are n slots remaining before the process terminates. The recursive equation for the value function can be written as,

$$V_n(Z) = \max_{a \in \mathcal{A}} \left[Z.\mathcal{R}(a) + \gamma \sum_{o \in \mathcal{O}} P(o|Z,a) V_{n-1}[T(Z|a,o)] \right], \tag{4.4}$$

where $0 < \gamma \leq 1$ is a discount factor for the expected reward and $P(o|Z,a) = \sum_{s_i=B}^{I} Z(s_i) \sum_{s_j=B}^{I} P_{s_i s_j}(a) P(o|s_j,a)$ is the probability of observing output o if the current information vector is Z and action a is taken. Therefore, the value for an information state Z is the value of the best action that can be taken from Z of the expected immediate reward for that action plus the expected discounted value of the resulting information state. Value function $V_n(Z)$ is piecewise, linear and convex [43]. It can be written as,

$$V_n(Z) = \max_{k} \left[\sum_{i=1}^{i=3} \alpha_i^k(n) Z(s_i) \right], \tag{4.5}$$

for some set of vectors, called α-vectors, $\alpha^k(n) = [\alpha_1^k(n), \alpha_2^k(n), \alpha_3^k(n)]$, $k = 1, 2, \cdots$. The exact numbers of $\alpha-$vectors depend on the numbers of action-observation pairs. It is clear from the above relation (4.5) that once the alpha vectors for various time-slots in the horizon are calculated, the policy that maximizes $V_n(I)$ for a given information vector is the optimal policy.

Algorithm for Calculating Alpha Vectors

There exist several algorithms (e.g., enumeration, witness and incremental pruning) to find the optimal policy for the formulated finite-horizon discounted reward POMDP problem,

where the algorithm calculates the best policy for a given information vector in each time-slot during the finite horizon. In [43], the authors have discussed different techniques for calculating the alpha vectors for (4.5) and their relative merits and limitations. In this paper, we use incremental pruning algorithm to calculate the alpha vectors over the horizon, which is shown to perform the best in [43]. The basic idea behind this algorithm is to form transformed value function sets for a particular action and all observations, and then combining all choices incrementally observation by observation (e.g., value functions for first and second observations are combined first, then the results are combined with third, and so on) to find dominant sets. The process is repeated for the other actions and then the alpha vector sets are obtained by combining and eliminating dominated sets.

PHY Optimal Policy with Every Time-Slot Sensing (POPETS)

Once the alpha vectors are determined for a problem, the next steps for finding optimal policy works as follows:

1. in every time-slot, the scheduler obtains the observation and it updates the information vector. The initial information vector is initialized randomly,
2. the value of information vector is plugged into the respective slot's alpha vector sets
3. the alpha vector that maximizes the value function for the information vector is the optimal alpha vector and the corresponding action is the optimal action.

4.3 Limited Sensing Policy

The optimal policy for the POMDP problem requires channel sensing in all the time-slots in a frame. However, sensing in all the time-slots consumes both the bandwidth and the power

for sensing. Since ACK/NAK information for the previous time-slot is already known at the link-layer. Using cross-layer interaction, the scheduler at the PHY can use those already available information to reduce the burden of sensing.

We propose a novel cross-layer policy with first time slot sensing (XLPFTS) using the forward algorithm that estimates and maintains the probability distribution of the states, also called belief, from both the sensing observation result and the feedback ACK/NAK observations. We assume that the transmitter senses the channel in the first time-slot and thereafter it uses feedback observation during the rest of the slots to update the belief of the states. The belief of the states in each time-slot is then used to pick up the best alpha vector and associated action using (4.5). We discuss the forward algorithm that deals with the updating and propagating the belief below.

Hidden State Belief Estimation

Suppose $O_{1:m} := o_1, o_2, \cdots, o_m$ denotes a given sequence of observations (either from sensor or from feedback). Therefore, the probability of state s_i given the observations can be written as:

$$f_{o:m}(s_i) = P(s^m = s_i | o_1, o_2, \cdots, o_m, \pi), \tag{4.6}$$

where π is the belief of the states at the starting time-slot. When current belief and the new observation are known, the belief of the hidden states can be updated iteratively as follows:

$$\mathbf{f}_{o:m}(s_i) = \mathbf{O}_d \mathcal{P}_s \mathbf{f}_{o:m-1}, \tag{4.7}$$

where $\mathbf{O}_d$ is the diagonal observation matrix whose diagonal elements $\mathbf{O}_d[i, i]$ are the observation probabilities for states $s_i \in \mathcal{S}$ and other elements are zeros.

After normalizing the probabilities so that the sum is equal to 1, we can write the

normalized belief vectors as follows:

$$\hat{\mathbf{f}}_{o:m} = \beta \mathbf{O}_d \mathcal{P}_s \hat{\mathbf{f}}_{o:m-1}, \tag{4.8}$$

where β is the normalizing factor.

Belief Update in the First Slot

In order to utilize unused spectrum opportunistically and at the same time avoid interference to the returning primary users, spectrum sensing is done periodically. Among the different spectrum sensing methods, energy detection is the most popular due to its simple design and smaller sensing time [12]. Without loss of generality, we continue our discussion using energy detection technique, where the collected energy after sampling and frequency domain operations forms the test statistics, $X(y)$ of the energy detector's received signal y. The probability density function (pdf), $p(y)$ of the test statistic can be approximated by a Gaussian distribution [15]. The cognitive user transmitter senses the channel energy and compares with two different thresholds ζ_1 and ζ_2 to determine the state of the primary user [19].

The probability of false alarm $P(\hat{B}|I)$, which is the probability of the sensor falsely declaring the presence of primary signal in lower state when it is actually in upper state, can be written as $Pr(X(y) > \zeta_1|I)$. The probability of mis-detection $P(\hat{I}|B)$, which is the probability of the sensor incorrectly declaring the presence of primary signal in state that is upper than actual state, can be written as $Pr(X(y) < \zeta_2|B)$. Similarly, other false alarm probabilities $P(\hat{U}|I)$ and $P(\hat{B}|U)$, and mis-detection probabilities $P(\hat{U}|B)$ and $P(\hat{I}|U)$ can be evaluated using appropriate thresholds. The diagonal observation matrix O_d, for observation $\hat{B}$ in (4.7), can be written as $O_d = \text{diag}(P(o_1|B),\ P(o_1|U),\ P(o_1|I))$.

Belief Update in the Other Slots

In a particular time-slot, in state s^t when the controller takes a particular action a^t, the cognitive transmitter obtains an observation using the feedback from the receiver. When the receiver receives the packet sent from the transmitter successfully, it sends an ACK. Therefore, when an ACK is received, the transmitter assumes that no collision occurred with primary user's transmission. The absence of ACK is interpreted as collision with the primary user's transmission.

Hence, the set of feedback observations can be written as $\mathcal{O}_f = \{q_1, q_2\}$={No Collision, Collision}. Although the actual states of the primary user's activity are hidden, the cognitive user gets an idea of them using the previous observations. The relationship between the actual state and the observation for each action can be expressed in terms of 3×2 feedback observation matrix and can be expressed as $\mathcal{Q} = [q_{ik}]$, where $q_{ik} = P(q^t = q_k | s^t = s_i i, a^t),\ q_k \in \mathcal{O}_f, s_i \in \mathcal{S}$. The diagonal observation matrix O_d can be written for ACK (no collision) feedback as follows: $O_d = \text{diag}(q_{11}, q_{21}, q_{31})$.

4.4 Simulation Results and Discussion

In this section, we present simulation results for the PHY-optimal policy and the cross-layer policy using Monte-Carlo technique for 10^6 time-slots. As discussed before, the belief of the states is updated using sensing information in each time-slot for POPETS. For XLPFTS case, it is updated using channel sensing information in the first time-slot and using previous ACK/NAK information in the other time-slots. We compare both policies with the fully observable optimal policy (FOOP) that gives maximum possible throughput over the simulation period. The throughput results for FOOP are obtained assuming that states are completely known and the action that gives maximum throughput without any collision

are chosen. For both POPETS and XLPFTS cases, the action for a particular time-slot is obtained by substituting the respective updated belief in (4.5). Note that the alpha vectors are obtained using incremental pruning algorithm.

We assume that spectrum sensing requires 10% (approximately 1ms [12]) of time in a slot. The duration of each slot is $T_{slot} = 10$ ms [44]. The horizon length (frame size), H is varied from 2 to 20. The number of radio frames for each scenario is found according to the frame size, H. Although any activity statistics of primary user are valid for the problem, without loss of generality, we consider three cases where the self-transition probabilities, $P_{st} = P_{s_i s_i},\ s_i \in \mathcal{S}$ are 0.99, 0.97 and 0.95. When in state B and I, the adjacent transition probability, $P_{s_i s_j},\ |i-j| = 1$ is $0.8(1-P_{s_i s_i})$ and other transition probability is $0.2(1-P_{s_i s_i})$. When in state U, both adjacent states are equally probable, i.e., $P_{s_i s_j} = 0.5(1-P_{s_i s_i}),\ |i-j| = 1$. We use the following rewards so that the occurrence of collision among primary user and cognitive user can be avoided: $R_B(a_1) = 0,\ R_U(a_2) = 1,\ R_I(a_3) = 2,\ R_I(a_2) = 1$, and others are -1. We use positive reward and negative reward for an action when it is expected and is not expected in a state respectively. That is, the negative value discourages the scheduler for taking actions when a higher positive reward exists. For example, when in state B, action a_2 and a_3 are not permitted as both of these two actions will introduce interference to the primary user. Therefore, the rewards corresponding to these actions in state B are negative. The reward for action a_1 is zero, which is better than negative reward, so the scheduler chooses a_1 over a_2 and a_3. In state U, our expected action is a_2 because a_3 will introduce interference and a_1 will miss spectrum opportunity. Likewise, in state I, expected action is a_3, but a_2 is permitted since it does not either introduce interference or miss spectrum opportunity. The reward is lower because the throughput obtained using a_2 is less than that using a_3. Action a_1 is not expected in state I as discussed above. Note that the reward matrices are not the same as throughput matrices. We assume that we receive

throughput of 1 and 2 for actions a_2 and a_3 respectively when no collision happened. In state $s_i \in \mathcal{S}$ collision occurs for action $a_j \in \mathcal{A}$ when $i < j$. We use 1 and 0 to express collision and successful events find average collision per-slot. We have found that the policy does not depend on the initial belief and therefore, it is initialized to steady-state vector.

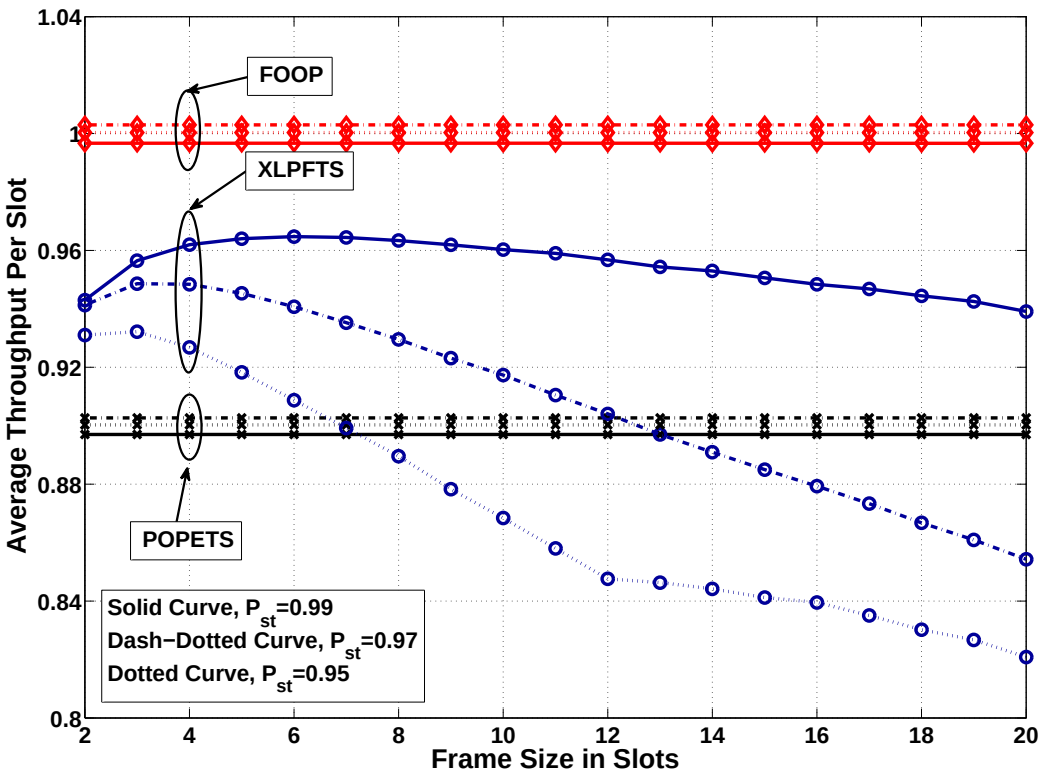

Figure 4.2: Throughput vs horizon size when sensing/feedback error is zero

In Figs. 4.2 and 4.3, we show the average throughput and the average collision for the three policies discussed above with self-transition probability, P_{st} as parameter and assuming zero sensing and feedback errors. It can be interestingly seen that when $P_{st} = 0.99$, the effective throughput obtainable in the XLPFTS is greater than the POPETS case for every size of the horizon. However, the average collision for XLPFTS case is slightly less than 0.5% while it is zero for POPETS. Since POPETS case loses $0.1T_{slot}$ sec in every slots and XLPFTS loses that only in first time-slot, the average throughput per slot is more for the latter. As

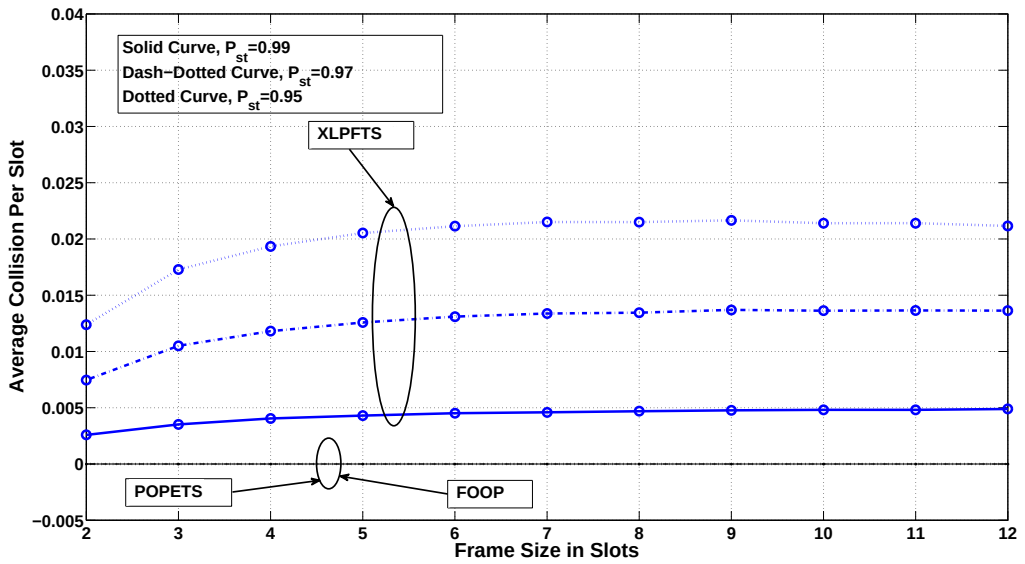

Figure 4.3: Collision vs horizon size when sensing/feedback error is zero

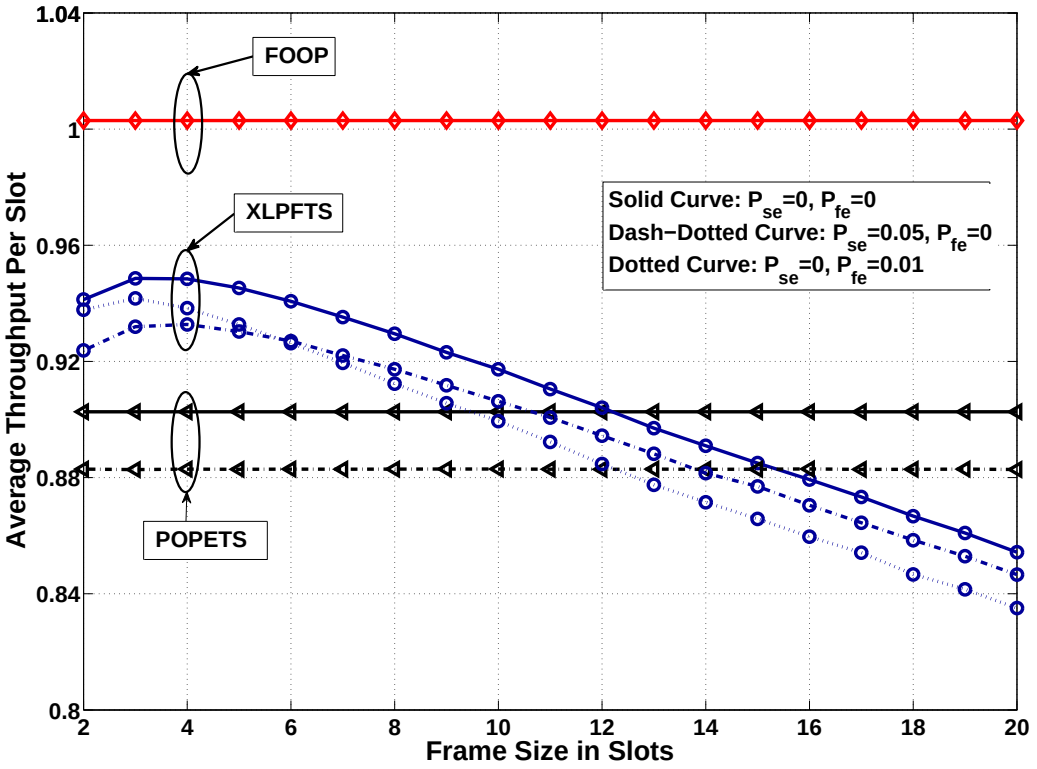

Figure 4.4: Throughput vs horizon size for non-zero sensing and feedback error

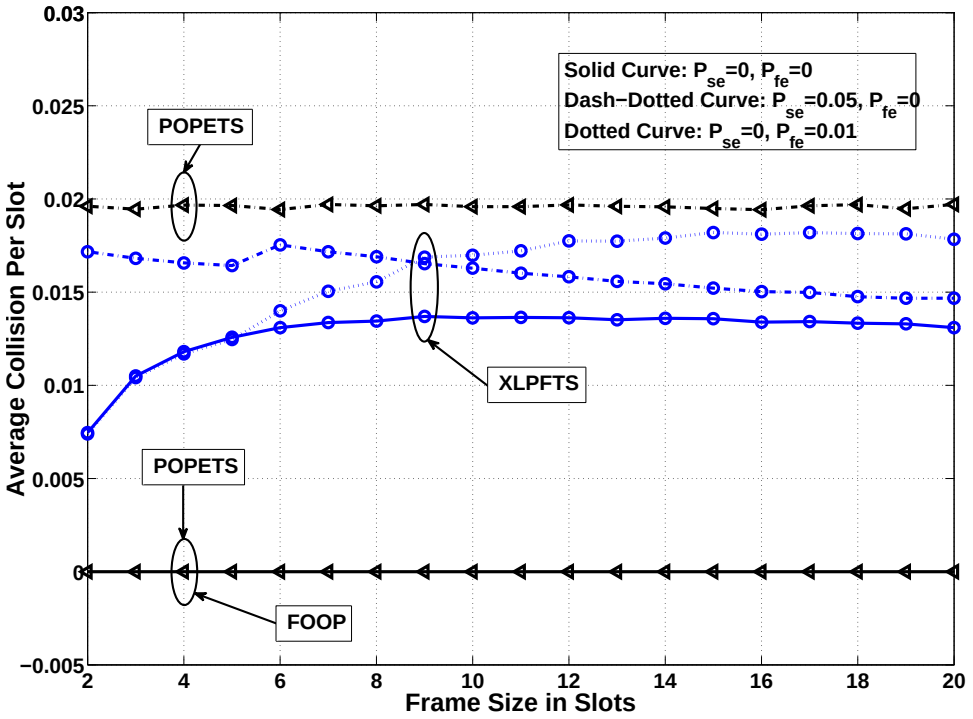

Figure 4.5: Collision vs horizon size for non-zero sensing and feedback error

the channel self-transition rate decreases to 0.97 and then to 0.95, XLPFTS case gives more throughput up to $H = 12$ and $H = 7$ respectively. The average collision also increases as the channel mixing rate and horizon size increases.

We show the effect of spectrum sensing error and feedback errors for $P_{st} = 0.97$ in Figs. 4.4 and 4.5 respectively. It can be noted from the figures that as the sensing error probability, $P_{se} = P_{MD} = P_{FA}$ increases to 0.05 from 0, the average throughput decreases and average collision is non-zero for POPETS case also. However, they are not dependent on the feedback error probability, P_{fe}. When both the sensing and/or the feedback error probabilities are non-zero, the average throughput decreases and average collision increases for XLPFTS case. However, up to $H = 6$, the loss of throughput due to sensing error is more than feedback error. The situations reverses after $H = 6$. The collision curves also exhibit the same trends, but switching happens at different value of H as can be seen in the Fig. 4.5.

4.5 Chapter Summary

We investigated the throughput and the collision performances of a cognitive radio system when the primary user has possibly three hidden states. We provided POMDP-based formulation and incremental-pruning algorithm based solution techniques to find alpha vectors needed to compute policy for a particular belief vector. For a particular belief vector in a particular time-slot, the power adaptation actions are found by plugging the belief vector in the alpha vector sets and by finding maximum value of the scalar products of them. We studied two policies: in order to track the belief, while first technique requires channel to be sensed in each time-slot, second technique requires channel sensing in the first time-slot only. In the other time-slots, ACK/NAK feedback from previous slot is used in the latter technique. We evaluated the throughput and the collision performances of both policies and compared them with fully observable optimal policy. Simulation results showed that the proposed cross-layer policy is more throughput efficient than the physical layer optimal policy, specially when the primary user's state transition rate is slower and/or frame size is smaller.

Chapter 5

Channel Access in Overlay Cognitive Radio System

In the previous chapters, we studied the performance of underlay and interweave cognitive communication system. In this chapter, we do the preliminary study of the last variant of the cognitive radio system called overlay cognitive radio system. In an overlay system, the cognitive user operates concurrently with primary user. In contrast to underlay system, the cognitive user assists the primary user communication while operating in overlay mode of transmission. In overlay mode, it is assumed that primary user information is available at cognitive user. The knowledge of the primary user's message is used to mitigate or cancel the interference at the primary and cognitive receiver. Relaying the primary user information plays a crucial role in an overlay system. On the other hand, orthogonal frequency and code division multiplexing (OFCDM) based access technology is considered as a good candidate for the next generation wireless standards [45, 46]. Hence, in this chapter, we evaluate the performance of an OFCDM based relay network and the analysis can be extended to the overlay cognitive radio system.

For wideband applications, code division multiple access (CDMA) based systems deployed on multicarriers could provide effective multiple access capabilities. First was the multicarrier direct-sequence CDMA [47] system where multicarrier modulation was used with time spreading. The other was the multicarrier CDMA [48] where multicarrier modulation and frequency domain spreading were used. Even though multicarrier CDMA provides frequency diversity, it is vulnerable to multiple access interference in frequency selective subcarriers. In order to realize the benefits from both systems, a multicarrier CDMA system was proposed in [49] where both frequency and time spreading codes were used according to the channel conditions. This proposed system was shown to provide frequency diversity while reducing the multiple access interference.

Channels can be selected orthogonally, and OFCDM system was proposed in [50]. OFCDM uses data spreading in both time and frequency domain, where each data stream is segmented into multiple substreams and spread over multiple channels and several OFCDM symbols, exploiting additional frequency and time diversity. OFDM technology is incorporated in standard IEEE 802.11 for wireless local area networks, in IEEE 802.16 for metropolitan area networks [51] and in LTE [52]. In [53], OFDM based two dimensional spreading was proposed for future 4G wireless networks [54] and field test was done by NTT DoCoMo to support the needs of OFCDM technology in future wideband communications [45]. There has been quite an amount of research work on channel grouping and allocation to further improve the performance in OFCDM systems. For example, channels are grouped and adaptively allocated in [55] to users by improving the signal to interference and noise ratio (SINR) while minimizing the multiple access interference.

On the other hand, the transmission range of the next generation wireless networks is limited due to the higher operating frequencies [56]. Cooperative cognitive relay systems can improve the throughput, coverage and the reliability [57, 58] in wideband wireless com-

munications. In order to get better performance, relaying was incorporated in the standard IEEE 802.16j (WiMAX) amendment and in 4G networks [59].

In future generations networks, OFCDM based relay networks would provide better performance. CDMA technique was introduced in relay systems in [60] [61] to take advantage of spread spectrum techniques. In [62], multicarrier CDMA decode-and-forward relay system performance was analyzed. The power allocation was analyzed in [63] for a CDMA based decode-and-forward relay system and cognitive relay networks are recently studied in different articles [64–66]. However, there have been not much work done for OFCDM based relay networks. In the future overlay cognitive systems, OFCDM based relaying would be more beneficial as mentioned earlier.

In this chapter, channel and power allocation schemes are proposed and analyzed for different scenarios for a two-hop decode-and-forward OFCDM based relay network. Our contributions in this chapter can be summarized as follows:

- Deriving the bit error performance of the proposed channel and power allocation schemes for a two-hop decode-and-forward OFCDM based cognitive relay network.
- Numerically evaluating the effect of considering the channel state information (CSI) of source-base station and source-relay in channel allocation.
- Numerically analyzing the BER performance for different power allocation ratio between the source and relay nodes.

The rest of the chapter is organized as follows: In Section 5.1, the system model for a two-hop relay network and a modified adaptive channel and power allocation algorithms are presented. In Section 5.2, relevant literature for one-hop and BER derivation for a two-hop OFCDM based decode-and-forward relay network are presented. Section 5.3 presents

the performance comparison for different channel and power allocation schemes for different time-frequency spreading codes. Finally, this chapter concludes in Section 5.4 with future work.

5.1 Two-hop Overlay System Model

We consider a two-hop wireless system where OFCDM is employed as multiple access technology. Users are denoted by U_k and total number of users is K (assumed to be even number). Odd numbered users $(U_1, U_3, \ldots, U_{K-1})$ are classified into one group and even numbered users $(U_2, U_4, \ldots, U_K)$ into another group as done in [62]. Further, it is assumed that there is an one-to-one mapping between two groups of users and they are paired (as partners) for cooperative relaying. Source nodes and relaying nodes are allocated separate channels (time slots) during the transmission. Each node transmits its own data as well as the estimated data of its partner which was received in the previous time slot.

All the users have their own spreading codes. Each partner node is aware of its own spreading code as well as its partner's spreading code. Every user's information is retransmitted using that user's spreading code. That is, source transmits its own information using its own spreading code. Relay node decodes and forwards the information of its partner using its partner's spreading code and, at the same time transmit its own information using its own code [67].

Fig. 5.1 shows a couple of transmission cycles to understand the pair-wise communication $(t = j, j+1)$and Table 5.1 shows 4 consecutive transmission time instances. The User 1 is considered as source and the User 2 as relay. Further, the binary data stream of user k is denoted by $\mathbf{b}_j^k = \pm 1$ and its estimate at the relay node by $\hat{\mathbf{b}}_j^k$ where $j \epsilon \aleph$ indicates the time instance.

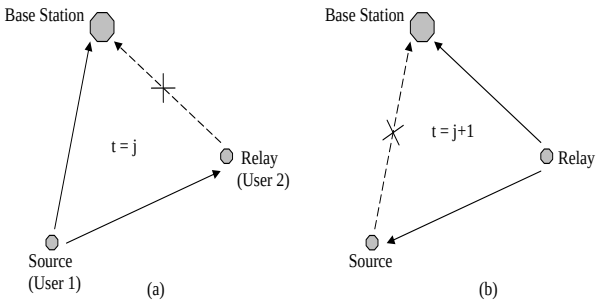

Figure 5.1: System model (a) at time $t = j$, (b) at time $t = j + 1$.

Transmitting node	Time instance			
	t=j	t=j+1	t=j+2	t=j+3
User 1	b_j^1	-	$\hat{b}_{j+1}^2, b_{j+2}^1$	-
User 2	-	$\hat{b}_j^1, b_{j+1}^2$	-	$\hat{b}_{j+2}^1, b_{j+3}^2$

Table 5.1: Two user cooperative communication during 4 time slots

In the analysis, the channel is assumed to be slowly varying with respect to the OFCDM symbol duration. It is also assumed that channel spacing is larger than the coherence bandwidth of the channel in a group and hence, frequency non-selective fading occurs on each channel within a channel group [3]. This allows the frequency domain channel to be modeled as:

$$H_{j,m}^k = \alpha_{j,m}^k e^{i\phi_{j,m}^k},$$

where $i = \sqrt{-1}$. The term $\alpha_{j,m}^k$ is the Rayleigh fading gain for the mth channel of the kth user during the jth transmitted bit. The phase is an uniformly distributed random variable over the interval $(0, 2\pi]$, which is assumed to be independent for each bit, user, and channel.

Channel and Power Allocation in a Relay Network

In this section, a modified adaptive channel allocation algorithm for an OFCDM based relay network is first proposed and then the power allocation parameters and the scenarios are discussed for the subsequent analysis.

Channel Allocation

In [55], an adaptive channel allocation algorithm was proposed for a single link transmission to improve the overall BER performance of an OFCDM system. The channels are assigned to users that are having higher SINR at the same time reducing the interference caused by this assignment to other users in the same channel group. This algorithm is modified later in this section for a decode-and-forward OFCDM based two-hop relay system.

In a two-hop relay system, there are 3 links, namely ($s \rightarrow r, s \rightarrow bs$ and $r \rightarrow bs$) that contribute to the overall BER performance of the system. As described earlier, the two consecutive time slot transmission from the source and the relay are assumed to fade independently; hence, the channel allocation is also done separately.

During the jth time slot, the source will transmit and, the base station and the cooperating relay node will receive on a same set of channel group ($G_{y,s}$). Therefore, the channel allocation algorithm is carried out based on the availability of the channel state information (CSI) of the links $s \rightarrow r$, and $s \rightarrow bs$.

We introduce a parameter ν ($0 \leq \nu \leq 1$), called *cooperative CSI (C-CSI)* which weighs in end-to-end SINR for a two-hop transmission and hence provides different impact on channel allocation. ν=0.5 means that the channel allocation algorithm tries to optimize both links ($s \rightarrow bs$ and $s \rightarrow r$) simultaneously giving equal weight. In this case, maximizing the SINR while minimizing the multiple access interference would be performed on both links together

with equal weight. When ν=1, the channel allocation is done solely based on the CSI of the link $s \rightarrow bs$ whereas when ν=0, it is solely on the CSI of the link $s \rightarrow r$. ν is therefore called *cooperative CSI* that adjusts the weight of different cooperative links.

Hereafter, the time instance j is dropped in the notations for simplicity. Decision variable (i.e., SINR) in channel allocation for a two-hop relay system for user k is defined giving different weights to cooperative links as:

$$\gamma_y^k = \nu \gamma_y^{k,bs} + (1-\nu)\gamma_y^{k,r}, \tag{5.1}$$

where $\gamma_y^{k,bs}$ and $\gamma_y^{k,r}$ are defined as SINR of user k belonging to channel group y at the base station and the relay node respectively and they are calculated as in (5.8).

The channel allocation algorithm is described briefly as follows:

(a) Channel group that has the largest SINR γ_y^k as defined in (5.1) for all k users is found as follows:

$$\gamma_{max}^k = \max\{\gamma_1^k, \gamma_2^k, \ldots, \gamma_Y^k\}.$$

The index denoted y_{max}^k is recorded.

(b) From the result in (**a**), the channel group with the smallest SINR is found as follows:

$$\gamma_{min} = \min\{\gamma_{max}^1, \gamma_{max}^2, \ldots, \gamma_{max}^K\}.$$

The index of the user with the lowest SINR value, denoted k_{min} is recorded.

(c) User k_{min} is assigned to the channel group $y_{max}^{k_{min}}$ and the SINR is re-calculated for that assigned group using (5.8). The algorithm is repeated until all the data streams are assigned.

The channel group with the highest SINR for each user will produce the best BER performance for each user (in step (a)). When the user with the smallest γ_{max}^{k} (in step (b)) is provisioned to the channel group first (in step (c)), it reduces the average fading gain in the group, and consequently reduces the amount of interference to other users.

Power Allocation

The source node and the relay node chip energies are denoted by ϵ_{c_s} and ϵ_{c_r} respectively. The total chip energy (ϵ_c) is kept as constant and can be written as

$\epsilon_c = \epsilon_{c_s} + \epsilon_{c_r}$. The cooperative power ratio λ ($0 \leq \lambda \leq 1$) is defined as:

$$\lambda = \frac{\text{source node power}}{\text{total power of source and relay nodes}} = \frac{\epsilon_{c_s}}{\epsilon_c}, \tag{5.2}$$

and ϵ_{c_r} can be defined as $(1-\lambda)\epsilon_c$. In the numerical analysis, the various power allocation strategies among the source and the relay node are discussed with different channel allocation schemes. Further, the BER performance analysis is carried out for two different scenarios.

- Case 1: Equal channel gains for all three links ($s \rightarrow bs$, $s \rightarrow r$ and $r \rightarrow bs$)
- Case 2: Strong source to relay link (ξ dB better than other two links). This case is more practical as one would normally resort to relay communication under this condition.

The power allocation strategies are discussed in the Section 5.3.

5.2 Bit Error Rate Analysis

In this section, BER performance for an one-hop OFCDM system with adaptive channel allocation is first reviewed and for the two-hop decode-and-forward OFCDM based relay system is derived later.

5.2.1 BER Derivation: One-hop (single link) Transmission

For a direct one-hop transmission, the adaptive channel allocation for an OFCDM system was proposed in [55]. In order to recover the data from User 1 at the receiver, the received signal is copied to the channel branches that are assigned to User 1 and then signal on each channel is restored to the baseband considering the phase response of the channel. Then each branch is multiplied by the synchronized time domain spreading sequence and the frequency domain pseudo-random chip. The despread signal is then multiplied by the fading gain, $\alpha^1_{j,m}$, according to the maximal ratio combining algorithm. Finally, the channels are summed, integrated over the bit period, and sampled to yield the decision variable for User 1 as:

$$Z^1_j = D^1_j + I^1_j + \eta^1_j, \tag{5.3}$$

where D^1_j is the desired signal, I^1_j is the interference from the other users on group y, $y = \{1, 2, \ldots, Y\}$, where Y is total number of channel groups and η^1_j is the noise term which is considered as the AWGN noise signal with a double-sided power spectral density of $N_o/2$ during j^{th} bit duration. Further, G_y, M_y and K_y denote the set of channels, number of channels and the number of users respectively occupying a group y simultaneously. Since we are not concerned with the absolute performance of the receiver/detection schemes, we could use any receiver. Maximal ratio combining receiver has been widely used in the literature [49, 55, 68–70] for similar work. A multi-user detection scheme such as minimum mean square error can also be used; however, it will not affect our conclusions, though one would expect relative BER performance degradation in maximal ratio combining receiver with an increase in the number of active users compared to multi-user detection schemes.

The desired signal can be written as [55] for a single link direct transmission,

$$D^1_j = N\sqrt{\varepsilon_c} b^1_j \sum_{m \epsilon G_y} (\alpha^1_{j,m})^2, \tag{5.4}$$

where ε_c is the chip energy and N is the length of the pseudo-random sequence.

The power of the desired signal for user 1 is determined by computing the variance D_j^1. Since the bit stream, $\mathbf{b}_j^1$ has zero mean, the power of the desired signal can be written as:

$$P_{D_j}^1 = \mathrm{Var}\big[D_j^1\big] = N^2\varepsilon_c\left[\sum_{m\epsilon G_y}(\alpha_{j,m}^1)^2\right]^2, \tag{5.5}$$

where Var[.] is the variance.

The interference term is calculated by considering the correlation between the received signals from all K_y users occupying channel group y simultaneously, with the time and frequency domain spreading sequences for User 1.

The interference power can be approximated as a Gaussian random variable when the number of users is moderate to large, and the input data stream is random [49] [71]. The resulting interference power is,

$$P_{I_j}^1 = N\varepsilon_c(K_y-1)\mathrm{E}\big[(\alpha_y)^2\big]\sum_{m\epsilon G_y}(\alpha_{j,m}^1)^2, \tag{5.6}$$

where $\mathrm{E}\big[(\alpha_y)^2\big]$ is the average fading gain for the K_y users and M_y channels in group y. It can be calculated as follows:

$$\mathrm{E}[(\alpha_y)^2] = \frac{1}{K_yM_y}\sum_{k\in G_y}\sum_{m\in G_y}(\alpha_{j,m}^k)^2.$$

The noise power at output of the correlation can be written as:

$$P_{\eta_j}^1 = \mathrm{Var}\big[\eta_j^1\big] = NN_o\sum_{m\epsilon G_y}(\alpha_{j,m}^1)^2. \tag{5.7}$$

Based on the equations (5.5)-(5.7), the SINR for User 1 during the jth bit assigned to channel group y, $\gamma_{j,y}^1$ can be written as:

$$\gamma_{j,y}^1 = \frac{N\varepsilon_c\sum_{m\epsilon G_y}(\alpha_{j,m}^1)^2}{(K_y-1)\varepsilon_c\mathrm{E}\big[(\alpha_y)^2\big]+N_o}. \tag{5.8}$$

Further, the probability of bit error can be determined for the jth bit as follows assuming BPSK modulation,

$$\Pr_{b_j}^1 = Q\left(\sqrt{2\gamma_{j,y}^1}\right). \tag{5.9}$$

5.2.2 BER Derivation: Two-hop Relay Transmission

Based on the results in the previous section for one-hop system, the BER performance of the two-hop relay system is derived in this section. Few additional notations $s{\rightarrow}r$, $s{\rightarrow}bs$ and $r{\rightarrow}bs$ are incorporated in the channel gain to differentiate the links, denoting source-relay link, source-base station link, and relay-base station link respectively. As shown in Fig. 5.1, the same source information is received at the base station (bs) during two consecutive time slots. In the jth time slot, the information is received from the source (s) and, during the $(j+1)^{\text{th}}$ time slot the information is decoded and forwarded by the corresponding relaying (r) node. The combined decision variables with equal confidence on both the links of User 1 after two consecutive time slots $(j, j+1)$ at the base station receiver can be written as below. The source node and the relay node chip energies are denoted by ϵ_{c_s} and ϵ_{c_r} respectively. The desired signal from (5.4) is:

$$D_{j+1,bs}^1 = D_{j,bs}^{1,s\rightarrow bs} + D_{j+1,bs}^{1,r\rightarrow bs} = N\left(\sqrt{\epsilon_{c_s}} b_j^1 \sum_{m\in G_{y,s}} (\alpha_{j,m}^{1,s\rightarrow bs})^2 + \sqrt{\epsilon_{c_r}} \hat{b}_{j+1}^1 \sum_{m\in G_{y,r}} (\alpha_{j+1,m}^{2,r\rightarrow bs})^2\right), \tag{5.10}$$

where $m\epsilon G_{y,s}$ is the set of channels in group y while source transmitting and, $\alpha_{j,m}^{1,s\rightarrow bs}$, $\alpha_{j+1,m}^{2,r\rightarrow bs}$ are the Rayleigh fading gain for the mth channel of the 1st user during the jth bit transmission in the link $s{\rightarrow}bs$ and, of the 2nd user during the $(j+1)^{\text{th}}$ bit transmission in the link $r{\rightarrow}bs$ respectively.

We can rewrite the desired decision variable at the base station on the condition of correct

($D^{1,c}_{j+1,bs}$) and incorrect ($D^{1,f}_{j+1,bs}$) decoding at the relay node as:

$$\begin{aligned} D^{1,c}_{j+1,bs} &= [D^1_{j+1,bs}|b^1_j = 1, \hat{b}^1_{j+1} = 1], \\ &= N(\sqrt{\epsilon_{c_s}} \sum_{m \in G_{y,s}} (\alpha^{1,s\to bs}_{j,m})^2 + \sqrt{\epsilon_{c_r}} \sum_{m \in G_{y,r}} (\alpha^{2,r\to bs}_{j+1,m})^2). \end{aligned} \tag{5.11}$$

$$\begin{aligned} D^{1,f}_{j+1,bs} &= [D^1_{j+1,bs}|b^1_j = 1, \hat{b}^1_{j+1} = -1], \\ &= N\big(\sqrt{\epsilon_{c_s}} \sum_{m \in G_{y,s}} (\alpha^{1,s\to bs}_{j,m})^2 - \sqrt{\epsilon_{c_r}} \sum_{m \in G_{y,r}} (\alpha^{2,r\to bs}_{j+1,m})^2\big). \end{aligned} \tag{5.12}$$

and the interference and noise power terms can be derived from (5.6) and (5.7) as shown in (5.13).

$$\begin{aligned} \Omega^1_{j+1,bs} &= N \sum_{m \in G_{y,s}} \big(\alpha^{1,s\to bs}_{j,m}\big)^2 \big((K_{y,s} - 1)\epsilon_{c_s} \mathrm{E}[(\alpha^{s\to bs}_{j,y})^2] + N^{s\to bs}_o\big), \\ &+ N \sum_{m \in G_{y,r}} \big(\alpha^{2,r\to bs}_{j+1,m}\big)^2 \big((K_{y,r} - 1)\epsilon_{c_r} \mathrm{E}[(\alpha^{r\to bs}_{j+1,y})^2] + N^{r\to bs}_o\big). \end{aligned} \tag{5.13}$$

Based on the above result, the probability of bit error can be determined for the jth bit for User 1 at the base station as:

$$\mathrm{Pr}^1_{j,bs} = \big(1 - \mathrm{Pr}^1_{j,r}\big)\, Q\left(\frac{\sqrt{2}(D^{1,c}_{j+1,bs})}{\sqrt{\Omega^1_{j+1,bs}}}\right) + \big(\mathrm{Pr}^1_{j,r}\big)\, Q\left(\frac{\sqrt{2}(D^{1,f}_{j+1,bs})}{\sqrt{\Omega^1_{j+1,bs}}}\right), \tag{5.14}$$

where $\Omega^1_{j+1,bs}$ is defined in (5.13) and $\mathrm{Pr}^1_{j,r}$ is defined as the probability of bit error of User 1 at the relay node while decoding before retransmitting to the base station. It can be calculated using (5.9) with

$$\gamma^1_{j,y} = \frac{N\epsilon_{c_s} \sum_{m \epsilon G_{y,s}} (\alpha^{1,s\to r}_{j,m})^2}{(K_{y,s} - 1)\epsilon_{c_s} \mathrm{E}\big[(\alpha^{s\to r}_y)^2\big] + N_o}. \tag{5.15}$$

5.2.3 Performance Analysis

The analysis for the overall BER performance is done in this section for the scheme where the channel allocation is done giving equal weight to the links $s\to bs$ and $s\to r$ (ν=0.5). This

analysis can be extended to other schemes as well. For the analytical purpose, equation (5.14) is simply denoted as:

$$P_e = (1 - e_r)e_c + e_r e_f, \tag{5.16}$$

where each term represents the corresponding term in (5.14). First, we consider the term $e_c = Q\left(\frac{\sqrt{2}(D^{1,c}_{j+1,bs})}{\sqrt{\Omega^1_{j+1,bs}}}\right)$. It can be assumed that both the links $s \rightarrow bs$ and $r \rightarrow bs$ have similar fading characteristics when the relay node is used for the diversity advantage. Hence, the number of channels and the total channel gains within a channel group can be assumed approximately the same in (8)-(10). Further, in an interference-limited system, the noise power can also be neglected compared to the interference power. Based on these assumptions, e_c can be approximated as:

$$e_c \approx Q\left(\frac{K(\sqrt{\epsilon_{c_s}} + \sqrt{\epsilon_{c_r}})}{\sqrt{\epsilon_{c_s} + \epsilon_{c_r}}}\right), \tag{5.17}$$

where K is constant for a fading block. It can be further simplified by substituting $\epsilon_{c_s} + \epsilon_{c_r} = \epsilon_c$ as:

$$e_c \approx Q\left(K(\sqrt{\lambda} + \sqrt{1-\lambda})\right). \tag{5.18}$$

Equation (5.18) is a convex function and it has the minimum when the power is equally shared between the source and the relay node (i.e., λ=0.5) as shown in the Fig. 5.2.

Similarly, it can be shown that the term e_f has the worst performance when λ=0.5. On the other hand, the term e_r monotonically decreases with λ as the $Q(.)$ function does. Therefore, the term $(1-e_r)$ is an increasing function. These observations are used to interpret the results later.

Higher E_b/N_o

The $s \rightarrow r$ link error probability (e_r) is comparatively minimal at higher E_b/N_o range even though the power allocation strategies vary at the source. In this case, the second term

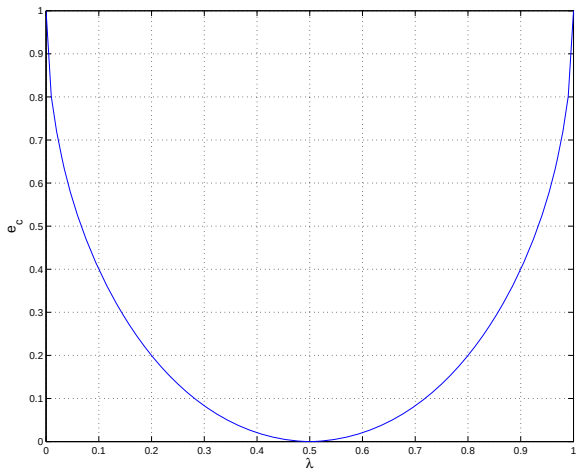

Figure 5.2: Normalized curve for e_c vs λ.

in (5.16), $e_r.e_f$, would be negligibly smaller compared to the other term $(1 - e_r)e_c$. As we discussed in previous section, when λ is closer to one, the the performance of e_c and $(1 - e_r)$ are getting worse; hence, the system performance is worse at higher E_b/N_o for higher λ. At lower λ, even though e_c is getting worse, $(1 - e_r)$ is improving and hence, slightly better performance can be noticed compared to higher λ values (this can be seen later in Fig. 5.5 at 20 dB).

Lower E_b/N_o

At lower E_b/N_o values, the $s \rightarrow r$ link performance will vary widely based on the received SINR at the relay node. If the transmit power is higher at the source node or $s \rightarrow r$ link is having better channel gains, the BER at the relay node would be better. At lower E_b/N_o values, the lower power allocation (lower λ) to the source node leads to higher BER (e_r) at the relay node. Further, the higher power allocation to the relay node makes the relay node transmit the incorrectly decoded bits with high power. This affects the term e_f further, but the performance of the term e_c remains almost the same irrespective to the power

allocation. Hence, the second term $e_r.e_f$ is highly determining the overall BER of the system at lower E_b/N_o (as shown later in the Fig. 5.5 at 0 dB for Case 1). The performance should be analyzed using both the terms in (5.16) when the link $s \rightarrow r$ has different channel gain compared to the other two links.

5.3 Numerical Results and Discussion

In this section, the simulation scenarios and the BER performance for different schemes are discussed. The BER performance results are numerically evaluated using Monte-Carlo simulation. The channel allocation is done based on the availability of the CSI between the links $s \rightarrow r$ and $s \rightarrow bs$. Channels are grouped so that within a group, all the channels undergo independent fading. Further, the uplink bandwidth is assumed to be 20MHz with 128 channels. There are 64 users grouped into two and paired. In one time slot, 32 users are assigned to the channel by the channel allocation algorithm. Each of the users is assumed to be traveling at a velocity of 5km/h, which corresponds to a Doppler frequency of 23.14Hz and to a coherence time of approximately 18μs. It is assumed that delay spread is 6.4μs which is common in urban areas [71].

The numerical simulation is carried out for the decode-and-forward OFCDM based two-hop relay system with different power allocation schemes. When a time domain spreading factor of 4 is utilized with a frequency domain processing gain of 8, it is denoted by 4×8. For the sake of comparison, we fix the total spreading factor to be 32. The total spreading factor is equal to the spreading factor in the time domain multiplied by the spreading factor in the frequency domain.

5.3.1 Channel Allocation

In this section, different channel allocation schemes are evaluated for a system with equal power sharing between the source and the relay nodes (λ=0.5).

Fig. 5.3(a) shows the different BER performance of a 4×8 (time x frequency) spread two-hop decode-and-forward relay system for different C-CSI (ν) values. From this figure, we can notice that the channel allocation of a decode-and-forward two-hop relay depends on the channel state information of the link $s \rightarrow r$ as further explained next.

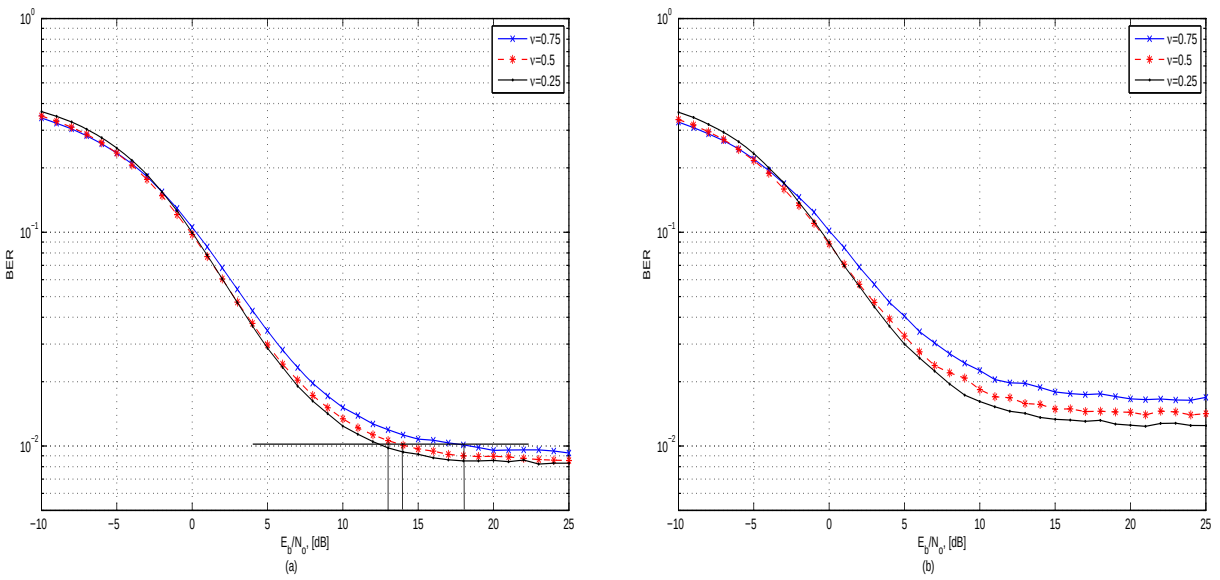

Figure 5.3: BER performance comparison for different spreading systems with different C-CSI (ν): (a) 4×8 (b) 8×4.

In a typical relay system, the CSI of the link $s \rightarrow bs$ is usually available. When the CSI of both links $s \rightarrow bs$ and $s \rightarrow r$ are available and equal weight is given (i.e., ν=0.5) in the channel allocation, it gives 4 dB gain over the channel allocation with ν=0.75, where channel allocation is done mainly based on the link $s \rightarrow bs$ at BER of 10^{-2}. Interestingly, when the channel allocation is done mainly based on the link $s \rightarrow r$ (ν=0.25), it outperforms

the allocation which is done mainly based on the link $s \rightarrow bs$ (ν=0.75) by 5 dB at BER of 10^{-2}. The decision variable at the receiver (bs) is considered during the decoding process giving equal weight on both the received signal from the source and the forwarded signal from its partner. Therefore, the incorrectly decoded bits at the relay node will cause higher error probability at the base station. At higher E_b/N_o, it is better to do the channel allocation considering mainly the inter-partner (source-relay) CSI, provided it is accurate.

Similar characteristic is observed in Fig. 5.3(b) for a system with spreading factor of 8×4. We can notice that the error floor improves when the value of ν decreases, i.e., the channel allocation is done giving higher weight to the link $s \rightarrow r$. The error floor is 0.0169 when ν=0.75 whereas it is 0.0125 when ν=0.25. The performance is highly interference-limited at higher E_b/N_o for higher time spreading schemes as shown in Fig. 5.3. Further, the error floors for the schemes 16×2 and2×16 are shown in Table 5.2 and explained in detail in Section 5.3.2.

In the case of a specific spreading factor (for example 8×4), different E_b/N_o values influence in selecting the index ν when both link CSIs are perfectly available. For example, even though ν=0.25 is performing better at higher E_b/N_o, for $E_b/N_o < 0$ dB, ν=0.5 is preferred over ν=0.25 for an 8×4 system as shown in Fig. 5.3. We also observed the significance of this selection in higher time spreading systems such as 16×2 and 32×1. Even though the selection of ν in channel allocation is less significant for the schemes with higher frequency spreading, it influences the schemes with higher time spreading.

In Fig. 5.4, BER performance is shown for different spreading factors, from higher (lower) time (frequency) spreading to lower (higher), by varying the parameter C-CSI (ν). At lower E_b/N_o, it is better to use higher spreading in time, and lower spreading in frequency as also reported in [55]. The *cross-over point* is defined as an E_b/N_o value around which the performance of the frequency spreading becomes better than the time spreading. In Fig.

5.4, when ν increases from 0.25 to 0.75, the cross-over point (E_b/N_o) value moves from 4 dB to 1 dB. It is also tabulated for different values of ν the Table 5.3 and it shows a relationship between the cross-over point (E_b/N_o) and the C-CSI (ν) which provide additional flexibility in operating environment for OFCDM systems between time and frequency spreading.

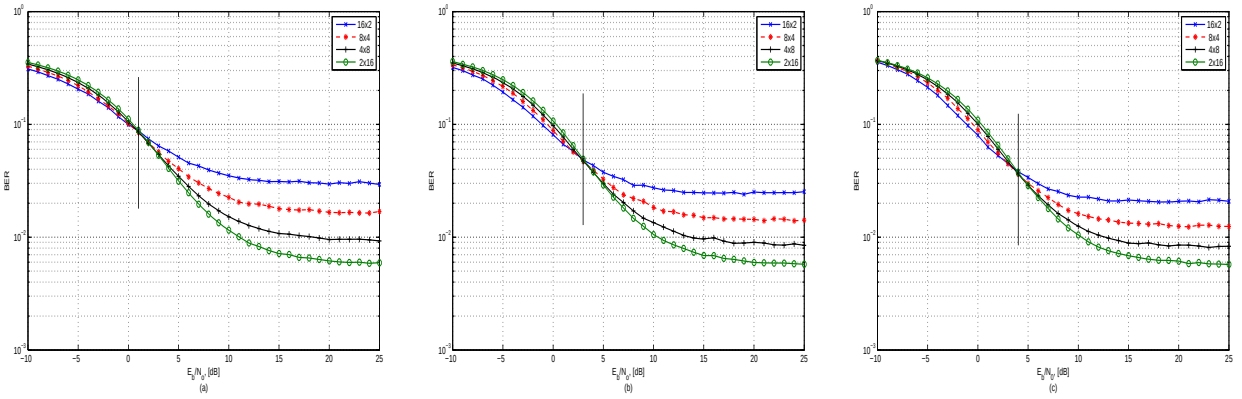

Figure 5.4: BER performance comparison with various spreading factor: (a) ν=0.25 (b) ν=0.5 (c) ν=0.75.

C-CSI (ν)	BER 16×2	BER 2×16
0.25	0.0208	0.0057
0.5	0.0253	0.0058
0.75	0.0294	0.0059

Table 5.2: Error floor for different spreading

C-CSI (ν)	E_b/N_o (dB)
0	5
0.25	4
0.5	3
0.75	1
1	-1

Table 5.3: Cross-over point from frequency to time spreading.

5.3.2 Power Allocation

In this section, different power allocation schemes are evaluated for a system where the channel allocation is done giving equal weight to the links $s \rightarrow bs$ and $s \rightarrow r$ (ν=0.5).

Different Source to Relay Channel Gains

Fig. 5.5 shows the BER performance for different cooperative power ratio (λ) at different E_b/N_o values for a 2×16 scheme for two different cases described in Section 5.1.

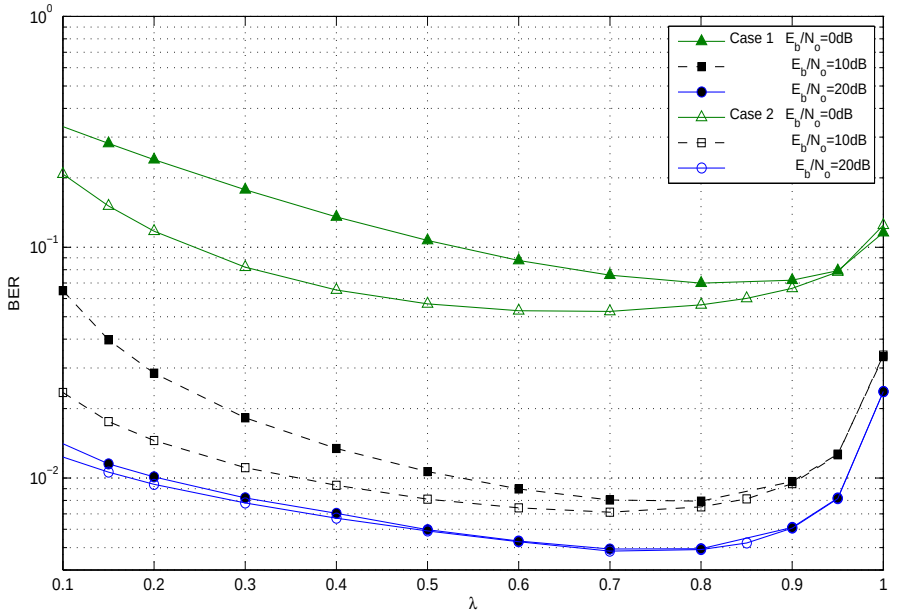

Figure 5.5: BER performance comparison for 2×16 scheme with different power allocation at E_b/N_o=0 dB,10 dB and 20 dB (ν=0.5).

For the equal link gain (Case 1, at higher E_b/N_o (20 dB)), the BER performance is optimum when $\lambda \approx 0.8$. When λ increases further, that is source node power is increased, the performance deteriorates at a faster rate than when λ decreases. Therefore, when λ takes the value less than the optimum, it is less sensitive to the BER performance and hence, it

is safe to operate in the region $0.6 \leq \lambda \leq 0.85$ with less than 10% performance degradation. On the other hand, at lower E_b/N_o values, the BER performance is also sensitive when λ decreases. Hence, the operating region shrinks to $0.75 \leq \lambda \leq 0.85$.

In the case of stronger $s \rightarrow r$ link (Case 2) considering here we consider ξ=5 dB, we can notice a similar trend at higher E_b/N_o values but at lower E_b/N_o values, Case 2 performance is better when lower power is allocated to the source node compared to Case 1. That is, the optimal cooperative power ratio moves towards $\lambda \approx 0.65$ for lower E_b/N_o values when the $s \rightarrow r$ has 5 dB better channel gain compared to the other two links as shown in Fig. 5.5.

Fig. 5.6(a) and Fig. 5.6(b) show the BER performance for different cooperative power ratio for both the cases when the channel allocation is done giving equal weight (ν=0.5) on both the links $s \rightarrow bs$ and $s \rightarrow r$. As we discussed earlier, at higher E_b/N_o, BER performance reaches the interference-limited error floor according to the power allocation scheme in both cases. Fig. 5.6(b) shows that when the channel gain on the link $s \rightarrow r$ is better, it gives better performance on low-to-moderate E_b/N_o region; but at higher E_b/N_o, it reaches the same error floors. Further, it shows 5 dB, 1.5 dB and 1 dB gains at λ=0.25, λ=0.5 and λ=0.75 respectively at BER of 10^{-2} for the system with better channel gain of 5 dB between the $s \rightarrow r$ link than the one having equal gain. Table 5.4 shows the above results.

	Required E_b/N_o at BER of 10^{-2}	
Power Allocation Ratio (λ)	Equal Gain	Strong $s \rightarrow r$ Link
0.25	8.25	7.25
0.50	10.5	8.0
0.75	17.0	13.0

Table 5.4: Performance comparison at BER of 10^{-2} for different λ (ν=0.5).

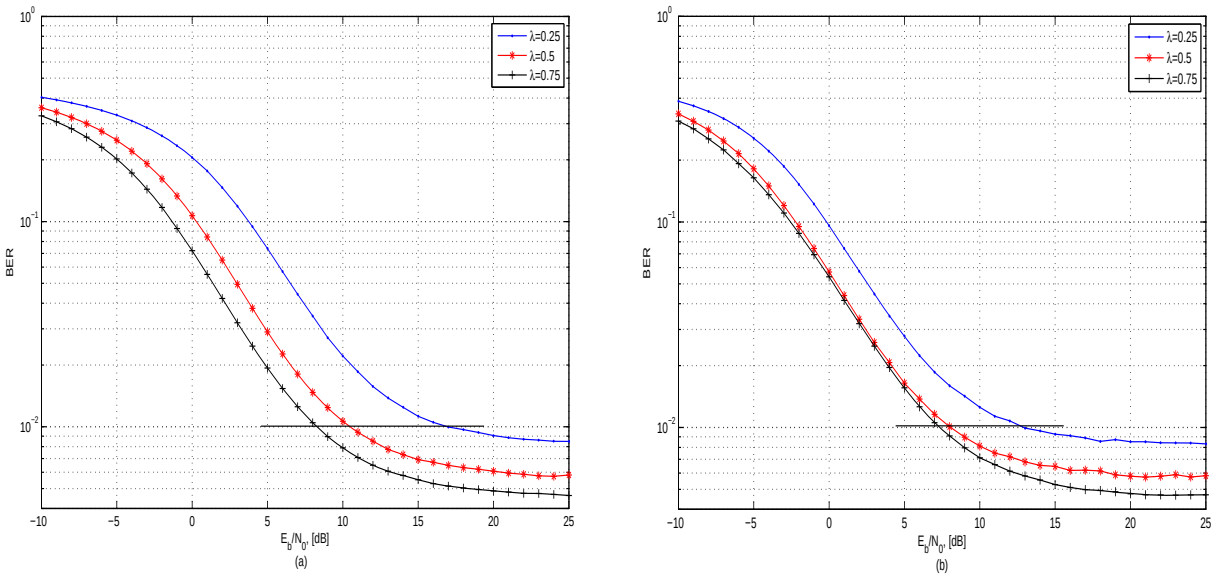

Figure 5.6: BER performance comparison for 2×16 scheme with C-CSI, ν=0.5, for various power allocation with: (a) Equal Channel Gain (Case 1) (b) 5 dB higher $s \rightarrow r$ link (Case 2).

We can notice at higher E_b/N_o when the link $s \rightarrow r$ is stronger, the interference-limited error remains the same for both the cases and there is no significant difference in optimal power allocation strategy (λ). On the other hand, at lower E_b/N_o values, different power allocation strategies have different impact.

Different Time-Frequency Spreading Schemes

Fig. 5.7 shows the BER performance of different spreading schemes (4×8, 8×4) for different E_b/N_o values. We notice the similar phenomena as discussed earlier for 2×16 scheme. We also notice that at low E_b/N_o (0 dB) the performance is better for an 8×4 scheme than the 4×8 scheme whereas, at higher E_b/N_o (10 dB, 20 dB), 4×8 scheme outperforms the other.

At lower E_b/N_o, the performance is limited by thermal noise. Higher number of groups with few channels lead to allocate channels with best channel conditions. Therefore, lower

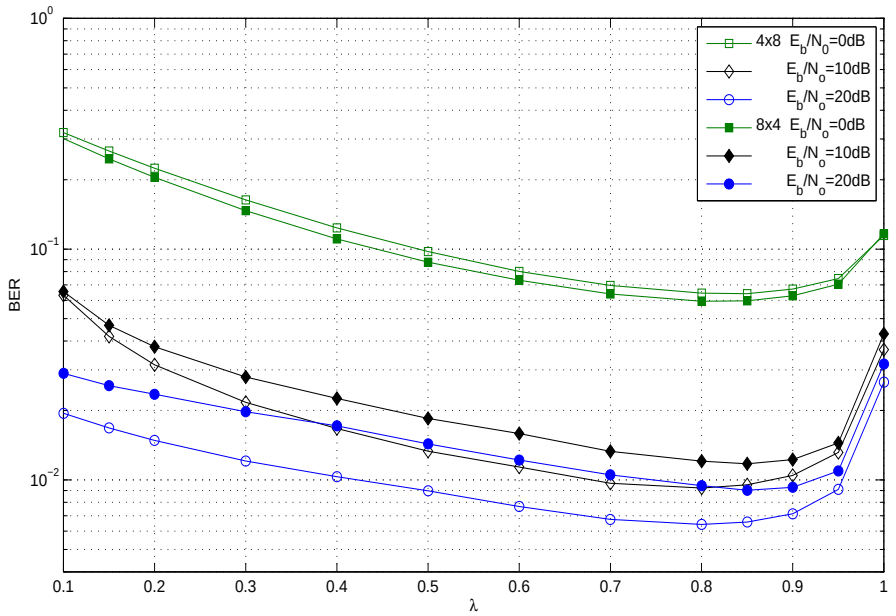

Figure 5.7: BER performance comparison for 4×8 and 8×4 schemes with different power allocation at E_b/N_o=0 dB,10 dB and 20 dB (ν=0.5).

frequency spreading with higher time spreading offers better performance. Also the multiple access interference is minimal since a relatively lower number of users is sharing each group of channels. On the other hand, at higher E_b/N_o, the system performance is limited by multiple access interference. Therefore, selecting a better channel does not necessarily offer better performance. Further, larger group size offers better frequency diversity and at higher E_b/N_o it is better to have higher frequency spreading with lower time spreading as also reported in [55].

The optimal power allocation strategy is not dependent on different spreading factors, but the power allocation affects differently at the extreme power allocation conditions ($\nu \approx 0/1$) for different spreading schemes.

5.4 Chapter Summary

We first proposed a cooperative CSI-based channel allocation algorithm for an OFCDM-based two-hop decode-and-forward relay system. Its BER performance was evaluated via Monte Carlo simulation. In the case of equal confidence given at the base station receiver for the source and its partner's forwarded data in a decode-and-forward OFCDM two-hop relay diversity system, CSI of the source-relay link (with lower *cooperative CSI*) influences the channel allocation at moderate to high E_b/N_o values. Further, when channel allocation is done giving higher weight on the CSI of the link $s \rightarrow bs$ (as ν is increased) the time-frequency spreading cross-over point moves towards lower E_b/N_o values.

Secondly we evaluated the power allocation schemes. There is an optimal power allocation between the source node and the relay node and that varies for different operating E_b/N_o values. When all three links have equal gains, the optimal power allocation ratio is $\lambda \approx 0.8$. Further, if a system has better $s \rightarrow r$ link, it will improve the performance at lower E_b/N_o values but not the interference-limited error floor. For a such system, at lower E_b/N_o values, the optimal power allocation ratio is $\lambda \approx 0.65$. Further, the optimal power allocation strategy is not highly dependent on different time-frequency spreading factors.

We can conclude from the above results that optimal power allocation between the source-relay nodes combined with proper channel allocation significantly improves the system performance of an OFCDM based decode-and-forward relay network.

This concept can be applied to the overlay cognitive system where the cognitive user acts as relay and assisting the primary user transmission. As the future work, the throughput performance of the overlay cognitive radio can be analyzed with the proposed channel and power allocation schemes.

Chapter 6

Conclusions and Future work

This dissertation mainly focused on channel access in cognitive radio communication. The main contributions of this dissertation are summarized as follows with the discussion of the future work:

6.1 Summary

First we considered an interweave cognitive radio system where cognitive user can only access the channel when the primary user is not active. As interfering with the primary user is strictly prohibited, cognitive user senses the channel every time before it transmits. In practice, cognitive user can sense only one channel at a time. Therefore, we considered first, an interweave cognitive radio system where a primary user accesses two primary channels. We developed an access scheme that considers primary user's occupancy and cognitive user's channel gain prediction in order to get an optimal channel switching threshold to maximize the cognitive user throughput. We mainly focused on a positively correlated primary user traffic. It was found that, when the primary user traffic is highly correlated or cognitive user is more dynamic (higher Doppler spread), it is not beneficial to switch the channel

frequently in order to gain long term throughput advantage. From our analysis, given that primary user occupancy statistics and cognitive user's relative movements (Doppler spread) are given, the proposed access scheme would instruct cognitive user to leave the current channel when its received SNR is below a certain threshold even if that channel is idle. We further investigated the channel access in a hybrid interweave-underlay cognitive radio system. Based on the primary user traffic characteristics and throughput ratio between the interweave and underlay mode of transmission, we proposed a transmission mode switching strategy between interweave and underlay modes. It was shown that, proper transmission mode selection based on our proposed access scheme can provide better throughput. In the previous analysis, we assumed perfect sensing but in practice, it is not true. Hence, we analyzed the performance of a hybrid interweave-underlay cognitive radio system with imperfect sensing. We formulated the problem as partially observable Markov decision process. We studied two policies in order to track the belief; while first technique requires channel to be sensed in each time-slot, second technique requires channel sensing in the first time-slot only. In other time-slots of a frame, ACK/NAK feedback from previous slot is used in the latter technique. We evaluated the throughput and the collision performances of both policies and compared them with fully observable optimal policy. Simulation results showed that the proposed frame-based sensing with ACK/NACK feedback policy is more throughput efficient than the policy with sensing every slot, specially when the primary user traffic is correlated and/or frame size is smaller.

Later we investigated the channel and power allocation on a cognitive relay based network. As in overlay cognitive radio systems, the relay nodes assist the primary transmission. We did the preliminary analysis on a decode-and-forward relay network with orthogonal frequency and code division multiplexing access scheme (OFCDM). We proposed a adaptive channel allocation scheme based on the channel gains between the source-destination and

source-cognitive relay node links. Also we proposed, how the frequency-time spreading need to be done based on the channel gains of source-destination and source-relay links. Apart from that, to achieve the better overall throughput, how the power should be allocated between source and relays nodes were also analyzed. Further, it was found that, the optimal power allocation strategy is not highly dependent on different time-frequency spreading factors. We observed that optimal power allocation between the source-relay nodes combined with proper channel allocation significantly improves the system performance of an OFCDM based decode-and-forward relay network.

6.2 Future Work

Even though several research contributions have been made in this dissertation for cognitive radio access schemes, there are a number of research topics to be explored as extensions of this work.

We assumed that cognitive user can sense only one channel at once, but there are many schemes with cooperative sensing and multiples channel sensing at a time in the literature. Performance improvement in the proposed access schemes with cooperative sensing needs to be evaluated. We considered only the interweave-underlay hybrid system, but in the future, cognitive radio should be more flexible to select the transmission modes between interweave-underlay-overlay. We would like to extend our work to a generalized framework for transmission mode selection with imperfect sensing Our research work rely on the availability/estimation of the primary user traffic characteristics. Uncertainty analysis on that parameter would be beneficial. We did most of the analysis on a positively correlated primary user traffic environment. Even though the analysis is similar, it is better to have and validate the findings on negatively correlated traffic. We have done channel-power allocation

on decode-and-forward OFCDM based relay network. This work can be extended on overlay network focusing on interference limitation to the primary receiver with different coding techniques.

Bibliography

[1] J. Mitola III and G. Q. Maguire Jr., "Cognitive radio: making software radios more personal," *IEEE Personal Commun. Mag.*, vol. 6, pp. 13–18, Aug. 1999.

[2] S. Srinivasa and S. A. Jafar, "Cognitive radios for dynamic spectrum access - The throughput potential of cognitive radio: A theoretical perspective," *IEEE Commun. Mag.*, vol. 45, pp. 73–79, May 2007.

[3] A. Goldsmith et al., "Breaking spectrum gridlock with cognitive radios: An information theoretic perspective," *Proceedings of the IEEE*, vol. 97, pp. 894–914, May 2009.

[4] Z. Wu and B. Natarajan, "Interference tolerant agile cognitive radio: Maximize channel capacity of cognitive radio," *in Proc. Consum. Commun. Networking Conf.*, pp. 1027–1031, Jan. 2007.

[5] Q. Zhao and B. M. Sadler, "A survey of dynamic spectrum access: Signal processing, networking, and regulatory policy," *IEEE Signal Processing Mag.*, pp. 79–89, May 2007.

[6] M. Gastpar, "On capacity under receive and spatial spectrum-sharing constraints," *IEEE Trans. Inf. Theory*, vol. 53, pp. 471–487, Feb. 2007.

[7] A. Ghasemi and S. Sousa, "Capacity of fading channels under spectrum-sharing constraints," *In Proc. IEEE Int. Conf. Commun. (ICC)*, vol. 10, no. 1, pp. 4373–4378, 2006.

[8] H. Suraweera et al., "Channel capacity limits of cognitive radio in asymmetric fading environments," *In Proc. IEEE Int. Conf. Commun. (ICC)*, pp. 4048–4053, May 2008.

[9] FCC Spectrum Policy Task Force, "FCC report of the spectrum efficiency working group," Nov. 2002.

[10] K. Son, B. Jung, S. Chong, and D. Sung, "Opportunistic underlay transmission in multi-carrier cognitive radio systems," *in Proc. IEEE Wireless Commun. Networking Conf.*, pp. 1–6, Apr. 2009.

[11] C. Lee, T. Liu, O. Oyman, and S. Vishwanath, "Limits on cognitive communications in the wideband regime," *In Proc. IEEE 3rd Int. Conf. Cognitive Radio Oriented Wireless Networks and Commun.*, pp. 1–6, 2008.

[12] H. Kim and K. G. Shin, "In-band spectrum sensing in IEEE 802.22 WRANs for incumbent protection," vol. 9, pp. 1766–1779, Dec. 2010.

[13] Q. Zhao et al., "Decentralized cognitive MAC for opportunistic spectrum access in ad hoc networks: a POMDP framework," *IEEE J. Select. Areas Commun.*, vol. 25, pp. 589–600, Apr. 2007.

[14] T. Zhang and D. Tsang, "Optimal cooperative sensing scheduling for energy-efficient cognitive radio networks," *In Proc. IEEE Int. Conf. on computer Commun.*, pp. 2723–2731, June 2011.

[15] Y. C. Liang, Y. Zneg, E. C. Peh, and A. T. Hoang, "Sensing-throughput tradeoff for cognitive radio networks," *IEEE Trans. on Wireless Commun.*, vol. 7, pp. 1362–1337, Apr. 2008.

[16] S. Senthuran, A. Anpalagan, and O. Das, "A predictive opportunistic access scheme for cognitive radios," *In Proc. IEEE Veh. Technol. Conf. (VTC)*, Sept. 2009.

[17] S. Senthuran, A. Anpalagan, and O. Das, "Opportunistic access with channel switching in a multi-channel cognitive radio system," *IEEE Trans. Veh. Technol.*, 2012 (under review).

[18] S. Senthuran, A. Anpalagan, and O. Das, "Opportunistic channel sharing based on primary user transition probabilities in dual mode cognitive radio networks," *In Proc. IEEE Int. Conf. Commun. (ICC)*, pp. 1–6, June 2011.

[19] S. Senthuran, A. Anpalagan, and O. Das, "Throughput analysis of opportunistic access strategies in hybrid underlay-overlay cognitive radio networks," *IEEE Trans. on Wireless Commun.*, vol. 11, pp. 2024–2035, June 2012.

[20] A. Karmokar, S. Senthuran, and A. Anpalagan, "POMDP-based cross-layer power adaptation techniques in cognitive radio networks," *In Proc. IEEE Global Telecommunications Conf.*, Dec. 2012 (accepted).

[21] S. Senthuran, A. Anpalagan, and O. Das, "Cooperative power allocation schemes and BER performance in decode-and-forward OFCDM based relay networks," *In Proc. IEEE Veh. Technol. Conf. (VTC)*, Sept. 2009.

[22] S. Senthuran, A. Anpalagan, O. Das, and S. Khan, "Effect of cooperative CSI in adaptive subcarrier allocation for OFCDM based decode-and-forward relay systems," *In Proc. IEEE Veh. Technol. Conf. (VTC)*, Sept. 2009.

[23] S. Senthuran, A. Anpalagan, and O. Das, "Cooperative subcarrier and power allocation for a two-hop decode-and-forward OFCDM based relay network," *IEEE Trans. on Wireless Commun.*, vol. 8, pp. 4797–4805, Sept. 2009.

[24] R. Knopp and P. A. Humblet, "Information capacity and power control in single-cell multiuser communications," *In Proc. IEEE Int. Conf. Commun. (ICC)*, vol. 1, pp. 331–335, June 1995.

[25] T. Yucek and H. Arslan, "A survey of spectrum sensing algorithms for cognitive radio applications," *IEEE Trans. Commun. Surveys & Tutorials*, vol. 11, pp. 116–130, First quarter 2009.

[26] K. Liu and Q. Zhao, "Link throughput of multi-channel opportunistic access with limited sensing," *In Proc. IEEE Int. Conf. on Acoustics, Speech and Signal Processing*, pp. 2997–3000, April 2008.

[27] Q. Zhao and A. Swami, "A survey of dynamic spectrum access: Signal processing and networking perspectives," *In Proc. IEEE Int. Conf. on Acoustics, Speech and Signal Processing*, vol. 4, pp. 1349–1352, April 2007.

[28] Q. Zhao, B. Krishnamachari, and K. Liu, "On myopic sensing for multi-channel opportunistic access: structure, optimality, and performance," *IEEE Trans. on Wireless Commun.*, vol. 7, pp. 5431–5440, Dec. 2008.

[29] E. N. Gilbert, "Capacity of a burst-noise channel," *Bell System Technical Journal*, vol. 39, pp. 1253–1265, Sept. 1960.

[30] H. S. Wang and N. Moayeri, "Finite-state Markov channel- a useful model for radio communication channels," *IEEE Trans. Veh. Technol.*, vol. 44, pp. 163–171, Feb. 1995.

[31] C. C. Tan and N. C. Beaulieu, "On first-order Markov modeling for the Rayleigh fading channel," *IEEE Trans. Commun.*, vol. 48, pp. 2032–2040, Dec. 2000.

[32] M. K. Simon and M. S. Alouini, *Digital Communication over Fading Channels.* New York: John Wiley & Sons, 2000.

[33] A. K. Karmokar, D. V. Djonin, and V. K. Bhargava, "Optimal and suboptimal packet scheduling over correlated time varying flat fading channels," *IEEE Trans. on Wireless Commun.*, vol. 5, pp. 446–456, Feb 2006.

[34] R. Menon, R. Buehrer, and J. Reed, "On the impact of dynamic spectrum sharing techniques on legacy radio systems," *IEEE Trans. on Wireless Commun.*, vol. 7, no. 11, pp. 4198–4207, 2008.

[35] Federal Communications Commission, Notice of Inquiry and Notice of Proposed Rulemaking, "Establishment of interference temperature metric to quantify and manage interference and to expand available unlicensed operation in certain fixed, mobile and satellite frequency bands," *ET Docket*, Nov. 2003.

[36] A. Papoulis, *Probability, Random Variables and Stochastic Processes.* McGraw-Hill Companies, 1991.

[37] A. Ghasemi and S. Sousa, "Spectrum sensing in cognitive radio networks: requirements, challenges and design trade-offs," *IEEE Commun. Mag.*, vol. 46, no. 4, pp. 32–39, 2008.

[38] A. Ghasemi and S. Sousa, "Interference aggregation in spectrum sensing cognitive wireless networks," *IEEE J. Select. Topics in Signal Process.*, vol. 2, pp. 41–56, Feb. 2008.

[39] M. K. Yoon, K. H. Lee, and J. B. Song, "Performance analysis of distributed cooperative spectrum sensing for underlay cognitive radio," *In Proc. IEEE Int. Conf. on Advanced Commun. Technology*, vol. 1, pp. 338–343, 2009.

[40] J. Hillenbrand, T. A. Weiss, and F. Jondral, "Calculation of detection and false alarm probabilities in spectrum pooling systems," *IEEE Commun. Lett.*, vol. 9, pp. 349–351, April 2005.

[41] S. Geirhofer, L. Tong, and M. Sadler, "Dynamic spectrum access in the time domain: Modeling and exploiting white space," *IEEE Commun. Mag.*, vol. 45, no. 5, pp. 66–72, 2007.

[42] B. Canberk, F. Akyildiz, and S. Oktug, "Primary user activity modeling using first-difference filter clustering and correlation in cognitive radio networks," *IEEE Trans. on Networking/ACM*, vol. 19, no. 1, pp. 170–183, 2011.

[43] A. R. Cassandra, M. L. Littman, and N. L. Zhang, "Incremental pruning: A simple, fast, exact method for partially observable Markov decision processes," *in Proc. of the Uncertainty in Artificial Intelligence, Providence, Rhose Island, USA*, pp. 54–61, July 1997.

[44] A. T. Hoang, Y. C. Liang, and Y. Zeng, "Adaptive joint scheduling of spectrum sensing and data transmission in cognitive radio networks," *IEEE Trans. Commun.*, vol. 58, pp. 235–246, Jan. 2010.

[45] Y. Kishiyama et al., "Transmission performance analysis of VSF-OFCDM broadband packet wireless access based on field experiments in 100-MHz forward link," *In Proc. IEEE Veh. Technol. Conf. (VTC)*, vol. 5, pp. 3328–3333, Sept. 2004.

[46] Y. Zhou, T.-S. Ng, J. Wang, K. Higuchi, and M. Sawahashi, "OFCDM: a promising broadband wireless access technique," *IEEE Commun. Mag.*, vol. 46, pp. 38–49, March 2008.

[47] V. M. DaSilva and E. S. Sousa, "Multicarrier orthogonal CDMA signals for quasi-synchronous communication systems," *IEEE J. Select. Areas Commun.*, vol. 12, pp. 842–852, June 1994.

[48] A. Chouly, A. Brajal, and S. Jourdan, "Orthogonal multicarrier techniques applied to direct sequence spread spectrum CDMA systems," *In Proc. IEEE Global Telecommunications Conf.*, pp. 1723–1728, Nov. 1993.

[49] C. W. You and D. S. Hong, "Multicarrier CDMA systems using time-domain and frequency-domain spreading codes," *IEEE Trans. Commun.*, vol. 51, pp. 17–21, Jan. 2003.

[50] K. Zheng, G. Zeng, and W. Wang, "Performance analysis for OFDM-CDMA with joint frequency-time spreading," *IEEE Trans. on Broadcasting*, vol. 51, pp. 144–148, March 2005.

[51] Y. Zhou et al., "OFCDM: a promising broadband wireless access technique," *IEEE Commun. Mag.*, vol. 46, pp. 38–49, March 2008.

[52] 3GPP TS36.300, "Evolved universal terrestrial radio access (E-UTRA) and evolved universal terrestrial radio access network (E-UTRAN): Overall description," vol. 11.2.0, pp. 37–41, July 2012.

[53] H. Atarashi, S. Abeta, and M. Sawahashi, "Broadband packet wireless access appropriate for high-speed and high-capacity throughput," *In Proc. IEEE Veh. Technol. Conf. (VTC)*, pp. 566–570, May 2001.

[54] B. J. Chang and C. H. Wu, "Adaptive load balancing MDP-based approach of two-dimensional spreading for VSF-OFCDM in 4G nextgeneration cellular communications," *IEEE Trans. Veh. Technol.*, vol. 58, pp. 1143–1156, March 2009.

[55] R. Caldwell and A. Anpalagan, "Adaptive subcarrier allocation in synchronous reverse links of a multicarrier CDMA system with time and frequency spreading," *IEEE Trans. Veh. Technol.*, vol. 57, pp. 1494–1501, May 2008.

[56] D. Soldani and S. Dixit, "Wireless relays for broadband access," *IEEE Commun. Mag.*, vol. 46, pp. 58–66, March 2008.

[57] J. N. Laneman and G. Wornell, "Distributed space-time-coded protocols for exploiting cooperative diversity in wireless networks," *IEEE Trans. Inf. Theory*, vol. 49, pp. 2415–2425, Oct. 2003.

[58] J. N. Laneman, D. Tse, and G. Wornell, "Cooperative diversity in wireless networks: Efficient protocols and outage behavior," *IEEE Trans. Inf. Theory*, vol. 50, pp. 3062–3080, Dec. 2004.

[59] M. Nohara et al, "IEEE 802.16j std.," *IEEE 802.16's Relay Task Group*, March 2006.

[60] A. Sendonaris, E. Erkip, and B. Aazhang, "User cooperation diversity. Part I. System description," *IEICE Trans. Commun.*, vol. 51, pp. 1927–1938, Nov. 2003.

[61] A. Sendonaris, E. Erkip, and B. Aazhang, "User cooperation diversity. Part II. Implementation aspects and performance analysis," *IEICE Trans. Commun.*, vol. 51, pp. 1939–1948, Nov. 2003.

[62] U. Oruthota and N. Rajatheva, "Cooperative diversity based multi-carrier CDMA system with decode and forward relays in Rayleigh fading channels," *Wireless Personal Communications*, vol. 58, pp. 503–523, June 2011.

[63] L. Zhao and Z. Liao, "On the power allocation for decode-and-forward cooperative transmission over Rayleigh fading channels," *In Proc. IEEE Veh. Technol. Conf. (VTC)*, pp. 1669–1673, Sept. 2007.

[64] J. Lee, H. Wang, J. G. Andrews, and D. Hong, "Outage probability of cognitive relay networks with interference constraints," *IEEE Trans. on Wireless Commun.*, vol. 10, pp. 390–396, Feb. 2011.

[65] S. Sagong, J. Lee, and D. Hong, "Capacity of reactive DF scheme in cognitive relay networks," *IEEE Wireless Communications Letters*, vol. 10, pp. 3133–3138, Oct. 2011.

[66] S. Huang, H. Chen, and Y. Zhang, "Optimal power allocation for apectrum sensing and data transmission in cognitive relay networks ," *IEEE Wireless Communications Letters*, vol. 1, pp. 26–29, Feb. 2012.

[67] T.-S. Yang, A. D. Hallen, and H. Hallen, "Reliable adaptive modulation aided by observations of another fading channel," *IEEE Trans. Commun.*, vol. 52, pp. 605–611, April 2004.

[68] Z. Li and M. Latva-aho, "Error probability of interleaved MC-CDMA systems with MRC receiver and correlated Nakagami-m fading channels," *IEEE Trans. Commun.*, vol. 53, pp. 919–923, June 05.

[69] K. Zheng, G. Zeng, and W. Wang, "Performance analysis for OFDM-CDMA with joint frequency-time spreading," *IEEE Trans. Broadcasting*, vol. 51, pp. 144–148, March 2005.

[70] X. Gui and T. S. Ng, "Performance of asynchronous orthogonal multicarrier CDMA system in frequency selective fading channel," *IEEE Trans. Commun.*, vol. 47, pp. 1084–1091, July 1999.

[71] Q. Chen, E. S. Sousa, and S. Pasupathy, "Multicarrier CDMA with adaptive frequency hopping for mobile radio systems," *IEEE J. Select. Areas Commun.*, vol. 14, pp. 1852–1858, Dec. 1996.